Dynamics Based Linearization and Control of an Autonomous Ground Vehicle

prepared by

Mohammad Eghtesad

Submitted to the University of Ottawa
as a partial fulfilment of the requirements for the degree of

Doctoral of Philosophy (PhD)
in
Mechanical Engineering

Ottawa-Carleton Institute for Mechanical and Aerospace Engineering
University of Ottawa
Ottawa, Ontario, Canada, K1N 5N6

September 1996

ISBN 0-612-19953-3

Canada

UNIVERSITÉ D'OTTAWA
UNIVERSITY OF OTTAWA

In the name of God

the Compassionate, the Merciful

With the hope of acceptance

by Imam Mahdi

for their prayers and patience

dedicated to my parents

Ali Eghtesad and Esmat Torabizadeh

and

for her sacrifice and support

dedicated to my wife

Maryam Najafi

Abstract

Several aspects of dynamics based motion control of autonomous ground vehicles have been studied. For example kinematic and dynamic modelling of the vehicle, path and motion planning, path following and trajectory tracking, stabilization to a manifold and a to a desired position with specified orientation have been considered.

Assuming the (ideal) rolling without slipping conditions for a wheel imposes the nonholonomic (non-integrable) constraints on the motion of the wheel and the vehicle. Nonholonomic systems are found not to be asymptotically stabilizable by a smooth state feedback laws.

In this research, first, kinematics and Newtonian dynamics of a tricycle with front wheel steering and driving are developed and then using the concepts of Lagrange equations of the first kind, the dynamic models of the tricycle in the form of $\dot{x} = f(x,u)$ with torque inputs are derived.

Nonlinear control theory and input-output feedback linearization as a systematic approach have been applied on these dynamic models of the vehicle. Cartesian space feedback linearization is utilized for trajectory tracking and asymptotic stabilization to a one dimensional manifold and simulation results are provided. Curvilinear space feedback linearization approach for asymptotic stabilization of two outputs with open-loop control of the third planar variable using a planned path between two end positions and orientations has been verified by simulations and implemented on an experimental setup.

Internal dynamics of the system has been investigated, and its dimension, state variable and stability have been analysed.

Acknowledgments

I would like to express my gratitude to my supervisor, Dr. Dan S. Necsulescu for his time, insight, bright ideas, support, guidance, patience and sincere attentions.

I am indebted to my colleagues in the control lab for their contributions, help, ideas, encouragement and advice, Jean, Rahim, Victor, Bumsoo, Kazuo, Emmanuel, Anthony, Michel and Sylvain.

I also would like to thank the advisory committee members, Professor J. Sasiadek and Professor A. Fahim for their suggestions and discussions, and the academic members and staff of the department of Mechanical Engineering, Ottawa-Carleton Institute for Mechanical and Aerospace Engineering and faculty of Engineering for their help.

I am very grateful to my wife and my daughters for their patience and understanding. I am also thankful to my parents for their support and encouragement.

Above all, I thank almighty God for making possible the seemingly impossible.

Table of Contents

List of Figures

Nomenclature

A1, A2, A3, A4	convenient parameters of steering angle and orientation angle
$\mathbf{a}$, $\mathbf{a}_1$, $\mathbf{a}_2$, $\mathbf{a}_3$	acceleration vectors of the origins of given frame with respect to inertial frame, but calculated in vehicle's moving frame
a_x , a_y	acceleration of the vehicle's centre of mass in the x-y frame
a_{x1} , a_{x2} , a_{x3}	acceleration of the wheels' in their directions
a_{y1} , a_{y2} , a_{y3}	acceleration of the wheels' perpendicular to their directions
b_1 , b_2 , b_3 , b_4	path coefficients
b	length of the vehicle's wheelbase
c	distance to the vehicle's centre of mass from the rear axle
CLAMOR	acronym used for the vehicle which stands for: "Cartesian Linearized Autonomous Mobile Observable Robot"
Den(δ), Num(δ)	functions of steering angle used in the dynamic equations
d	a distance
dA	infinitesimal area
dF_f	infinitesimal friction force
dM_f	infinitesimal friction resultant moment
E(x)	decoupling matrix, in the relationship between the inputs and the outputs
F_f	friction force
F_{x2} , F_{y2} , F_{x3} , F_{y3}	internal forces in given directions between rear wheels and main body of the vehicle
F_{FSAx} , F_{FSAy}	internal forces in given directions between steering assembly and main body of the vehicle
F_{SAx} , F_{SAy}	internal forces in given directions between steering assembly and front wheel
f(x)	a vector, function of the state vector
f_i	a set of vectors, "i" represents an integer

G_i	a set of matrices, "i" represents an integer
G_{x1} , G_{x2} , G_{x3}	contact forces of the wheels in wheels' directions
G_{y1} , G_{y2} , G_{y3}	contact forces of the wheels perpendicular to wheels' directions
g_i	a set of vectors, "i" represents an integer
$\mathbf{h(x)}$	outputs vector as a function of the states vector
I , J	inertial frame unit vectors
I_{x1} , I_{x2} , I_{x3}	rotational moment of a wheel about its axis of rotation
I_{y1} , I_{y2} , I_{y3}	rotational moment of a wheel perpendicular to its axis of rotation in plane
I_{SAx} , I_{SAy}	rotational moment of steering assembly about given direction
i , j	vehicle's moving frame unit vectors
J_1 , J_2 , J_3	rotational moment of a wheel about the vertical axis
J_0	rotational moment of the main body of the vehicle
J_{SA}	rotational moment of the steering assembly
K_i	a set of matrices, "i" represents an integer
k	vertical unit vector
k_1 , k_2 , k_3	control parameters
l	distance between the vehicle's rear wheels
M	total mass of the vehicle
M_f	friction resultant moment
M_{x2} , M_{x3} , M_{z2} , M_{z3}	internal moments in given directions between rear wheels and main body of the vehicle
M_{FSAx} , M_{FSAy}	internal moments in given directions between steering assembly and main body of the vehicle
M_{SAx} , M_{SAz}	internal moments in given directions between steering assembly and front wheel
m_1 , m_2 , m_3	masses of the given wheels
m_0	mass of the main body of the vehicle
m_{SA}	mass of the steering assembly

n	normal distance from current point to a path
O , O_1 , O_2 , O_3	origins of vehicles and given wheels moving frames
Q_1 to Q_{14}	convenient constant of vehicles dimensions and dynamical parameters
p	an integer representing the order of derivatives
p_i	a set of integers representing the rank of a set of matrices
$\mathbf{R}$, $\mathbf{R}_1$, $\mathbf{R}_2$, $\mathbf{R}_3$	position vectors from inertial frame origin to moving frames origins
$\mathbf{R(x)}$	a vector, function of the state vector, representing the rest of the equation
r_1 , r_2 , r_3	radius of a given wheel
$\mathbf{S}_i$	a set of matrices, "i" represents an integer
s	arc length along a path
$\mathbf{T}$	a transformation matrix
$\mathbf{u}$	inputs vector
$\mathbf{u}_i$, u_1 , u_2	intermediate input vector and its components
$\mathbf{V}$, $\mathbf{V}_1$, $\mathbf{V}_2$, $\mathbf{V}_3$	velocity vectors of the origins of given frame with respect to inertial frame, but calculated in vehicle's moving frame
V_{dA}	velocity of the infinitesimal area
V_x , V_y , V_s , V_n	velocities of the vehicle's centre of mass in the x-y and s-n frames
V_{x1} , V_{x2} , V_{x1}	velocities of the wheels' in their directions
V_{y1} , V_{y2} , V_{y1}	velocities of the wheels' perpendicular to their directions
W_1	share of the weight taken by the front wheel
X	horizontal inertial coordinate
$\mathbf{x}$	states vector
x , x_1 , x_2 , x_3	non-inertial coordinates along the frame of the vehicle and wheels
x_t , y_t	path frame
Y	horizontal inertial coordinate, perpendicular to X
$\mathbf{y}$	outputs vector
y , y_1 , y_2 , y_3	non-inertial coordinates perpendicular to x, x_1 , x_2 and x_3, respectively
Z	vertical coordinate

z , z_1 , z_2 , z_3	vertical coordinates of given frames
α	an angle
α_1 , α_2 , α_3	angular displacements of the wheel
β	path parameter
δ	steering angle
θ	vehicle orientation as angle between vehicle heading and inertial X axis
θ_d	angle between tangent to the path and inertial X axis
ρ	radius of curvature
ρ_i	a set of integers representing the rank of a set of matrices
ρ_1 , ρ_2 , ρ_3	position vectors from vehicle's center of mass to given wheel in x-y frame
η	an integer
κ	reciprocal to radius of curvature
σ , σ_1	two constant functions
τ_s , τ_d	steering and driving torques
ψ	orientation error
ω_1 , ω_δ	angular velocities of front wheel about driving and steering directions.
ω_2 , ω_3	angular velocities of the rear wheels
ω_θ , ω_ψ	angular velocity of the vehicle's frame relative to the X axis and orientation error velocity

Generally derivatives will be shown as:

$$\dot{x} = \frac{dx}{dt}$$

$$\ddot{x} = \frac{d^2x}{dt^2}$$

$$x^{(i)} = \frac{d^{(i)}(x)}{dt^{(i)}}$$

Chapter 1

Introduction

1-1 Background

For the past few years, research interest in autonomous vehicles, i.e., mobile robots and automated guided vehicles(AGVs) has grown. There are a variety of potential and active applications of these vehicles in industrial, household, military, security, space, office automation and scientific laboratory systems, and some examples are material handling inside factories, cleaning an industrial waste site, maintaining a nuclear plant, inspecting and repairing underwater structures, assembling structures in outer space, fire fighting, bomb removing, window cleaning and aiding the disabled.

Active attempts to build and analyse mobile devices started immediately after world war II. The first AGVs were made in 1950's. But, the true ancestor of AGVs was developed in 1960's at Stanford University [1]. Also, Shakey, the first serious autonomous mobile robot was built in late 1960's at Stanford Research Institute [1]. Although the historic origins of AGVs and mobile robots are quite different, today they resemble each other in many respects, particularly in their increasing use of faster and more powerful onboard signal and data processing microprocessors for control and communication [1]. The motion of an AGV is restricted to certain predefined paths, and once the guidance mechanism is installed a new path can be achieved only by rebuilding

this mechanism. A more flexible AGV must be capable of following different paths and to be so it must be programmable for path selection. On the other hand, the interest in land vehicles has shifted to make them be able to move independently in remote, unstructured, and hazardous environments. The challenge has been to allow these systems to make independent, intelligent decisions as the situation changes and perform various actions without human intervention. As a result, more sophisticated vehicles with on and off board control devices and sensors are needed to make independent decisions and actions. Today the use of autonomous (or semi autonomous) vehicles as a support for conceptual and experimental work in advanced robotics and vehicular systems is as strong as ever.

An autonomous ground vehicle is composed of these basic groups of components:

- Mechanical assembly including the platform, driving and assembly subsystems, energy conversion and transmission and coasting and braking.

- Electronic components and interfaces, electrical components and onboard power: Electronic components and interfaces such as amplifiers, digital to analog and analog to digital convertors and specially sensors. Electrical components such as switches and relays provide trouble shooting and easier operation. Also, batteries are widely used to provide onboard power for actuators and onboard computing devices.

- Navigational systems such as guidepaths for AGVs, inertial navigation systems, laser scanning and beacons, ultrasonic and optical devices, dead reckoning and so on. Different combinations of these systems can be used to prcduce satisfactory results.

- Onboard computing facilities and controllers to handle many tasks at different levels of control.

Each of these components and their assembly and combinations need careful consideration in order that the best design and performance can be achieved.

1-2 Research Objectives

There are several problems arising when designing autonomous ground vehicles: sensor data acquisition, interpretation and integration, real world modelling, path planning and navigation, map presentation, vehicle design and modelling, machine learning and decision making for navigation, actuator control for vehicles with complicated dynamics, global monitoring and control of the vehicular system as a whole. These problems are direct or indirect consequence of having those four groups of components and solving them demands knowledge of control, electrical, computer, optical and mechanical engineering.

This research focuses on those issues which require mechanical engineering knowledge, including modelling, kinematics and dynamics, open and closed loop control, path and motion planning, path following and trajectory tracking and stabilization.

These issues are common between robot manipulators and ground vehicles, but unlike manipulators which are holonomic systems, wheeled vehicles are nonholonomic. A kinematic constraint in differential form is holonomic if it is integrable and this constraint is called nonholonomic if it is not integrable.

A conventional wheel has only two degrees of freedom, since its third DOF in a planar pair model(wheel with the ground) is omitted when the sideway component of wheel velocity is set to be zero to eliminate sideway slip. This assumption together with the assumption that the wheel roils without slip are called ideal rolling conditions. Ideal rolling conditions impose kinematic constraints on the wheel motion that are not integrable.

The primary objective of this research is to contribute to the solutions of the dynamics based motion control problems of nonholonomic ground vehicles. Dynamic modelling is more accurate, more realistic and more complex. Also,

- Dynamics based control makes it possible to control directly input force and

torque commands to the system. It also allows to take the dynamic parts of the system like suspension and wheels into consideration.

- There are some "dynamic constraints" like motor-torque limits that should be considered and in this case their saturation should be avoided. On the other hand, ideal rolling conditions could be verified by checking the wheel-ground contact forces. These can be done much more easily if dynamics based control is used.

- Nonholonomic constraints which govern the motion of autonomous(or semi-autonomous) wheeled vehicles are kinematic constraints (between velocities and general coordinates) and that is why controllability, stabilization and following(tracking) properties of kinematic and dynamic models are the same.

Using differential geometric control theory, it has been shown that nonholonomic systems are (weakly)controllable from any starting point [2]. Also, applying Brockett's theorems regarding nonholonomic systems results that these systems are not smooth state feedback asymptotically stabilizable [2,3,4].

In this research nonlinear control theory is applied to study the motion control problems of an autonmous ground vehicle. Feedback linearization, which is a systematic approach to nonlinear control systems, is used. This method works very well for minimum-phase systems which can be asymptotically stabilized by smooth state feedback controllers. Nonholonomic systems are not minimum-phase and their internal dynamics stability problem remains to be solved. This internal dynamics is examined, its state variable is found, and its stability for trajectory tracking and path following procedures(asymptotic) and for point stabilization(bounded) is investigated.

1-3 The Vehicle

The autonomous vehicle modelled and used in this research report, CLAMOR, is a three-wheeled vehicle with the front wheel steering and driving and has five mechanical parts (Figure 1-1):

- A rigid structure to which the other parts are attached,

- Two rear wheels,

- A front wheel,

- Steering assembly, attached to the front wheel, the main body and the steering and driving motors.

The vehicle is moving on a flat horizontal surface and this motion is studied under ideal rolling assumptions.

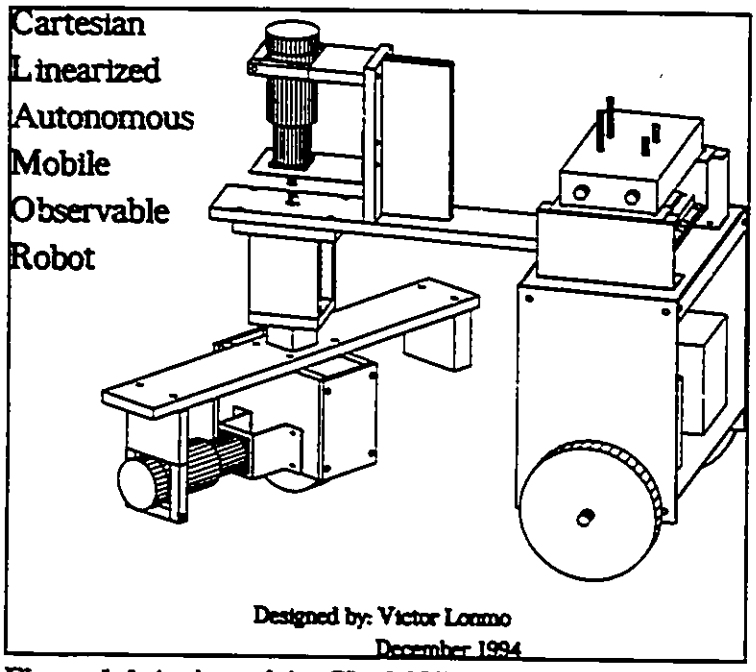

Figure 1-1 A view of the CLAMOR platform

1-4 Outline of the Thesis

This thesis is organized as follows:

Chapter 1- Related issues like a brief history, applications and the components of autonomous ground vehicles are reviewed as the background. Objectives of the

research and a brief description of the vehicle modelled and utilized in this thesis are also included in this chapter.

Chapter 2- Existing literature has been surveyed and the most recent relevant contributions to the open and closed loop control of autonomous vehicles are discussed. Different possible configurations of the vehicles and their kinematic and dynamic modelling have been reviewed.

Chapter 3- Existing kinematic and dynamic models of the described vehicle has been updated the complete set of equations has been found. This set of equations can be rearranged to obtain (almost) minimal systems of differential equations that can be used to control the vehicle.

Chapter 4- Exact input-output feedback linearizations of Cartesian and curvilinear space dynamic models have been performed. It is found that the vehicle's internal dynamics is one dimensional. Steering angle by analytical examination and by physical discussion is determined to be the only internal dynamics state. This internal dynamics as long as the vehicle keeps moving forward is found to be stable. Then, theoretically, trajectory tracking and path following procedures are asymptotically stabilizable by applying feedback linearization. By further examination of wheel-ground contact area, bounded stability of the internal dynamics for the case of point(position with orientation) stabilization of the vehicle is validated.

Chapter 5- The suggested methods as solutions to the motion control problems of the autonomous vehicle are described in this chapter. Previous chapters results are used to show how exact input-output feedback linearization in Cartesian and curvilinear spaces can be utilized to serve as these solutions.

Chapter 6- Simulation and experimental results are presented and compared. Discussion and comments follow these results.

Chapter 7- This chapter comprises of a summary and conclusions, contributions, and recommendations for future work.

Appendix A- Algebraic manipulation to reduce the number of required equations

is performed in this appendix. These equations are needed in order to find the (almost)minimal set of differential equations containing both inputs and outputs of the control systems.

Appendix B- Results of PD, time-varying and discontinuous control laws for kinematic models are obtained from the original publications. They are presented with discussion and some comments on the results.

Chapter 2

Literature Survey

A variety of branches of science and engineering are incorporated in the research of autonomous ground vehicles. The knowledge of those branches is employed to look from different angles in various aspects of mobile robots and AGVs. Consequently, an enormous number of publications are relevant to this research area.

The literature has been surveyed to provide a comprehensive background on the pertinent aspects of the research of the autonomous ground vehicles. Kinematic and dynamic modelling and motion control strategies of these vehicles are particularly reviewed.

2-1 Configurations of Wheeled Autonomous Vehicles

The most familiar wheel layout for a vehicle is a four wheel configuration in which the wheels are placed at the corners of a rectangle. Often, the two rear wheels are used for driving and the two front for differential steering. Alternative arrangements include front wheel drive, four wheel drive, and four wheel steering allowing some limited sideway motion [5,6].

One way to simplify the complications of four wheel vehicles is to replace the coupled steering wheels with one wheel and keep the rear wheels driven. Still the two rear wheels must rotate at slightly different speeds for accurate control of turning [7,8]. Another motor configuration for three wheel vehicles is to have two rear wheels independently driven and the front wheel idle caster. In order to steer this vehicle the

rear wheels should be driven at different speeds [9,10]. The vehicle modelled in this research is a tricycle with the front wheel steering and driving [11-13].

Campion et al [14] classified different possible configurations of combinations of four types of wheels: three conventional: (fixed, centred orientable and off-centred orientable) and one Swedish (or omnidirectional) wheel. Based on the number of degrees of freedom they can be classified in six groups.

The vehicles mentioned so far have two degrees of freedom. There is a kinematic relation between their orientations and speeds, a nonholononic constraint. The systems with nonholonomic constraints have some motion control problems which are hard to overcome. To avoid these problems one idea is to use omnidirectional vehicles. These vehicles have the ability to achieve decoupled dynamics(in position and orientation) for following paths and avoiding obstacles, but they are more complicated and may need suspension to avoid tipping over. Because they are in their early stages, they are not fast enough. This type of wheels will not be dealt with in this research.

2-2 Modelling, Kinematics and Dynamics

The word "modelling" refers to the use of Newtonian, Lagrangian or Hamiltonian dynamics to produce a system of differential-algebraic equations as the model of the vehicle or nonholonomic system in $\dot{x}=f(x,u)$ form, where **x** is the state vector and **u** is the input vector. Bloch and McClamroch and d'Andrêa-Novel et al have applied two different diffeomorphisms to have their models [3,15,16]. Saha and Angeles also studied kinematics and dynamics of a nonholonomic system [17]. They applied the same method as d'Andrêa-Novel et al used for their modelling which is called Orthogonal Complement method. Since the orthogonal complement of a system is not unique, they introduced a simpler one called natural orthogonal complement [18]. More

details and components of a vehicular system can be modelled and further simplified as presented in the books by Ellis and Wong [19,20].

Muir and Neuman [21] proposed simplified configurations of robot vehicles modelled under the design assumptions:

1) The wheeled mobile robot is built from rigid mechanisms,

2) There is zero or one steering link per wheel,

3) All steering axes are perpendicular to the surface of motion,

and the operational assumptions:

4) The surface is a smooth plane,

5) No translational slip occurs between the wheel and the floor,

6) The rotational friction at the point of contact is small enough for the wheel to turn freely about a vertical axis through that point.

Wheeled mobile robots are considered as multiple closed-link chains, with higher pairs of contact points between wheels and surfaces, with reduced degrees of freedom due to nonholonomic constraints. They also introduced Instantaneously Coincident coordinates as the inertial frame coinciding with the moving vehicle body frame at each instant of time to simplify their matrix equations of multibody robotic mechanisms.

Necsulescu et al [12] directly used Newton-Euler equations to model their vehicle's dynamics. In this research, intermediate and advanced multibody dynamics are applied to derive the kinematic and dynamic equations of our vehicle [22-24].

2-3 Controllability

Since nonholonomic vehicles are nonlinear systems, nonlinear control theory, in which the concept of controllability is related to the dimension of the corresponding control Lie Algebra, should be used [25-28]. Campion et al proved that both kinematic and dynamic model of nonholonomic systems satisfy the strong accessibility rank condition and stated that this property implies controllability [2,26]. Barraquand and Latombe [29] discussed accessibility, local and weak controllability and local weak controllability and showed that for the case of less than 4-trailer nonholonomic

vehicles(front wheel drive) are controllable.

2-4 Open-Loop Control: Path and Motion Planning and Steering.

There has been a great deal of work on robot motion planning. Maps and diagrams are the tools in motion planning which require the use of classical geometry, topology, algebraic geometry, algebra and computational geometry [30]. Extending those works to nonholonomic systems is not direct and easy because "a robot may be physically incapable of following a path that changes direction by a large amount at single point, partly due to the degrees of mobility of the robot and partly due to the inability of motors to achieve infinite acceleration" [31]. This made the researchers choose the strategy of considering the paths that satisfy the nonholonomic constraints. This strategy leads to what is called "nonholonomic motion planning". Some examples are the papers in the book by Canny and Li [32].

One direction in nonholonomic motion planning focuses on correcting the mentioned problem, while using the same tools, maps and diagrams. One example is Barraquand and Latombe's on mobile robots and optimal maneuvering [33]. Schwartz and Sharir [34] worked on piano mover's problem, while Tournassoud and Jehl [35] addressed the problem of turning a vehicle in a corridor. Laumond [36] showed that a two DOF mobile robot with a bounded gyration radius can follow any trajectory within the admissible configuration space at the expense of extensive maneuvers if this space is in a domain with connected interior.

Another direction in nonholonomic motion planning uses analytical approaches. This type of contribution is based on first bringing a given number of outputs, by the same number of inputs, to their desired values and then, by using different tools, bringing the rest of states to their desired numbers. Based on those tools this direction can be divided into these categories [37]:

- Differential geometric or differential algebraic techniques, by using iterated Lie brackets or recursive averaging method as in the papers by Lafferriere and Sussman

[38] and L. Gurvits [39].

- Geometric phases by using Stoke's theorem by Mukherjee and Anderson [40].

- Parametrization of the inputs by using a family of sinusoids at integrally related frequencies or gradient descent algorithm by Murray and Sastry [41] and Divelbiss and Wen [42].

These methods that were developed for the systems without drift can be extended to power and chained forms but are not yet available to the systems with general form of drift including steering [43,44]. More references can be found in [37].

A related field to geometric phase type of contributions considers various paths, classified as follows [45]:

1) Piece-wise continuous paths,

2) Continuous paths,

3) Continuous orientation paths,

4) Continuous curvature paths and

5) Continuous curvature derivative paths.

The goal is to find smooth paths which satisfy some order of optimality of the curvature of the path. Kanayama and Miyake [46] introduced clothoid pairs and proposed the connection of two postures with zero end curvatures. Nelson [47] introduced the use of polar polynomials for arc turns (to replace circle arcs) and Cartesian polynomials (to replace circular arc-arc or arc-line-arc segments for line change maneuvers). In Nelson's proposal the equations have closed forms, unlike the case in Kanayama and Miyake's. Kanayama and Hartman [48] used the squares of path curvature and path curvature derivative as two cost functions to find circular arcs and the set of cubic spirals as the answers to the path planning problem of symmetric postures (position with orientation). The idea presented in this paper is that in order to have a good dead reckoning (position sensing using odometry), the path has to be of continuous curvature. The continuity of the curvature and its derivative is achieved by using steering angle (or its derivatives) as the input to the system. Their open loop

approach does not explicitly address other parameters that may affect the dynamics of the vehicle when travelling along the path.

2-5 Path Following and Trajectory Tracking

Closed-loop control approaches for following the planned paths and motions have been mentioned under various names like: locomotion control, path control, path tracking, trajectory tracking and path following. "Locomotion control" works as a flexible interface between path planner and motor-wheel system [45]. To differentiate between current and reference postures, v and ω(heading and angular velocities) are chosen as inputs and a PID controller is used to make e_x, e_y and e_θ (errors in Cartesian positions and orientation) go toward zero. "Path control" separates the path errors (between measured and reference states) into tangential and normal while the velocity errors into two heading and speed errors and uses these four values in compensating for differences between steering angles and driving angular velocities of the reference and actual systems [11]. Hemami et al [8] used linear equations for slip angles and side forces from vehicle dynamics models and assume the steering angle as the only input to upgrade the linear proportional controller of their previous works to a nonlinear one. Later, Hemami et al [49] used a time-variant linearized version of the dynamic model of their system and applied optimal control theory to design a controller for "path tracking". Their cost function contained a quadratic function of position and orientation errors and steering angle. Kanayama et al [50] analysed the stability of their proposed controller for tracking using the Lyapunov direct method. They assumed heading and angular velocities of the vehicle as the inputs and a simple Cartesian kinematic set of equations for stable tracking. They also noticed that tracking a virtual vehicle makes the reference posture time-variable and the system by definition becomes non-autonomous, a fact that usually is ignored in the literature.

One of the most quoted papers in control of mobile robots is the paper by Graettiger and Krogh [51] in which they suggest time rescaling for travelling along the

path in order to satisfy torque constraints and other constraints for vehicles. Many contributors have focused on path following as apposed to trajectory tracking because time assignment changes can be made. Dahl and Neilson [52] using the "s", path parameter, applied this idea for on-line change of the nominal trajectory . Canudas de Wit and Roskam [53] modified the feedback law presented by Dahl and Neilson. Sørdalen and Canudas [54] extended their work on stabilization, to path following problem. They proved that if the desired path is composed of a sequence of straight lines and circle segments and there are two vectors of desired velocities and maximum deviations at connecting points between each two consecutive segments(velocities could be negative or zero), then a feedback law guaranties following that path.

Having steering angle(or its derivatives) as the main state of he control law causes some error in positioning of the system. Shin et al [55] suggested a feedforward component in the control system to compensate for that error if the steering dynamics is modelled exactly by a first order system. They also used a fifth-order equation of the path parameter "s" as the error along the path to replan the path at each control cycle. After converting the new path into steering angle, this accounted for the feedback part of their controller . They stated that considering the kinematics and assuming the point at the middle of the rear axle as the point on the path (and not the centre of mass) kinematically separates the velocity control and steering control, but they also mentioned that these two variables are dynamically coupled.

Samson [56] uses "s", "y"(normal to the path from the current point to the desired one) and θ(orientation) as the states and not the usual Cartesian coordinates. By applying Lyapunov direct method, he shows that with one input it is possible to make y and θ follow their desired values. The advantage of this approach is that it leaves the other input (heading velocity) to control the third variable "s". Most of the models presented in the above approaches were kinematic. For dynamic models, feedback linearization is one of suggested methods and the references will be quoted later.

2-6 Stabilization. Asymptotic stabilization to a manifold or a point.

One of the most challenging features of motion control of nonholonomic systems in general and vehicles with ideal rolling assumptions in particular has been asymptotic stabilization. Brockett by two theorems showed the "necessary" conditions for the existence of a continuously differentiable (smooth) feedback control law for the system of $\dot{x}=f(x,u)$ with $f(x_0,0)=0$ which makes x_0 asymptotically stable [4]. Several researchers, among them Samson and Ait-Abderrahim [57], have shown that for the systems they have studied condition (iii) of the first theorem is not satisfied. Because their linearized matrix was not square and therefore not controllable, they had to use the second theorem in that paper of Brockett for critical situations, but condition (iii) was not satisfied and thus that system was not stabilizable by smooth state feedback laws. Bloch and McClamroch [3] using their diffeomorphism of the nonholonomic systems showed that the equation $\dot{x}_3=0$ is the zero dynamics of the system which is obviously not locally asymptotically stable. This system has as many zero eigenvalues as the degree of nonholonomy is. Campion et al [2] using condition (iii) proved this global result that neither the kinematic nor the dynamic model of the systems having nonholonomic constraints can be made asymptotically stable by smooth feedback laws. This (local result versus global) is one of the differences between the diffeomorphisms these two groups of researchers have used.

Given that nonholonomic systems are not full state asymptotically stabilizable, the question is how many outputs can be made asymptotically stable. Bloch and McClamroch [3] and in [58] with Reyhanoglu using their diffeomorphism and Campion et al in [2] with their modelling showed that in the case of "n" generalized coordinates with "m" nonholonomic constraints, the control system with a smooth feedback is asymptotically stabilizable to a "n-m" dimensional manifold.

The second question is about the possibility of non smooth (discontinuous) feedback control laws. Sussmann [59] proved the existence of stabilizing piecewise continuous state feedback laws for a class of nonlinear systems. This class includes

kinematic and dynamic models of nonholonomic control systems. One discontinuous controller for mobile robots was proposed by Canudas de Wit and Sordalen [9] for a simple kinematic model subject to a feedback law with exponential rate of convergence. They introduced a family of the circles passing through origin with $\theta = 0$ at origin and the current position(and not necessarily current orientation) of the vehicle. They used two inputs, the arc length "a" for circles and, the difference between current orientation (θ_d) and the angle θ between the tangent of the circle at the current position and x-axis, α. Because the straight line between current position and the origin is always shorter than any arc length, "a" and "α" will converge to zero with an exponential rate. A different approach to constructing piecewise continuous controllers has been developed by Astolfi [60] and Aicardi et al [61]. There a nonsmooth state transformation is used and then a smooth time-invariant feedback is applied to stabilize the transformed system. In the original coordinates the resulting feedback is discontinuous. Recently sliding mode approach has been proposed [62]. The disadvantage of the sliding mode controllers is that they may cause chattering.

Another approach to the stabilization of nonholonomic systems to a single point is due to Samson and Ait-Abderrahim [57] in which they, using the idea of stability of tracking a virtual vehicle, proposed time-varying feedback laws with the exogenous variable "time". Samson [10] developed a time-varying feedback law for a simple kinematic based model in the mobile frame which makes the cart converge to zero posture. Samson in a later [56] paper uses path variables rather than Cartesian coordinates and obtains the same final result. In his next paper [63], Samson adds steering to the model and makes the system equations as a system without drift. The simulations show a low rate of convergence with a difficult dynamics to follow.

Coron [64] proves that accessibility rank condition on $R^n - \{0\}$ is sufficient to guarantee the existence of a global periodic time-varying feedback control law for driftless systems, but does not present a systematic approach. Pomet in [65] and Coron and Pomet in [66] present a rigorous result for this problem. In their experimental work,

M'Closkey and Murray [67] demonstrated that smooth time-periodic feedback laws may not steer mobile robots to a small neighbourhood of the desired configuration in a reasonable amount of time. Then non-smooth time-varying control laws were suggested. Time-varying controllers have also been proposed for chained and power forms [68,69].

2-7 Nonlinear Control Theory: Feedback Linearization.

There has been a growing interest in the applications of nonlinear control techniques. Almost every physical system is fundamentally nonlinear. A linear system approach is often taken into design of a controller based on a linear approximation of the system about a desirable operating point or a rich set of output trajectories. Under reasonable conditions, the linear controller can be used to stabilize and regulate the system about the operating point or reference trajectory. This system is valid in a very small neighbourhood of the desired point or trajectory and a time-varying compensator has to be designed. Few methods are available to design such compensators. Another approach is time scheduling, but few analytical results prove the effectiveness of this method [70]. Robust methods were developed to enlarge the region where such linear controllers can effectively control the nonlinear system.

For a nonholonomic system in general and a vehicle with ideal rolling conditions in particular, of course one of the goals is trajectory tracking or path following, but the linear approximation is valid for a small region and not a long trajectory or path. For these systems linear approximation results in a non-square matrix, and the system becomes uncontrollable [57]. The alternative approach is to use nonlinear control theory and in particular input-output feedback linearization. This method is useful for tracking and stabilization of nonlinear systems with stable internal dynamics(see Slotine [74] and Isidori [25]). Examples of applying this method to vehicles and mobile robots are given in Necsulescu et al [13] and d'Andrea et al [75]. Yun and Yamamoto [76] for dynamic model of a two rear wheels driven mobile robot used feedback linearization and showed that its internal dynamics is stable if the vehicle keeps moving forward. Deng and

Brady [77] developed a controller design for trajectory tracking of a dynamic model of a tricycle with front wheel steering and driven. Sarkar et al [78] did the same thing for path following of a vehicle with two driving wheels.

2-8 General Comments on the Literature

- While most of contributions for autonomous vehicles are for kinematic models, the way to start from the kinematic based approaches to extend them to more elaborate models is not explored. Recently more interest in dynamic models has been shown.

- It has been largely accepted that nonlinear control theory and its techniques have to be used to treat nonholonomic systems, but they have hardly been systematically used. Recent use of power and chained systems are exceptions.

- Stability of trajectory tracking for a simple kinematic case without steering using a Lyapunov function has been proven. For a more complicated dynamic (including steering) model just feedback linearization has been reported to be used [13, 75-78].

- It has been proven that nonholonomic systems are not asymptotically stabilizable using smooth state feedback laws. Two alternative approaches for stabilization of these systems have been proposed by Samson(time-varying feedback laws)[10] and by Sussmann [59], and Canudas and Sørdalen(discontinuous feedback laws using a family of circles)[9], but, both have been applied on very simple kinematic examples. Later Samson [63] added steering to his model.The problem for time-varying controllers so far is its poor dynamic behaviour. It has been experimentally shown that smooth time-periodic feedback laws may not steer vehicles to a small neighborhood of the desired position and orientation in a reasonable amount of time and nonsmooth time-varying laws have been suggested [67, 37].

- In a few research works that include steering, the complete dynamics based modelling and the internal stability have not been covered, and in most of these researches δ (the steering angle or its derivatives) and v(heading velocity or its

corresponding angular velocity) have been used as outputs. These methods cannot correct any offset in position by using feedback from δ, since δ is compared with δ_d(desired) at each time and before δ approaches δ_d, the errors in position have occurred and cannot be recovered. One way is to add a feedforward part to the controller [55].

- Lately Cartesian space and curvilinear(path variables) space methods have been distinguished as different possibilities for outputs. The corresponding method of Cartesian positions control in curvilinear variables (s, n) has not been analytically explored.

Chapter 3

Kinematic and Dynamic Equations and Dynamic Models

3-1 Kinematic Equations

3-1-1 Cartesian Space Kinematics

Wheeled vehicles correspond to multibody mechanisms and require multiple reference frames chosen in such a way as to facilitate the development of kinematic and dynamic equations as well as dynamic models [12,51]. For the case of planar motion of a three-wheel vehicle with rigid structure and wheels, one inertial and four moving reference frames are chosen (Figure 3-1). One moving frame x, y, z is attached to the vehicle main body (x-axis along the vehicle, y-axis parallel to the rear axle with the origin O at centre of mass and z-axis opposite the gravity direction). Three others x_i ,y_i ,z_i(i=1,2,3), with origins O_i , are attached to the three wheels (x_i-axes along the direction of motion of the wheels and z_i-axes parallel to z). x_1 ,y_1 ,z_1 frame can be considered with different origins on z_1-axis to be used for both front wheel and steering assembly. A global inertial frame X, Y, Z is chosen with Z parallel to z.

To determine the moving reference frames positions and orientations with regard to the inertial frame, the vectors $\mathbf{R}$, $\mathbf{R}_i$ (i=1,2,3) for absolute positions of the origins and the orientation angles θ of x, x_2, x_3 and $\theta+\delta$ of x_1 with respect to X are defined. Therefore, the transformation between the unit vectors i , j of x, y frame and I , J of the inertial frame X , Y will be (Figure 3-1):

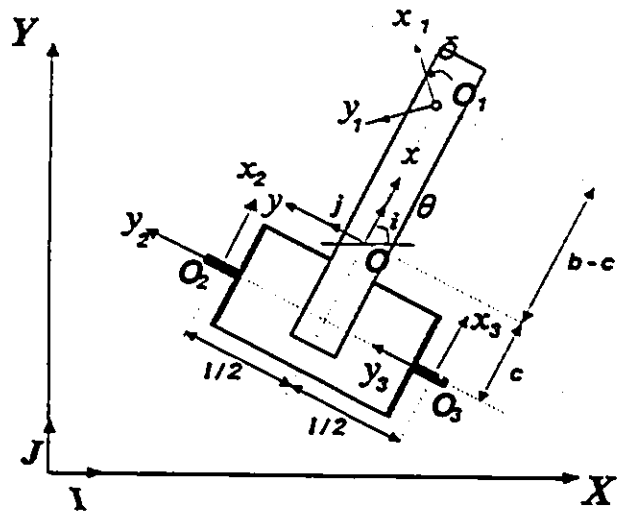

Figure 3-1 The reference frames of the vehicle.

$$\begin{bmatrix} i \\ j \end{bmatrix} = \begin{bmatrix} \cos\theta & \sin\theta \\ -\sin\theta & \cos\theta \end{bmatrix} \begin{bmatrix} I \\ J \end{bmatrix} = T \begin{bmatrix} I \\ J \end{bmatrix} \tag{3-1}$$

Also, three geometric relations:

$$R_i = R + T^T \rho_i \qquad (i = 1,2,3) \tag{3-2}$$

represent 6 scalar holonomic constraints. Here ρ_i are relative positions of the origins O_i (i=1,2,3) with respect to x-y frame origin, O (Figure 3-2):

$$\rho_1 = (b-c)i \tag{3-3}$$

$$\rho_2 = -ci + (l/2)j \tag{3-4}$$

$$\rho_3 = -c\,i - (l/2)j \qquad (3\text{-}5)$$

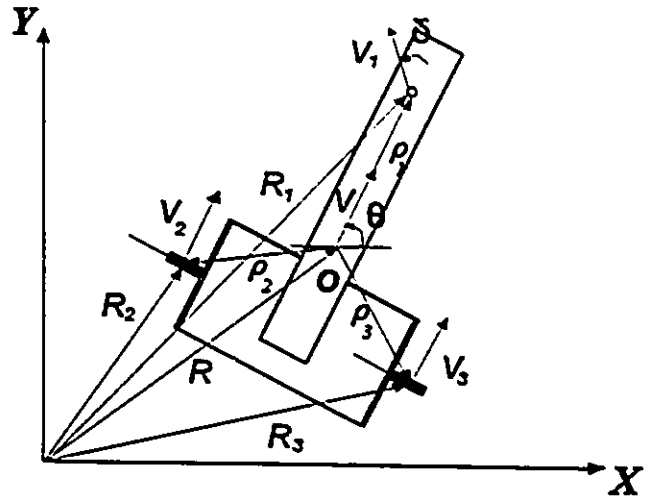

Figure 3-2 Position vectors and velocity diagram for no slip conditions.

Absolute velocities of the origins O_i expressed in X ,Y frame are obtained by differentiation, (Note $\dot{\rho}_i=0$, because of the rigid body assumption):

$$\dot{R}_i = \dot{R} + \omega \times T^T \rho_i \qquad (i = 1,2,3) \qquad (3\text{-}6)$$

where $\omega = \dot{\theta}k$ is the angular velocity of the moving frame x-y-z with respect to X,Y,Z. The absolute velocities V and V_i (i=1,2,3) expressed in x, y frame are given by:

$$V = V_x i + V_y j \qquad (3\text{-}7)$$

while in X-Y frame: $\dot{R} = \dot{X} I + \dot{Y} J$

From Equations (3-1) and (3-7), $\dot{R}$ can be written in this matrix form:

$$\begin{bmatrix} \dot{X} \\ \dot{Y} \end{bmatrix} = T^T \begin{bmatrix} V_x \\ V_y \end{bmatrix} \tag{3-8}$$

Similarly, for the velocities of the origins of x_i ,y_i ,z_i (i=1,2,3) frames:

$$V_i = V_{xi} i + V_{yi} j = V_x i + V_y j + \omega \times \rho_i \tag{3-9}$$

combining (3-3 to 3-5) and (3-9) gives:

$$V_1 = V_x i + [V_y + (b-c)\dot{\theta}] j \tag{3-10}$$

$$V_2 = [V_x - (l/2)\dot{\theta}] i + (V_y - c\dot{\theta}) j \tag{3-11}$$

$$V_3 = [V_x + (l/2)\dot{\theta}] i + (V_y - c\dot{\theta}) j \tag{3-12}$$

Absolute accelerations of the origins O_i of x_i , y_i frames (i=1,2,3) expressed in X, Y frame are obtained by differentiation, again. (Note ρ_i=0 , because of the rigid body assumption):

$$\ddot{R}_i = \ddot{R} + \dot{\omega} \times T^T \rho_i + \omega \times (\omega \times T^T \rho_i) \qquad (i=1,2,3) \tag{3-13}$$

where $\dot{\omega} = \ddot{\theta} k$ is the angular acceleration along z axis of moving frame x, y with respect to X, Y. The absolute accelerations a and a_i (i=1,2,3) expressed in x, y frame

are:

$$a = a_x i + a_y j \tag{3-14}$$

and with repect to X-Y frame: $\bar{R} = \bar{X} I + \bar{Y} J$

or, together with Equation (3-1) in this matrix form:

$$\begin{bmatrix} \bar{X} \\ \bar{Y} \end{bmatrix} = T^T \begin{bmatrix} a_x \\ a_y \end{bmatrix} \tag{3-15}$$

Also, for the accelerations of the origins of x_i ,y_i ,z_i (i=1,2,3) frames:

$$a_i = a_{xi} i + a_{yi} j = a_x i + a_y j + \dot{\omega} \times \rho_i + \omega \times (\omega \times \rho_i) \tag{3-16}$$

combining Equations (3-1 to 3-5) and (3-16) gives:

$$a_1 = [a_x - (b-c)\dot{\theta}^2] i + [a_y + (b-c)\ddot{\theta}] j \tag{3-17}$$

$$a_2 = [a_x + c\dot{\theta}^2 - (l/2)\ddot{\theta}] i + [a_y - c\ddot{\theta} - (l/2)\dot{\theta}^2] j \tag{3-18}$$

$$a_3 = [a_x + c\dot{\theta}^2 + (l/2)\ddot{\theta}] i + [a_y - c\ddot{\theta} + (l/2)\dot{\theta}^2] j \tag{3-19}$$

Also, from Figure (3-1), differentiating of angular velocities of the wheels for front

wheel will give:

$$\begin{aligned}\dot{\omega}_1 &= \dot{\omega}_1 i_1 + \omega_1 \dot{i}_1 \\ &= \dot{\omega}_1 i_1 + (\dot{\theta}+\dot{\delta}) k \times \omega_1 i_1 \\ &= \dot{\omega}_1 i_1 + (\dot{\theta}+\dot{\delta}) \omega_1 j_1\end{aligned} \tag{3-20}$$

and for rear wheels (i=2,3):

$$\begin{aligned}\dot{\omega}_i &= \dot{\omega}_i i + \omega_i \dot{i} \\ &= \dot{\omega}_i i + \dot{\theta} k \times \omega_i i \\ &= \dot{\omega}_1 i + \dot{\theta} \omega_i j\end{aligned} \tag{3-21}$$

The constraints for velocities, Equations (3-10 to 12), and for accelerations, Equations (3-17 to 19), were obtained from the holonomic constraint, Equation (3-2). The assumptions with repect to the contact between the wheels and the ground impose further constraints. The wheel angular speeds $\omega_i = \dot{\alpha}_i$ (i=1,2,3) about their axes y_i and the absolute velocities $\mathbf{V}_i$ of the origins O_i expressed in x, y frame are linked by the following differential constraints (ideal rolling assumptions, Figure 3-2),

$$V_1 = \begin{bmatrix} V_{x1} \\ V_{y1} \end{bmatrix} = \begin{bmatrix} r_{w1}\omega_1 \cos\delta \\ r_{w1}\omega_1 \sin\delta \end{bmatrix} \tag{3-22}$$

$$V_2 = \begin{bmatrix} V_{x2} \\ V_{y2} \end{bmatrix} = \begin{bmatrix} r_{w2}\omega_2 \\ 0 \end{bmatrix} \tag{3-23}$$

$$V_3 = \begin{bmatrix} V_{x3} \\ V_{y3} \end{bmatrix} = \begin{bmatrix} r_{w3}\,\omega_3 \\ 0 \end{bmatrix} \tag{3-24}$$

where r_{wi} (i=1,2,3) are the radii of the wheels and δ is the front wheel steering angle. The six differential scalar constraints given by Equations (3-22 to 24) will be reduced to five independent constraints if it is taken into account that Equations (3-11 and 3-12) give:

$$V_{y2} = V_{y3} \tag{3-25}$$

such that $V_{y2} = 0$ in Equation (3-23) implies in this case $V_{y3} = 0$, which makes the second equation of (3-24) redundant. Equation (3-22) contains the nonholonomic constraint:

$$\frac{V_{y1}}{V_{x1}} = \tan\delta \tag{3-26}$$

while the other differential constraints are integrable. The dynamic model contains, however, reaction forces between the wheels and the ground which are associated with these differential constraints and for this reason all differential constraints are retained. The 13 coordinates used for determining the motion of the vehicle structure (x, y, θ) and the wheels (x_1, y_1, x_2, y_2, x_3, y_3, α_1, α_2, α_3, δ) are subject to 6 scalar holonomic constraints given by Equation (3-2) and 5 independent differential constraints out of the 6 constraints given by Equations (3-22 to 24). Consequently, the vehicle has only two degrees of freedom.

By eliminating V_{xi} and V_{yi} from the differential constraints for velocities, Equations (3-22 to 24), using the derivative of the holonomic constraints (3-2) in the form given in Equations (3-10 to 12), the following 5 independent scalar differential constraints will result:

$$V_x = r_{w1}\omega_1 \cos\delta \tag{3-27}$$

$$V_y + (b-c)\dot{\theta} = r_{w1}\omega_1 \sin\delta \tag{3-28}$$

$$V_x - (l/2)\dot{\theta} = r_{w2}\omega_2 \tag{3-29}$$

$$V_y - c\dot{\theta} = 0 \tag{3-30}$$

$$V_x - (l/2)\dot{\theta} = r_{w3}\omega_3 \tag{3-31}$$

Also, from Equations (3-28) and (3-30):

$$V_y = \frac{c}{b} r_{w1}\omega_1 \sin\delta \tag{3-32}$$

Equations (3-1), (3-8), (3-27) and (3-32) give:

$$\dot{X} = V_x\cos\theta - V_y\sin\theta = r_{w1}\omega_1(\cos\delta\cos\theta - \frac{c}{b}\sin\delta\sin\theta) \tag{3-33}$$

$$\dot{Y} = V_x\sin\theta + V_y\cos\theta = r_{w1}\omega_1(\cos\delta\sin\theta + \frac{c}{b}\sin\delta\cos\theta) \tag{3-34}$$

The nonholonomic constraint in terms of V_x , V_y and δ results from Equations (3-27) and (3-32):

$$\tan\delta = \frac{bV_y}{cV_x} \tag{3-35}$$

The constraints for accelerations can be obtained by taking derivatives of V_i (i=1,2,3), Equation (3-9):

$$\begin{aligned} V_i &= V_{xi}\,i + V_{yi}\,j \\ a_i &= \dot{V}_i = \dot{V}_{xi}\,i + \dot{V}_{yi}\,j + V_{xi}\,\dot{i} + V_{yi}\,\dot{j} \end{aligned} \tag{3-36}$$

But, for pure rotation of unit vectors i and j, Equation (3-21), the following derivatives can be taken:

$$\begin{aligned} \dot{i} &= \dot{\theta}k \times i = \dot{\theta}j \\ \dot{j} &= \dot{\theta}k \times j = -\dot{\theta}i \end{aligned} \tag{3-37}$$

Equations (3-36) and (3-37) give:

$$a_i = \begin{bmatrix} a_{xi} \\ a_{yi} \end{bmatrix} = \begin{bmatrix} \dot{V}_{xi} - \dot{\theta}V_{yi} \\ \dot{V}_{yi} + \dot{\theta}V_{xi} \end{bmatrix} \tag{3-38}$$

Equations (3-22 to 24) and (3-39) can be used to obtain:

$$a_1 = \begin{bmatrix} a_{x1} \\ a_{y1} \end{bmatrix} = \begin{bmatrix} r_{w1}\dot{\omega}_1\cos\delta - r_{w1}\omega_1\dot{\delta}\sin\delta - r_{w1}\omega_1\dot{\theta}\sin\delta \\ r_{w1}\dot{\omega}_1\sin\delta + r_{w1}\omega_1\dot{\delta}\cos\delta + r_{w1}\omega_1\dot{\theta}\cos\delta \end{bmatrix} \tag{3-39}$$

$$a_2 = \begin{bmatrix} a_{x2} \\ a_{y2} \end{bmatrix} = \begin{bmatrix} r_{w2}\dot{\omega}_2 \\ r_{w2}\dot{\theta}\omega_2 \end{bmatrix} \tag{3-40}$$

$$a_3 = \begin{bmatrix} a_{x3} \\ a_{y3} \end{bmatrix} = \begin{bmatrix} r_{w3}\dot{\omega}_3 \\ r_{w3}\dot{\theta}\omega_3 \end{bmatrix} \tag{3-41}$$

Eliminating a_{xi} and a_{yi} from the constraints for accelerations, Equations (3-39 to 41) using Equations (3-17 to 19) will result in the following 6 differential constraints in scalar form:

$$r_{w1}\dot{\omega}_1\cos\delta - r_{w1}\omega_1(\dot{\delta}+\dot{\theta})\sin\delta = a_x - (b-c)\dot{\theta}^2 \tag{3-42}$$

$$r_{w1}\dot{\omega}_1\sin\delta + r_{w1}\omega_1(\dot{\delta}+\dot{\theta})\cos\delta = a_y + (b-c)\dot{\theta} \tag{3-43}$$

$$r_{w2}\dot{\omega}_2 = a_x + c\dot{\theta}^2 - (l/2)\dot{\theta} \tag{3-44}$$

$$r_{w2}\dot{\theta}\omega_2 = a_y - c\dot{\theta} - (l/2)\dot{\theta}^2 \tag{3-45}$$

$$r_{w3}\dot{\omega}_3 = a_x + c\dot{\theta}^2 + (l/2)\dot{\theta} \tag{3-46}$$

$$r_{w3}\dot{\theta}\omega_3 = a_y - c\dot{\theta} + (l/2)\dot{\theta}^2 \tag{3-47}$$

Only five independent constraints result out of the six given by Equations (3-42 to 47). Eliminating $a_y - c\dot{\theta}$ between Equations (3-45) and (3-47), taking the derivative of the resulting equation and using Equation (3-44) will give Equation (3-46).

3-1-2 Curvilinear Space Kinematics

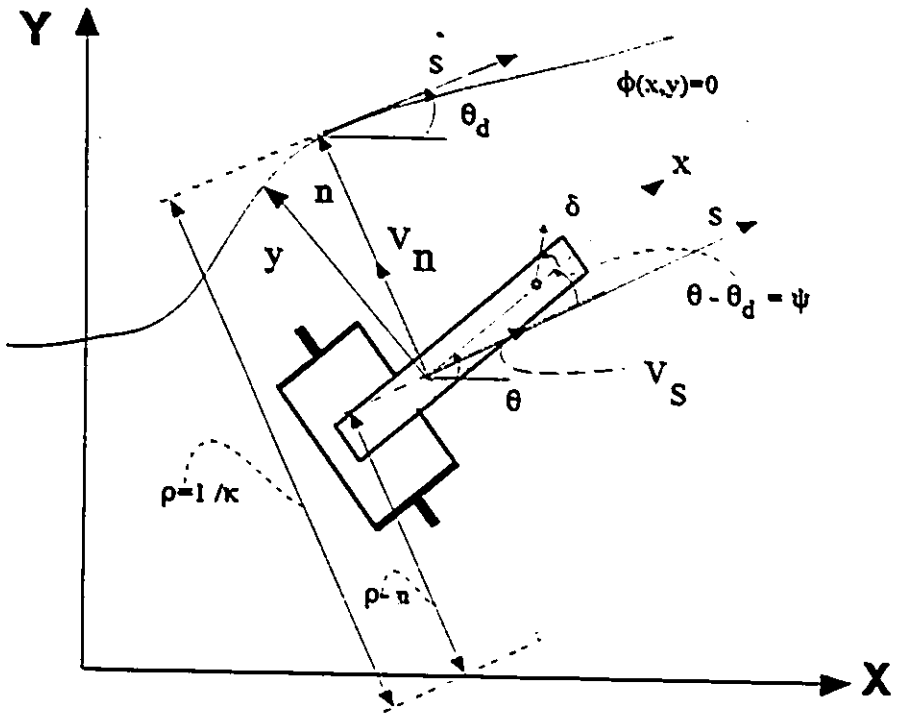

Figure 3-3 Curvilinear space variables s, n and ψ.

Following [56], it can be assumed that $\phi(x, y)=0$ is a smooth planar curve along which the vehicle is supposed to move. ϕ is either open and infinite or closed on itself and its curvature has successive derivatives uniformly bounded along ϕ. The radius of any circle (containing ϕ at two or more points) whose interior does not contain any point of the curve, is bounded from below by some positive number r_{min}. In this case, introducing s, (the arc length along ϕ) and n, (the distance from the vehicle to the curve,

along the normal at each point, passing through the centre of curvature), will constitute a Frenet frame, the curvilinear coordinate system of s and n. The angle θ_d is between s and X and the difference between θ and θ_d is denoted by ψ. The radius of curvature at each point is denoted by ρ and its reciprocal by κ [76].

The velocity of the vehicle has the components V_x , V_y in the x, y frame and V_s , V_n in the s-n frame. They are related by rotational transformations (Figure 3-3):

the tangential component along ϕ: $$V_s = V_x\cos\psi - V_y\sin\psi \tag{3-48}$$

and normal to ϕ : $$V_n = V_x\sin\psi + V_y\cos\psi \tag{3-49}$$

Also, the proportion $\frac{\dot{s}}{V_s}=\frac{\rho}{\rho-n}$ from Figure (3-3) gives:

$$\dot{s} = \frac{\rho}{\rho-n} V_s = \frac{1}{(1-n\kappa)}V_s \tag{3-50}$$

Equations (3-48 to 50) will result in:

$$\begin{aligned}\dot{s} &= \frac{V_x\cos\psi - V_y\sin\psi}{(1-n\kappa)} \\ &= \frac{r_{wl}\omega_1(\cos\delta\cos\psi - \frac{c}{b}\sin\delta\sin\psi)}{(1-n\kappa)}\end{aligned} \tag{3-51}$$

$$\dot{n} = r_{wl}\omega_1(\cos\delta\sin\psi + \frac{c}{b}\sin\delta\cos\psi) \tag{3-52}$$

From kinematic textbooks [22-24] and Equation (3-51):

$$\dot{\theta}_d = \frac{\dot{s}}{\rho} = \dot{s}\,\kappa$$

$$= \frac{r_{wl}\omega_1(\cos\delta\cos\psi - \frac{c}{b}\sin\delta\sin\psi)\kappa}{(1-n\kappa)} \qquad (3\text{-}53)$$

Curvilinear space kinematics will be utilized in section 3-3-2.

3-2 Dynamic Equations

A Newtonian dynamic model of the vehicle is derived using free body diagrams for the rigid structure of a vehicle (Figure 3-4), for each of the 3 wheels (Figure 3-5) and for steering assembly (Figures 3-6 and 3-7) [12]. For the rigid structure, three equations can be written for the planar translation and the rotation about axis Z. For each wheel, five equations of motion can be obtained for the planar translation (x_i , y_i) and for the rotation about the x_i , y_i and z_i axes. Also for steering assembly, these five equations can be written in x_1 ,y_1 ,z_1 frame. The 23 Newton-Euler equations of motion using absolute accelerations expressed in the x-y frame are the following :

a) for the rigid structure of the vehicle (Figure 3-4)

$$m_0\, a_x = F_{x2} + F_{x3} + F_{FSAx}\cos\delta - F_{FSAy}\sin\delta \qquad (3\text{-}54)$$

$$m_0\, a_y = F_{y2} + F_{y3} + F_{FSAx}\sin\delta + F_{FSAy}\cos\delta \qquad (3\text{-}55)$$

$$J_0\ddot{\theta} = (l/2)(-F_{x2}+F_{x3}) + (b-c)(F_{FSAx}\sin\delta + F_{FSAy}\cos\delta) - c(F_{y2}+F_{y3}) - \tau_s - M_{z2} - M_{z3} \qquad (3\text{-}56)$$

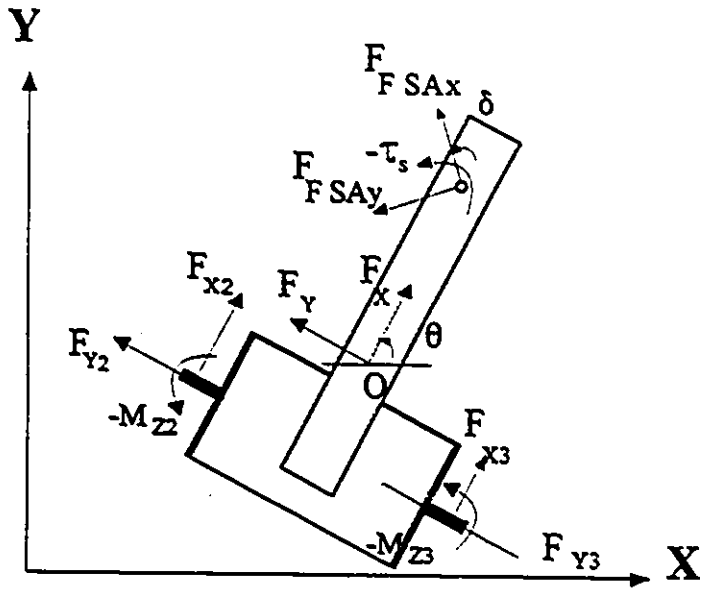

Figure 3-4 Free body diagram of the rigid structure of the vehicle.

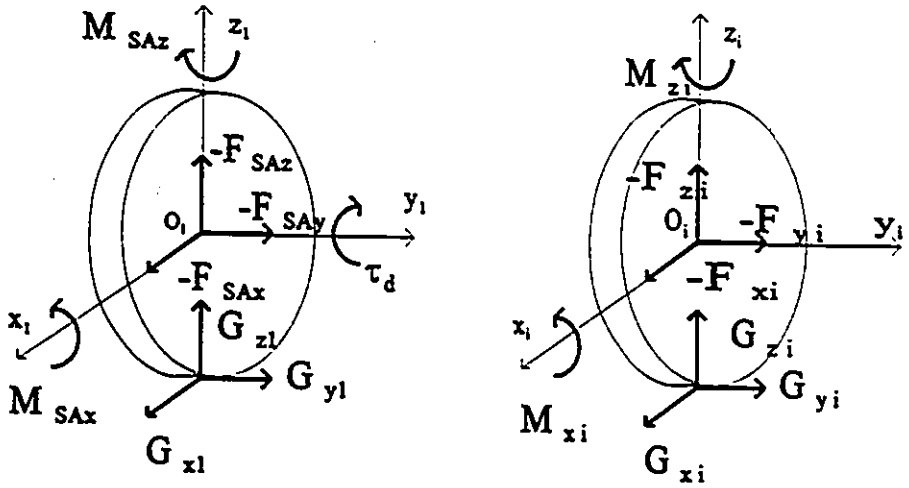

(a) (b)

Figure 3-5 Free body diagrams for front wheel (a) and rear wheels i=2,3 (b).

b) for the front wheel (Figure 3-5a)

$$m_1 a_{x1} = (G_{x1} - F_{SAx})\cos\delta - (G_{y1} - F_{SAy})\sin\delta \quad (3\text{-}57)$$

$$m_1 a_{y1} = (G_{x1} - F_{SAx})\sin\delta + (G_{y1} - F_{SAy})\cos\delta \quad (3\text{-}58)$$

$$-I_{x1}\ \omega_1(\dot{\theta}+\dot{\delta}) = G_{y1} r_{w1} + M_{SAx} \quad (3\text{-}59)$$

$$I_{y1}\dot{\omega}_1 = \tau_d - G_{x1} r_{w1} \quad (3\text{-}60)$$

$$J_1\ (\dot{\theta}+\dot{\delta}) = M_{SAz} \quad (3\text{-}61)$$

c) for the rear wheels (Figure 3-5b)

$$m_2 a_{x2} = G_{x2} - F_{x2} \quad (3\text{-}62)$$

$$m_2 a_{y2} = G_{y2} - F_{y2} \quad (3\text{-}63)$$

$$-I_{x2}\ (\omega_2\ \dot{\theta}) = G_{y2} r_{w2} + M_{x2} \quad (3\text{-}64)$$

$$I_{y2}\dot{\omega}_2 = -G_{x2} r_{w2} \quad (3\text{-}65)$$

$$J_2\ddot{\theta} = M_{z2} \tag{3-66}$$

$$m_3 a_{x3} = G_{x3} - F_{x3} \tag{3-67}$$

$$m_3 a_{y3} = G_{y3} - F_{y3} \tag{3-68}$$

$$-I_{x3}(\omega_3 \dot{\theta}) = G_{y3} r_{w3} + M_{x3} \tag{3-69}$$

$$I_{y3}\dot{\omega}_3 = -G_{x3} r_{w3} \tag{3-70}$$

$$J_3\ddot{\theta} = M_{z3} \tag{3-71}$$

d) for the steering assembly (Figures 3-6 and 3-7)

$$m_{SA} a_{x1} = (F_{SAx} - F_{FSAx})\cos\delta - (F_{SAy} - F_{FSAy})\sin\delta \tag{3-72}$$

$$m_{SA} a_{y1} = (F_{SAx} - F_{FSAx})\sin\delta + (F_{SAy} - F_{FSAy})\cos\delta \tag{3-73}$$

$$I_{SAz}(\ddot{\theta} + \ddot{\delta})\omega_1 = s_b F_{FSAy} + s_a F_{SAy} + M_{FSAx} - M_{SAz} \tag{3-74}$$

$$I_{SAy}\dot{\omega}_1 = -s_b F_{FSAx} - s_a F_{SAx} + M_{FSAy} - \tau_d \qquad (3\text{-}75)$$

$$J_{SA}(\ddot{\theta}+\ddot{\delta}) = \tau_s - M_{SAz} \qquad (3\text{-}76)$$

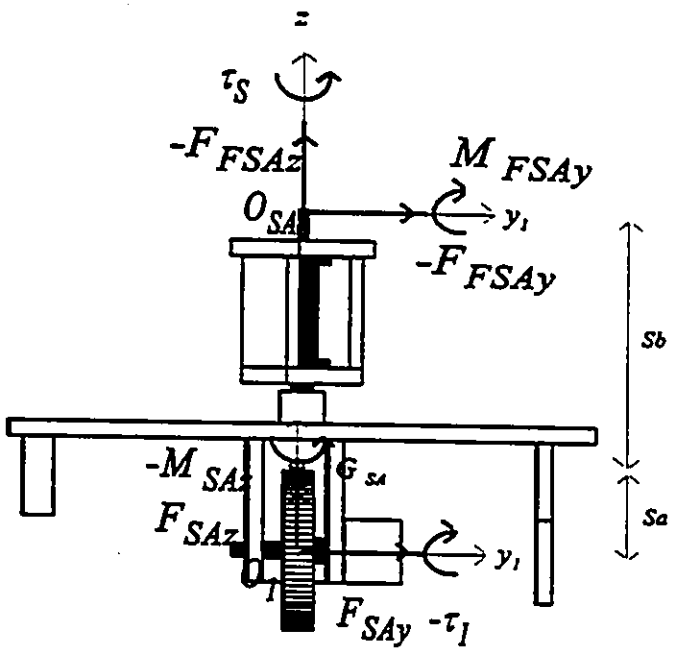

Figure 3-6 Steering assembly front view.

where

m, J_0 are the mass and the moment of inertia, about an axis parall to Z, for the rigid structure of the vehicle,

m_i, I_{xi}, I_{yi}, J_i (i=1,2,3) are the mass and the moment of inertia about x_i, y_i and z_i, respectively, for each wheel,

m_{SA},I_{SAx},I_{SAy},J_{SA} are the mass and the moment of inertia about x_1 , y_1 and z_1 , respectively, for steering assembly,

s_a ,s_b are the distance from steering assembly centre of mass to centre of the front wheel and to the rigid structure, respectively.

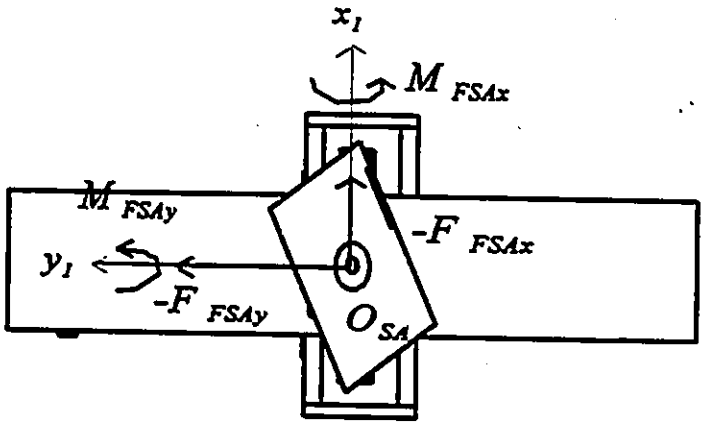

Figure 3-7 Steering assembly top view.

3-3 Dynamic Models

3-3-1 Cartesian Space Dynamic Model

Dynamic models for model based controllers require minimum size dynamic models for real time computations. So far, kinematic variables x, y, x_i, y_i, α_i (actually in differential form $\omega_i=\dot{\alpha}_i$ (i=1,2,3)), θ and δ have been used, and it has been shown that V_x, V_y, V_{xi}, V_{yi}, a_{xi}, a_{yi} (i=1,2,3) can be written using those variables (Equations 3-22 to 25, 3-32 and 3-39 to 41). Equations (3-28 and 3-30) give:

$$\dot{\theta}=\frac{1}{b}r_{w1}\omega_1\sin\delta \qquad (3\text{-}77)$$

This equation with (3-29) and (3-31) show that ω_2 and ω_3 also can be eliminated leaving just x ,y, θ, δ and ω_1. Since X and Y are projections of the absolute position in X, Y frame, they will be used instead of the projections x and y in x, y frame.

In the dynamic equations F_{xi}, F_{yi}, M_{xi}, M_{zi} (i=2,3), G_{xi}, G_{yi} (i=1,2,3), F_{SAx}, F_{SAy}, M_{SAx}, M_{SAz}, F_{FSAx}, F_{FSAy}, M_{FSAx}, M_{FSAy}, τ_s and τ_d have been introduced. τ_s (steering torque) and τ_d (driving torque) are actuator torques and in a dynamic model have to be chosen as the inputs. G_{xi}, G_{yi} (i=1,2,3) are wheel-ground (contact) forces and the rest are internal forces and moments.

Reaction forces between bodies and wheel-ground unilateral friction (contact) forces can be eliminated from the dynamic model. In a reduced form of the dynamic model, x, y (or X, Y), θ, δ, ω_1 and/or their derivatives as the state variables and τ_s and τ_d as the inputs should be present. The elimination of the reaction and contact forces and moments is presented in the Appendix A. The differential equations containing the state variables and the inputs are Equations (3-33, 34, 77) and (A-71, 78, 79):

$$\dot{X} = V_x\cos\theta - V_y\sin\theta = r_{w1}\omega_1(\cos\delta\cos\theta - \frac{c}{b}\sin\delta\sin\theta) \qquad (3\text{-}33)$$

$$\dot{Y} = V_x\sin\theta + V_y\cos\theta = r_{w1}\omega_1(\cos\delta\sin\theta + \frac{c}{b}\sin\delta\cos\theta) \qquad (3\text{-}34)$$

$$\dot{\theta}=\frac{1}{b}r_{w1}\omega_1 si \qquad (3\text{-}77)$$

$$\dot{\omega}_1 = \frac{\tau_d - Num(\delta) r_{wl}^2 \omega_1 \omega_\delta - \frac{r_{wl}\sin\delta}{b}\tau_s}{Den(\delta)} \tag{A-71}$$

$$\dot{\delta} = \omega_\delta \tag{A-78}$$

$$\dot{\omega}_\delta = \tau_s\left[\frac{1}{J_{SA}+J_1} + \frac{r_{wl}^2\sin^2\delta}{b^2 Den(\delta)}\right] - \left(\frac{r_{wl}}{b}\sin\delta\right)\left[\frac{\tau_d}{Den(\delta)}\right] + \frac{r_{wl}}{b}\omega_1\omega_\delta\left[\frac{Num(\delta)}{Den(\delta)} r_{wl}^2 \sin\delta - \cos\delta\right] \tag{A-79}$$

3-3-2 Curvilinear Space Dynamic Model

In order to have the minimum size curvilinear space dynamic model, similar discussion to the one for Cartesian space minimum size dynamic model will lead to this conclusion that the same variables have to be taken with this difference that Cartesian space coordinates (X, Y, θ) are to be replaced with their corresponding curvilinear space variables (s, n, ψ) (Figure 3-3). The differential equation containing ψ will be resulted by subtracting (3-53) from (3-77):

$$\psi = \dot{\theta} - \dot{\theta}_d = \frac{1}{b} r_{wl}\omega_1 \sin\delta - \frac{[r_{wl}\omega_1(\cos\delta\cos\psi - \frac{c}{b}\sin\delta\sin\psi)]\kappa}{(1-n\kappa)} \tag{3-78}$$

Also, similar to ω_θ:

$$\omega_\psi = \dot{\psi} = \dot{\theta} - \dot{\theta}_d \tag{3-79}$$

Rewriting Equations (3-51 and 52) and (A-71, 78, 79) together with (3-78), the minimum size curvilinear space dynamic model of the vehicle will be:

$$\dot{s} = \frac{r_{wl}\omega_1(\cos\delta\cos\psi - \frac{c}{b}\sin\delta\sin\psi)}{(1-n\kappa)} \tag{3-51}$$

$$\dot{n} = r_{wl}\omega_1(\cos\delta\sin\psi + \frac{c}{b}\sin\delta\cos\psi) \tag{3-52}$$

$$\omega_\psi = \frac{1}{b}r_{wl}\omega_1\sin\delta - \frac{[r_{wl}\omega_1(\cos\delta\cos\psi - \frac{c}{b}\sin\delta\sin\psi)]\kappa}{(1-n\kappa)} \tag{3-80}$$

$$\dot{\omega}_1 = \frac{\tau_d - Num(\delta)r_{wl}^2\omega_1\omega_\delta - \frac{r_{wl}\sin\delta}{b}\tau_s}{Den(\delta)} \tag{A-71}$$

$$\dot{\delta} = \omega_\delta \tag{A-78}$$

$$\dot{\omega}_\delta = \tau_s\left[\frac{1}{J_{SM}+J_1}+\frac{r_{wl}^2\sin^2\delta}{b^2 Den(\delta)}\right]-\left(\frac{r_{wl}}{b}\sin\delta\right)\left[\frac{\tau_d}{Den(\delta)}\right]$$

$$+\frac{r_{wl}}{b}\omega_1\omega_\delta\left[\frac{Num(\delta)}{Den(\delta)}r_{wl}^2\sin\delta-\cos\delta\right] \qquad \text{(A-79)}$$

Chapter 4

Feedback Linearization and Internal Dynamics

4-1 Feedback Linearization

Feedback linearization is an approach to nonlinear control design. The central idea of the approach is to algebraically transform a nonlinear system dynamic into a (fully or partially) linear one, so that linear control techniques can be applied [71]. In input-output feedback linearization the basis is to find a direct and simple relation between the system outputs and the control inputs [71]. To generate this direct relationship, the derivatives of the outputs should be taken until the inputs all appear in the equations. In this case:

$$y^p = E(x)\,u + R(x)$$

where y is the outputs vector, p is an integer representing the order of derivatives, E(x) is the matrix of the relationship between the outputs and the inputs, x is the states variables vector , u is the inputs vector and R(x) represents the rest of the equation which is a function of the state variables. E(x) is called decoupling matrix. If the determinant of the decoupling matrix is zero, differentiation should continue. When this matrix becomes non-singular, then;

$$u = E^{-1}(x)\,y^p - E^{-1}(x)\,R(x)$$

A linear control law in terms of y and its derivatives which satisfies the stability conditions will guarantee the stability of the external dynamics of the control system. The internal dynamics of the system should ne analysed separately [25,71].

4-1-1 Cartesian Space Feedback Linearization

Given that the vehicle has two degrees of freedom and two inputs (τ_s , τ_d) are applied to the system, only two out of the six states (X, Y, θ, δ, ω_h, ω_1) can be controlled [25]. If for Cartesian space feedback linearization the coordinates X and Y are chosen as the outputs, the first derivatives are Equations (3-33 and 34) [13]:

$$\begin{aligned} \dot{X} &= r_{w1}\omega_1(\cos\delta\cos\theta - \frac{c}{b}\sin\delta\sin\theta) \\ \dot{Y} &= r_{w1}\omega_1(\cos\delta\sin\theta + \frac{c}{b}\sin\delta\cos\theta) \end{aligned} \tag{4-1}$$

No inputs are present and obviously E(x) = . Taking another derivative and using (A-71):

$$\begin{aligned} \ddot{X} &= r_{w1}[A_1 \frac{\tau_d - Num(\delta) r_{w1}^2 \omega_1 \omega_\delta - \frac{r_{w1}\sin\delta}{b}\tau_s}{Den(\delta)} - \omega_1(A_2\omega_\theta + A_3\omega_\delta)] \\ \ddot{Y} &= r_{w1}[A_2 \frac{\tau_d - Num(\delta) r_{w1}^2 \omega_1 \omega_\delta - \frac{r_{w1}\sin\delta}{b}\tau_s}{Den(\delta)} + \omega_1(A_1\omega_\theta - A_4\omega_\delta)] \end{aligned} \tag{4-2}$$

where;

$$\begin{aligned} A_1 &= \cos\delta\cos\theta - \frac{c}{b}\sin\delta\sin\theta \;;\; A_2 = \cos\delta\sin\theta + \frac{c}{b}\sin\delta\cos\theta \\ A_3 &= \sin\delta\cos\theta + \frac{c}{b}\cos\delta\sin\theta \;;\; A_4 = \sin\delta\sin\theta - \frac{c}{b}\cos\delta\cos\theta \end{aligned} \tag{4-3}$$

and;

$$Num(\delta) = \frac{l}{2b}Q_7(\sin^2\delta - \cos^2\delta) + Q_{12}\sin\delta\cos\delta \tag{A-72}$$

$$Den(\delta) = I_{yl} + [Q_6\cos^2\delta + \frac{c}{b^2}Q_8\sin^2\delta - \frac{l}{b}Q_7\sin\delta\cos\delta]r_{wl}^2 \qquad \text{(A-73)}$$

τ_s and τ_d, both appear, but it can be easily shown that, det E(x) = 0. Before taking one more derivative, this intermediate inputs should be introduced:

$$u_1 = [u_{l1}\ ,\ u_{l2}]^T = [\tau_d - \frac{r_{wl}\sin\delta}{b}\tau_s\ ,\ \tau_s]^T \qquad \text{(4-4)}$$

Then;

$$\begin{aligned} X^{(3)} = {} & r_{wl}A_1[\frac{\dot{u}_{l1} - r_{wl}^2\omega_\delta(\dot{Num}\ (\delta)\omega_1 + Num\ (\delta)\dot{\omega}_1) - \dot{Den}\ (\delta)\dot{\omega}_1}{Den\ (\delta)}] \\ & - r_{wl}\omega_1(A_3 + \frac{Num\ (\delta)A_1}{Den\ (\delta)})[\frac{u_{l2}}{J_{SA}+J_1} - \frac{r_{wl}}{b}(\dot{\omega}_1\sin\delta + \omega_1\omega_\delta\cos\delta)] \\ & - r_{wl}[2(A_2\omega_\theta + A_3\omega_\delta)\dot{\omega}_1 + (A_1\omega_\theta - A_4\omega_\delta)\omega_1\omega_\theta - (A_4\omega_\theta - A_1\omega_\delta)\omega_1\omega_\delta + A_2 \end{aligned} \qquad \text{(4-5)}$$

$$\begin{aligned} Y^{(3)} = {} & r_{wl}A_2[\frac{\dot{u}_{l1} - r_{wl}^2\omega_\delta(\dot{Num}\ (\delta)\omega_1 + Num\ (\delta)\dot{\omega}_1) - \dot{Den}\ (\delta)\dot{\omega}_1}{Den\ (\delta)}] \\ & - r_{wl}\omega_1(A_4 + \frac{Num\ (\delta)A_2}{Den\ (\delta)})[\frac{u_{l2}}{J_{SA}+J_1} - \frac{r_{wl}}{b}(\dot{\omega}_1\sin\delta + \omega_1\omega_\delta\cos\delta)] \\ & + r_{wl}[2(A_1\omega_\theta - A_4\omega_\delta)\dot{\omega}_1 - (A_2\omega_\theta + A_3\omega_\delta)\omega_1\omega_\theta - (A_3\omega_\theta + A_2\omega_\delta)\omega_1\omega_\delta + A_1\dot{\omega}_\theta \end{aligned} \qquad \text{(4-6)}$$

The following are used in Equations (4-5) and (4-6):

$$\begin{aligned}\dot{A}_1 &= -(\cos\delta\sin\theta+\frac{c}{b}\sin\delta\cos\theta)\omega_\theta \\ &\quad -(\sin\delta\cos\theta+\frac{c}{b}\cos\delta\sin\theta)\omega_\delta \\ &= -A_2\omega_\theta - A_3\omega_\delta\end{aligned} \tag{4-7}$$

and;

$$\begin{aligned}\dot{A}_2 &= A_1\omega_\theta - A_4\omega_\delta \\ \dot{A}_3 &= -A_4\omega_\theta + A_1\omega_\delta \\ \dot{A}_4 &= A_3\omega_\theta + A_2\omega_\delta\end{aligned} \tag{4-8}$$

To see if, det E(x) = 0 or not, (Equations 4-5 and 4-6):

$$\begin{bmatrix}\dot{X}^{(3)} \\ \dot{Y}^{(3)}\end{bmatrix} = E(x)\dot{u}_t + R(x) = \begin{bmatrix}\dfrac{r_{wl}A_1}{Den(\delta)} & -r_{wl}[A_3+A_1\dfrac{Num(\delta)}{Den(\delta)}]\omega_1 \\ \dfrac{r_{wl}A_2}{Den(\delta)} & -r_{wl}[A_4+A_1\dfrac{Num(\delta)}{Den(\delta)}]\omega_1\end{bmatrix}\begin{bmatrix}\dot{u}_{t1} \\ u_{t2}\end{bmatrix} + R(x) \tag{4-9}$$

such that:

$$\det E(x) = \frac{r_{wl}^2(-A_1A_4+A_2A_3)\omega_1}{Den(\delta)} \tag{4-10}$$

with:

$$
\begin{aligned}
A_2A_3 - A_1A_4 &= (\cos\delta\sin\theta + \frac{c}{b}\sin\delta\cos\theta)(\sin\delta\cos\theta + \frac{c}{b}\cos\delta\sin\theta) \\
&\quad -(\cos\delta\cos\theta - \frac{c}{b}\sin\delta\sin\theta)(\sin\delta\sin\theta - \frac{c}{b}\cos\delta\cos\theta) \\
&= \sin\delta\sin\theta\cos\delta\cos\theta + \frac{c}{b}(\sin^2\delta\cos^2\theta + \cos^2\delta\sin^2\theta) \\
&\quad + \frac{c^2}{b^2}\sin\delta\sin\theta\cos\delta\cos\theta \\
&\quad -\sin\delta\sin\theta\cos\delta\cos\theta + \frac{c}{b}(\cos^2\delta\cos^2\theta + \sin^2\delta\sin^2\theta) \\
&\quad - \frac{c^2}{b^2}\sin\delta\sin\theta\cos\delta\cos\theta \\
&= \frac{c}{b}(\sin^2\delta\cos^2\theta + \cos^2\delta\sin^2\theta + \cos^2\delta\cos^2\theta + \sin^2\delta\sin^2\theta) \\
&= \frac{c}{b}(\cos^2\theta + \sin^2\theta) \\
&= \frac{c}{b}
\end{aligned}
\qquad (4\text{-}11)
$$

which means;

$$
\det E(x) = \frac{c\, r_{wf}^2\, \omega_1}{b\, Den(\delta)} \qquad (4\text{-}12)
$$

This shows that det E(x) = 0 if, $\omega_1 = 0$ or $c = 0$. Also, from Equation (4-9):

$$
\begin{bmatrix} \dot{u}_{11} \\ u_{12} \end{bmatrix} = E^{-1}(x)\left[\begin{bmatrix} \dot{X}^{(3)} \\ \dot{Y}^{(3)} \end{bmatrix} + R(x)\right] = \begin{bmatrix} -r_{wf}\left[A_4 + A_1\frac{Num(\delta)}{Den(\delta)}\right]\omega_1 & r_{wf}\left[A_3 + A_1\frac{Num(\delta)}{Den(\delta)}\right]\omega_1 \\ \frac{-r_{wf}A_2}{Den(\delta)} & \frac{r_{wf}A_1}{Den(\delta)} \end{bmatrix} \frac{\left[\begin{bmatrix} \dot{X}^{(3)} \\ \dot{Y}^{(3)} \end{bmatrix} + R(x)\right]}{\det E(x)} \qquad (4\text{-}13)
$$

4-1-2 Curvilinear Space Feedback Linearization

Similar to the previous case, two inputs (τ_s , τ_d) are available, and at most two out of six states (s, t, θ, δ, ω_δ , ω_1) can be controlled [25]. If s and n we are chosen, the first derivatives are Equations (3-51 and 52) [76]:

$$\dot{s} = \frac{r_{wl}\omega_1(\cos\delta\cos\psi - \frac{c}{b}\sin\delta\sin\psi)}{(1-n\kappa)}$$
$$\dot{n} = r_{wl}\omega_1(\cos\delta\sin\psi + \frac{c}{b}\sin\delta\cos\psi) \qquad (4\text{-}14)$$

Obviously, E(x) = 0. Taking another derivative:

$$\ddot{s}(1-n\kappa) = r_{wl}[A_1\frac{\tau_d - Num(\delta)r_{wl}^2\omega_1\omega_\delta - \frac{r_{wl}\sin\delta}{b}\tau_s}{Den(\delta)} - \omega_1(A_2\omega_\psi + A_3\omega_\delta)] + \dot{s}(\dot{n}\kappa + n\dot{\kappa})$$
$$\ddot{n} = r_{wl}[A_2\frac{\tau_d - Num(\delta)r_{wl}^2\omega_1\omega_\delta - \frac{r_{wl}\sin\delta}{b}\tau_s}{Den(\delta)} + \omega_1(A_1\omega_\psi - A_4\omega_\delta)] \qquad (4\text{-}15)$$

where;

$$A_1 = \cos\delta\cos\psi - \frac{c}{b}\sin\delta\sin\psi$$
$$A_2 = \cos\delta\sin\psi + \frac{c}{b}\sin\delta\cos\psi$$
$$A_3 = \sin\delta\cos\psi + \frac{c}{b}\cos\delta\sin\psi \qquad (4\text{-}16)$$
$$A_4 = \sin\delta\sin\psi - \frac{c}{b}\cos\delta\cos\psi$$

τ_s and τ_d , both appear, but, det E(x) = 0 . Then the next derivative should be taken:

$$
\begin{aligned}
& s^{(3)}(1-n\kappa)-2\dot{s}(\dot{n}\kappa+n\dot{\kappa})-\ddot{s}(\ddot{n}\kappa+2\dot{n}\dot{\kappa}+n\ddot{\kappa}) \\
& \quad = r_{wl}A_1\left[\frac{\dot{u}_{l1}-r_{wl}^2\omega_\delta(\dot{Num}\ (\delta)\omega_1+Num\ (\delta)\dot{\omega}_1)-\dot{Den}\ (\delta)\dot{\omega}_1}{Den\ (\delta)}\right] \\
& \quad -r_{wl}\omega_1\left(A_3+\frac{Num\ (\delta)A_1}{Den\ (\delta)}\right)\left[\frac{u_{l2}}{J_{SA}+J_1}-\frac{r_{wl}}{b}(\dot{\omega}_1\sin\delta+\omega_1\omega_\delta\cos\delta)\right] \\
& -r_{wl}[2(A_2\omega_\psi+A_3\omega_\delta)\dot{\omega}_1+(A_1\omega_\psi-A_4\omega_\delta)\omega_1\omega_\psi-(A_4\omega_\psi-A_1\omega_\delta)\omega_1\omega_\delta+A_2\dot{\omega}_\psi
\end{aligned}
\tag{4-17}
$$

$$
\begin{aligned}
n^{(3)} &= r_{wl}A_2\left[\frac{\dot{u}_{l1}-r_{wl}^2\omega_\delta(\dot{Num}\ (\delta)\omega_1+Num\ (\delta)\dot{\omega}_1)-\dot{Den}\ (\delta)\dot{\omega}_1}{Den\ (\delta)}\right] \\
&\quad - r_{wl}\omega_1\left(A_4+\frac{Num\ (\delta)A_2}{Den\ (\delta)}\right)\left[\frac{u_{l2}}{J_{SA}+J_1}-\frac{r_{wl}}{b}(\dot{\omega}_1\sin\delta+\omega_1\omega_\delta\cos\delta)\right] \\
&\quad + r_{wl}[2(\dot{A}_1\omega_\psi-A_4\omega_\delta)\dot{\omega}_1-(A_2\omega_\psi+A_3\omega_\delta)\omega_1\omega_\psi-(A_3\omega_\psi+A_2\omega_\delta)\omega_1\omega_\delta+A_1\dot{\omega}_\psi\omega_1]
\end{aligned}
\tag{4-18}
$$

In Equations (4-17 and 4-18), the following were used:

$$
\begin{aligned}
\dot{A}_1 &= -(\cos\delta\sin\psi+\frac{c}{b}\sin\delta\cos\psi)\omega_\psi \\
&\quad -(\sin\delta\cos\psi+\frac{c}{b}\cos\delta\sin\psi)\omega_\delta \\
&= -A_2\omega_\psi-A_3\omega_\delta
\end{aligned}
\tag{4-19}
$$

and

$$\begin{aligned}\dot{A}_2 &= A_1\omega_\psi - A_4\omega_\delta \\ \dot{A}_3 &= -A_4\omega_\psi + A_1\omega_\delta \\ \dot{A}_4 &= A_3\omega_\psi + A_2\omega_\delta\end{aligned} \tag{4-20}$$

To verify if, det **E(x)** = 0 or not :

$$\begin{bmatrix} s^{(3)} \\ n^{(3)} \end{bmatrix} = E(x)\dot{u}_i + R(x) = \begin{bmatrix} \dfrac{r_{wl}A_1}{Den(\delta)(1-n\kappa)} & -\dfrac{r_{wl}[A_3 + A_1\dfrac{Num(\delta)}{Den(\delta)}]}{(1-n\kappa)}\omega_1 \\ \dfrac{r_{wl}A_2}{Den(\delta)} & -r_{wl}[A_4 + A_2\dfrac{Num(\delta)}{Den(\delta)}]\omega_1 \end{bmatrix} \begin{bmatrix} \dot{u}_{i1} \\ u_{i2} \end{bmatrix} + R(x \tag{4-21}$$

such that:

$$\det E(x) = \frac{r_{wl}^2(-A_1A_4 + A_2A_3)\omega_1}{Den(\delta)(1-n\kappa)} \tag{4-22}$$

with;

$$\begin{aligned} A_2A_3 - A_1A_4 &= (\cos\delta\sin\psi + \frac{c}{b}\sin\delta\cos\psi)(\sin\delta\cos\psi + \frac{c}{b}\cos\delta\sin\psi) \\ &\quad -(\cos\delta\cos\psi - \frac{c}{b}\sin\delta\sin\psi)(\sin\delta\sin\psi - \frac{c}{b}\cos\delta\cos\psi) \\ &= \frac{c}{b} \end{aligned} \tag{4-23}$$

which means:

$$\det E(x) = \frac{\frac{c}{b} r_{wl}^2 \omega_1}{Den(\delta)(1-n\kappa)} \tag{4-24}$$

This shows that det E(x) = 0 if, $\omega_1 = 0$ or c = 0 . Also, from Equation (4-21):

$$\begin{bmatrix} \dot{u}_{l1} \\ u_{l2} \end{bmatrix} = E^{-1}(x)\left[\begin{bmatrix} s^{(3)} \\ n^{(3)} \end{bmatrix} + R(x)\right] = \begin{bmatrix} -r_{wl}[A_4 + A_1 \frac{Num(\delta)}{Den(\delta)}]\omega_1 & \frac{r_{wl}[A_3 + A_1 \frac{Num(\delta)}{Den(\delta)}]}{(1-n\kappa)}\omega_1 \\ \frac{-r_{wl}A_2}{Den(\delta)} & \frac{r_{wl}A_1}{Den(\delta)(1-n\kappa)} \end{bmatrix} \frac{\left[\begin{bmatrix} s^{(3)} \\ n^{(3)} \end{bmatrix} + R(x)\right]}{\det E(x)} \tag{4-25}$$

4-2 Controller Design

4-2-1 Cartesian Space Controller Design

A simple linear controller design for $X^{(3)}$ and $Y^{(3)}$ gives:

$$\begin{bmatrix} X^{(3)} \\ Y^{(3)} \end{bmatrix} = \begin{bmatrix} X^{(3)_d} \\ Y^{(3)_d} \end{bmatrix} + k_1 \begin{bmatrix} \ddot{X}_d - \ddot{X} \\ \ddot{Y}_d - \ddot{Y} \end{bmatrix} + k_2 \begin{bmatrix} \dot{X}_d - \dot{X} \\ \dot{Y}_d - \dot{Y} \end{bmatrix} + k_3 \begin{bmatrix} X_d - X \\ Y_d - Y \end{bmatrix} \tag{4-26}$$

X_d and Y_d and their derivatives are zero for stabilization at the origin and non-zero for tracking. The torque inputs τ_d and τ_s can be calculated using Equations (4-5, 4-6) and (4-26).

4-2-2 Curvilinear Space Controller Design

Same type of linear controller as the one for Cartesian space can be used for curvilinear coordinates s and n:

$$\begin{bmatrix} s^{(3)} \\ n^{(3)} \end{bmatrix} = -k_1 \begin{bmatrix} \ddot{s} \\ \ddot{n} \end{bmatrix} - k_2 \begin{bmatrix} \dot{s} \\ \dot{n} \end{bmatrix} - k_3 \begin{bmatrix} s - s_d \\ n \end{bmatrix} \tag{4-27}$$

4-3 Internal Dynamics

To find the dimension of the internal dynamics, Singh's inversion algorithm can be used [77]. This algorithm starts by defining $S_0(x, y) = h(x) - y$, where y is the outputs vector and $h(x)$ is the vector of outputs expressed using the states vector x.

Taking derivative of S_0 and having $\dot{x} = f(x) + g(x)u$ gives:

$$\dot{S}_0(x, y, \dot{y}, u) = \frac{\partial S_0}{\partial x} f(x) + \frac{\partial S_0}{\partial x} g(x)u + \frac{\partial S_0}{\partial y} \dot{y} = f_0(x, y, \dot{y}) + g_0(x, y)u$$

where u is the inputs vector. Let ρ_0 denote the rank of g_0, $p_0 = m$ (the number of inputs) and $p_1 = p_0 - \rho_0$. A $p_1 \times p_0$ matrix K_0 can be chosen in such a way that $K_0 g_0 = 0$. Now the vector $S_1 = K_0 f_0$. At each step:

$$\dot{S}_k(x, y, \dot{y}, y^{(k+1)}, u) = \frac{\partial S_k}{\partial x} f(x) + \frac{\partial S_k}{\partial x} g(x)u + \frac{\partial S_k}{\partial y} \dot{y} + \ldots + \frac{\partial S_k}{\partial y(k)} y^{(k+1)}$$

$$= f_k(x, y, \dot{y}, y^{(k+1)}) + g_k(x, y, \dot{y}, y^{(k)})u$$

Also, at each step the matrix $G_k = [\, G_{k-1} \quad g_k \,]^T$ can be constructed with proper numbers for rows and columns of each of them. Two matrices T_k and K_k can be chosen in such a way that $T_k G_k + K_k g_k = 0$. By denoting ρ_k as the rank of G_k, the following equation will be true: $p_{k+1} = p_k - (\rho_k - \rho_{k-1})$. The matrix $S_{k+1} = T_k F_{k-1} + K_k f_k$ can be set with $F_k = [\, F_{k-1} \quad f_k \,]^T$. When one of G_k's has rank m this algorithm ends and $n - \mu = n - (\sum p_k)$ shows the size of the internal dynamics of the system where n is the number of the states. In this case, for Cartesian space dynamic model we have: n=6 with $x = [\, X\ Y\ \theta\ \delta\ \omega_1\ \omega_\delta \,]$, $u = [\dot{\omega}_1\ \omega_\delta]^T$

, $\mathbf{h(x)} = [X \;\; Y]$ and $S_0 = [X\text{-}y_1 \;\; Y\text{-}y_2]^T$. Taking derivative of S_0 gives:

$$\dot{S}_0=[r_{w1}\omega_1 A_1-\dot{y}_1 \quad r_{w1}\omega_1 A_2-\dot{y}_2]^T \tag{4-28}$$

with $g_0=0$ and $\rho_0=0$, $p_0=2$ and $p_1=2$. For the next step $K_0=I_2$ can be selected as the identity matrix of rank 2. Then; $S_1=[r_{w1}\omega_1 A_1-\dot{y}_1 \quad r_{w1}\omega_1 A_2-\dot{y}_2]^T$
Taking derivative of S_1 gives:

$$\dot{S}_1=\begin{bmatrix} r_{w1}[\dot{\omega}_1 A_1-\omega_1(A_2\omega_\theta+A_3\omega_\delta)]-\ddot{y}_1 \\ r_{w1}[\dot{\omega}_1 A_2-\omega_1(A_1\omega_\theta+A_4\omega_\delta)]-\ddot{y}_2 \end{bmatrix} \tag{4-29}$$

with $g_1=\begin{bmatrix} r_{w1}A_1 & 0 \\ r_{w1}A_2 & 0 \end{bmatrix}$, $\rho_1=1$ and $p_2=1$. By choosing $T_1=[0 \;\; 0]$ and $K_1=[-A_2 \;\; A_1]^T$, S_2 will be:

$$S_2=r_{w1}\omega_1[(A_1^2+A_2^2)\omega_\theta+(A_2A_3-A_1A_4)\omega_\delta]+A_2\ddot{y}_1-A_1\ddot{y}_2 \tag{4-30}$$

Since $\dot{\omega}_1$ and $\dot{\omega}_\delta$ both appear in the derivative of S_2 the algorithm ends here with, $\rho_2=2$, $p_3=p_2-(\rho_2-\rho_1)=0$ and $\mu=\Sigma p_k=2+2+1+0=5$. Since n=6, the system's internal dynamics is one dimensional.

4-3-1 Zero Dynamics

Knowing the dimension of the internal dynamics, its structure by using zero dynamics algorithm defined in [25] and [71] can be found. This dynamics plays a role similar to that of the "zeros" of the transfer function in a linear system [25]. It consists of "zeroing the outputs" (and their derivatives) in order to find the states (equal to some numbers or in form of some differential equations) and the inputs that keep outputs (and their derivatives) identically zero for all times.

If the Cartesian coordinates X and Y are selected as the outputs, the following steps result:

1) X=0 and Y=0

2) $\dot{X} = r_{wl} A_1 \omega_1 = 0$ and $\dot{Y} = r_{wl} A_2 \omega_1 = 0$. These mean $\omega_1=0$ or $A_1=0=A_2$. Because of their definitions A_1 and A_2 can not be zero at the same time, and the only feasible result is $\omega_1=0$.

3) $\ddot{X} = r_{wl}(A_1\dot{\omega}_1 + \dot{A}_1\omega_1) = 0$ and $\ddot{Y} = r_{wl}(A_2\dot{\omega}_1 + \dot{A}_2\omega_1) = 0$. Since it is already known that $\omega_1=0$ and A_1 and A_2 cannot be equal to zero at the same time, the only conclusion is $\dot{\omega}_1 = 0$.

4) Higher order derivatives of X and Y equal to zero. Because of their structure, the only conclusion can be $\omega_1^{(k)} = 0$.

Thus, this algorithm does not give direct information about the other states, θ, δ and ω_δ. Equation (3-77) and $\omega_1=0$ give: $\dot{\theta}=0$ and Equation (A-79), $\omega_1 = 0$ and $\tau_s = 0 = \tau_d$ (inputs are zero for zero dynamics) give: $\dot{\omega}_\delta=0$ i.e., ω_δ=const and $\delta=\delta(t)$. Then δ should be the internal dynamics variable.

Another way to find the internal dynamics state variable is to use the physics of the vehicle. If this dynamics is θ, the vehicle cannot make any moves(X, Y and ω_1 and their derivatives are zero), thus it is not zero dynamics, but δ can keep changing since the front wheel, which theoretically has just point contact with the ground, can rotate about a vertical axis at constant speed ω_δ=const even when vehicle is stationary($\omega = 0$). This physical interpretation leads to this conclusion that the vehicle's zero dynamics is "δ". It should be noted that this is the same for Cartesian X and Y or curvilinear s and n.

One more point to make here is that, although the vehicle has three wheels and each of them has one nonholonomic constraint, because the two rear wheels have the same structure for their nonholonomic constraints ($V_{y2} = 0 = V_{y3}$), the number of independent nonholonomic constraints is reduced to two. Moreover, it is known that internal dynamics is one dimensional, which means that the number of independent nonholonomic constraints

should be one. In fact the state "θ" governing the relations $V_{y2} = 0 = V_{y3}$ and the state "δ" governing the nonholonomic constraint of the front wheel ($\tan\delta = \frac{b}{c}\frac{V_y}{V_x}$) are related by the holonomic constraint ($\dot{\theta} = \frac{r_{wl}}{b}\omega_1 \sin\delta$).

4-3-2 Internal Stability for Non-vanishing ω_1

In zero dynamics, the behaviour of the internal dynamics when the system is stationary is studied and it is interested to see if some states can keep changing while the outputs and their derivatives and the inputs are zero. For nonholonomic vehicles the zero dynamics is not null. For CLAMOR, the internal dynamics state is steering angle δ which means steering assembly can keep rotating when centre of mass position, velocity and acceleration and driving and steering torques all are zero.

An alternative discussion for path following and trajectory tracking would be to analyse the stability of internal (steering) dynamics while the system is moving. (A-75) is the governing equation for steering dynamics. To examine unforced stability, it is assumed that steering torque is equal to zero. The equation:

$$\ddot{\delta} + \frac{r_{wl}}{b}\omega_1 \cos\delta\,\dot{\delta} + \frac{r_{wl}}{b}\dot{\omega}_1 \sin\delta = 0 \qquad (4\text{-}31)$$

and its approximate linearized form around $\delta = 0$ where $\sin\delta \approx \delta$ and $\cos\delta \approx 1$;

$$\ddot{\delta} + \frac{r_{wl}}{b}\omega_1 \dot{\delta} + \frac{r_{wl}}{b}\dot{\omega}_1 \delta = 0 \qquad (4\text{-}32)$$

have no closed-form solutions. By assuming that ω_1 is constant, Equations (4-31) will be reduced to:

$$\ddot{\delta}+\frac{r_{wl}}{b}\omega_1\cos\delta\dot{\delta}=0 \tag{4-33}$$

which has a solution of the type $\delta=\tan^{-1}[(\tan v+h)/c_1]$ where v is a linear function of time and a nonlinear function of h where $h=\frac{r_{wl}\omega_1}{b}$ and c_1 is a constant. This solution is indefinite when $t\to\infty$. Also Equation (4-32) will be reduced to:

$$\ddot{\delta}+\frac{r_{wl}}{b}\omega_1\dot{\delta}=0 \tag{4-34}$$

which its solution is bounded but not asymptotically stable around zero.

One interesting suggestion is given by Yun and Yamamoto [73]. If the vehicle's motion under some conditions is (asymptotically)stable around $\delta=0$, then assuming that it moves along a straight line, without loss of generality inertial X direction (with may be some fluctuation around this line) is acceptable. If these conditions are found, the result stands and if some conditions under which the system's motion is unstable are found, there may be a chance of recovery later. This is the case because the unstable mode may oppose the initial assumption of moving on a straight line. This recovery has to satisfy the conditions for (asymptotic)stability around zero or other possible configurations. Then;:

$$\begin{aligned}\dot{X}&=\pm f(t)\\ \dot{Y}&=o\end{aligned} \tag{4-35}$$

Inverting (3-8) gives:

$$\begin{aligned}V_x&=\dot{X}\cos\theta+\dot{Y}\sin\theta\\ V_y&=-\dot{X}\sin\theta+\dot{Y}\cos\theta\end{aligned} \tag{4-36}$$

Rewriting (3-35) and including (4-35 and 36) give:

$$\tan\delta=\frac{bV_y}{cV_x}=\frac{b(-\dot{X}\sin\theta+\dot{Y}\cos\theta)}{c(\dot{X}\cos\theta+\dot{Y}\sin\theta)}$$
$$=\frac{b[-f(t)\sin\theta]}{c[f(t)\cos\theta]}$$
$$=\frac{-b\tan\theta}{c} \qquad (4\text{-}37)$$

or for $\omega_1 \neq 0$,

$$\delta=\tan^{-1}\left(\frac{-b\tan\theta}{c}\right) \qquad (4\text{-}38)$$

Taking derivative of δ will result in:

$$\dot{\delta}=\frac{1}{\left(1+\frac{b^2}{c^2}\tan^2\theta\right)}\left(-\frac{b}{c}\frac{1}{\cos^2\theta}\right)\dot{\theta} \qquad (4\text{-}39)$$

where:

$$\frac{d}{dt}\tan^{-1}u=\frac{1}{1+u^2}\frac{du}{dt} \quad ; \quad \frac{d}{dt}\tan u=\frac{1}{\cos^2 u}\frac{du}{dt}$$

Equations (3-77) and (4-39) give:

$$\dot{\delta}=\frac{-b\left(\frac{r_{wl}}{b}\omega_1\sin\delta\right)}{c\left(1+\frac{b^2}{c^2}\tan^2\theta\right)\left(\frac{1}{\cos^2\theta}\right)}=\frac{-r_{wl}\omega_1\sin\delta}{\left(c\cos^2\theta+\frac{b^2}{c}\sin^2\theta\right)} \qquad (4\text{-}40)$$

or:

$$\dot{\delta}+\frac{r_{wl}\omega_1}{(c\cos^2\theta+\frac{b^2}{c}\sin^2\theta)}\sin\delta=0 \tag{4-41}$$

To solve this differential equation, the variable separation method should be used:

$$\frac{d\delta}{\sin\delta}=-\frac{r_{wl}\omega_1}{(c\cos^2\theta+\frac{b^2}{c}\sin^2\theta)}dt \tag{4-42}$$

The solution is:

$$\ln\tan\frac{\delta}{2}=-\int\frac{r_{wl}\omega_1}{(c\cos^2\theta+\frac{b^2}{c}\sin^2\theta)}dt \tag{4-43}$$

or:

$$\delta=2\tan^{-1}[\exp(-\int\frac{r_{wl}\omega_1}{(c\cos^2\theta+\frac{b^2}{c}\sin^2\theta)}dt)]+const. \tag{4-44}$$

By assuming that $\delta(t_0)=0$, then, const.= 0. A sufficient condition to have this variable approaching zero is that the integrant be bounded from below by a number a) 0. Which means;

$$\delta \prec 2\tan^{-1}(e^{-\alpha t})$$

$$with;\ \lim_{t\to\infty}(e^{-\alpha t})\to 0 \Rightarrow \lim_{t\to\infty}\delta\to 0 \tag{4-45}$$

In this case the sufficient condition for stability of the internal dynamics is that ω_1 be

bounded by a number $\omega_{min} > 0$. (r_{w1} and c are positive), which means as long as the vehicle keeps moving forward, its internal dynamics is stable. Also, if vehicle moves backward its motion will be unstable.

4-3-3 Internal Dynamics for $\omega_1 = 0$. Wheel-Ground Contact Area.

When $\omega_1=0$ and the vehicle is stopped, the Equation (4-31) will be reduced to $\dot{\delta} = 0$. This comes from the fact that for simplicity it is usually assumed that the contact between wheel and ground happens at a point or a line(with the width of the wheel), the reality is that, because of the weight of the wheel and the fact that wheel is not completely rigid, there is an area of contact [79], which is known as Hertzian surface (Figure 4.1). As a result, contact friction leads not only to a resultant force applied to the center of the area but also to a non-

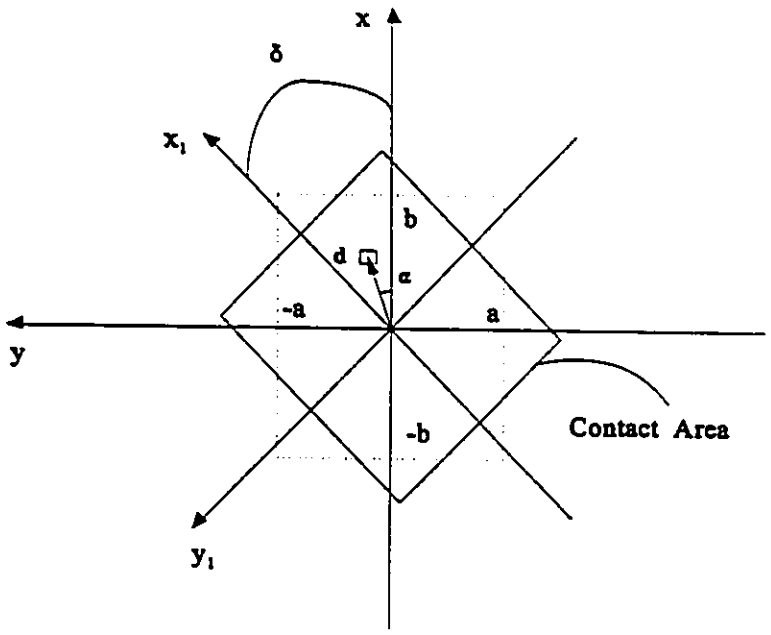

Figure 4-1 Wheel-ground contact area.

vanishing moment of forces about the vertical axis through the center of that area [79].

This moment is determined in this section and its effect is shown on motion of the steering wheel for small and relatively large, but not very large, steering angles. By considering a differential area of dA which is located at d from the center of the area and makes an angle of α degree from x-axis. This small area is rotated by angle δ. Friction force dF_f (Figure 4-2) will resist this motion and, the resultant of those forces on the whole area is denoted $G_{xl}i_1 + G_{yl}j_1$. (Fig. 3-5) The resultant of multiplication of the arm d by the friction force dF_f, $dM_f = d \times dF_f$, is:(Figure 4-2)

$$M_f = \iint dM_f = \iint d \times dF_f$$

$$= \iint |d| (\cos(\alpha + \delta)i + \sin(\alpha + \delta)j) \times \mu W_1 \frac{V_{dA}}{V_{dA}} dA \qquad (4\text{-}46)$$

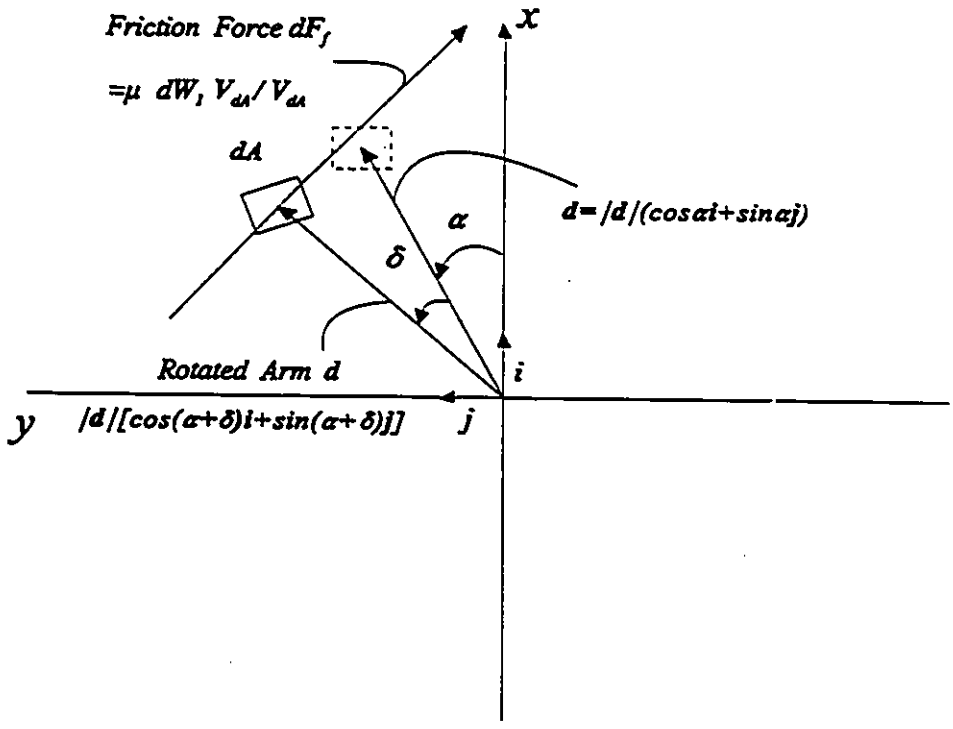

Figure 4-2 The infinitesimal area and friction force.

where W_1 is the share of the front wheel of total weight and $dW_1 = W_1\, dA$ is the part of W_1 acting on dA and V_{dA} is the velocity of the infinitesimal area. Double integral indicates that the integrant should be calculated for the whole contact area. For simplicity it is assumed that the shape of contact area remains the same throughout turning and since the vehicle is close to the end $\omega_1 \approx 0$ and V_{dA} is only turning velocity of each point:

$$\frac{V_{dA}}{V_{dA}} = \sin(\alpha+\delta)i - \cos(\alpha+\delta)j \tag{4-47}$$

Then:

$$\begin{aligned} M_f &= -\mu W_1 \int |d| dA\, k \\ &= -\mu W_1\, \sigma_1\, k \\ &= -\sigma\, k \end{aligned} \tag{4-48}$$

where σ_1 is a constant function of the size of the area and σ is a function of the size of contact area, wheel material, type of wheel-ground contact, weight of the vehicle, etc. M_f should be added to Equation (A-75) with this note that it opposes the steering motion. The result is:

$$\begin{aligned} \tau_s &= (J_{SA} + J_1)(\ddot{\delta} + \ddot{\theta}) + M_f \\ &= (J_{SA} + J_1)[\ddot{\delta} + \frac{r_{wl}}{b}(\dot{\omega}_1 \sin\delta + \omega_1 \dot{\delta}\cos\delta)] + \sigma \frac{\dot{\delta}}{|\dot{\delta}|} \end{aligned} \tag{4-49}$$

Equation (4-49) is a non-homogenous nonlinear differential equation. Rather than attempt to calculate σ from Equations (4-46) or (4-48), it is sufficient here to observe that σ is nonzero in practical situations. This conclusion permits to clarify the internal stability for the case of driving angular velocity $\omega_1 = 0$ and $\tau_s = 0$. Equation (4-49) shows that, the friction term transforms a marginally stable system for $\sigma = 0$ into a bounded stable system

for $\sigma \neq 0$. In fact, as usual, dry friction term leads to energy dissipation during motion and eventually to sticking in the vicinity of the desired orientation. In the experiments, the result of the friction term on motion stability when slowing down toward the end of the path will be investigated.

Chapter 5

Motion Control of an Autonomous Ground Vehicle

As mentioned earlier, the main focus of this research is on motion control problems of autonomous ground vehicles including kinematic and dynamic modelling, path and motion planning, path following and trajectory tracking and stabilization. To have a system that represents some reality of an actual vehicle but remains somehow simple to model and work with, a tricycle with front wheel steering and driving was chosen. Eventually, the dynamic models found based on kinematic and dynamic equations of the vehicle were nonlinear and motion control problems of relatively long trajectories and far desired positions could not be dealt with by linearized approximation of the system.

The emphasis of this thesis, to solve the motion control problems, is to apply systematic approaches that can be extended, by some adjustments, to more complicated models. Feedback linearization is one systematic technique in nonlinear control theory that by transforming the control system into a linear one and by applying a linear controller for the transformed system could stabilize the original system around a point or about a trajectory. This technique has been used to solve nonlinear control problems and a known version of it which is called computed torque method is proven to work for robotic systems. But those systems are holonomic and wheeled vehicles are nonholonomic. Application of this technique to nonholonomic vehicles trajectory tracking and stabilization to a manifold were suggested and used by d'Andrêa-Novel et

al [72], Yun and Yamamoto [73], Deng and Brady [74], Sarkar et al and Necsulescu et al [13]. Since by feedback linearization, a smooth feedback will be applied to the system, it cannot directly contribute to asymptotic stabilization of the overall nonholonomic system. Nonholonomic systems have an internal dynamics which its dimension is equal to the number of independent nonholonomic constraints and because feedback linearization only treats the external dynamics of the system, internal dynamics remains to be examined separately.

5-1 Kinematic and Dynamic Modelling

Kinematic and dynamic equations of the motion of the system were obtained in chapter 3. These equations by means of the concepts of Lagrange equations of the first kind, i.e., by algebraically eliminating internal and contact forces and moments, as performed in Appendix A, will be reduced into (almost) minimum size dynamic models of the form $\dot{x}=f(x,u)$ (section 3-3). The minimal models could be obtained by presenting the system in body moving frame and not inertial frame (for Cartesian space). In that case the six-state variable model could be reduced to a five-state variable model, since $\dot{y}=c\dot{\theta}$ (Equation 3-30) would make one of "y" or "θ" redundant.

5-2 Feedback Linearization

Input-output feedback linearization technique was applied to the dynamic models with X-Y and s-n as outputs and τ_s and τ_d as inputs. To be completed, this approach needed a dynamic extension(derivatives of the inputs should be taken in order to succeed) and the result was the appearance of the third derivative of the position, jerk, in the transformations of output equations (section 4-1). Consequently, the third order linear control laws, Equations (4-26) and (4-27), for the linearized system have three parameters to be chosen and some "trial and error" is required to determine the appropriate values. One reason is that as a result of feedback linearization

transformation, all nonlinearities are contained in the loop between the jerk inputs to the linearized system and the inputs to the nonlinear system, τ_s and τ_d. The result is that the overall system does not necessarily project the changes in the linear controller gains as expected and even relatively small change in one of these parameters may cause somehow drastic changes in the overall performance of the system. On the other hand, the behavior of the system not only is affected by system's external dynamics but also by its internal dynamics. The internal dynamics of the system is not a part of linearization procedure, so the effect of this nonlinear dynamics will make it more difficult to have some kind of regulation on changing the linear gains of input-output feedback linearization approach.

Figure 5-1 shows the feedback Linearization loop of the system.

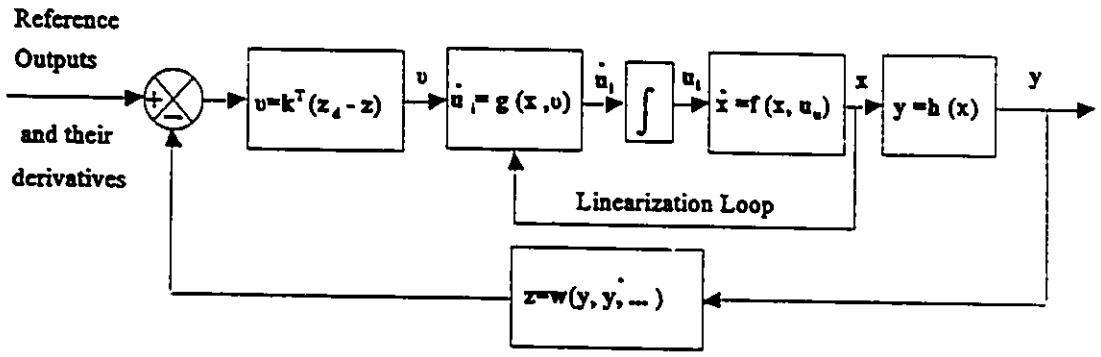

Figure 5-1 Dynamically extended input-output feedback linearization loop of the vehicle.

with;

Cartesian Space	Curvilinear Space
$x = [X,\ Y,\ \theta,\ \omega_1,\ \delta,\ \omega_\delta]^T$	$x = [s,\ n,\ \psi,\ \omega_1,\ \delta,\ \omega_\delta]^T$
$y = [X,\ Y]^T$	$y = [s,\ n]^T$
$\upsilon = [X^{(3)},\ Y^{(3)}]^T$	$\upsilon = [s^{(3)},\ n^{(3)}]^T$

Cartesian Space	Curvilinear Space
$z = [X, Y, \dot{X}, \dot{Y}, \ddot{X}, \ddot{Y}, 0, 0]^T$	$z = [s, n, \dot{s}, \dot{n}, \ddot{s}, \ddot{n}, 0, 0]^T$
$z_d = [X_\Phi, Y_\Phi, \dot{X}_d, \dot{Y}_d, \ddot{X}_d, \ddot{Y}_d, X_d^{(3)}, Y_d^{(3)}]^T$	$z_d = [s_d, 0, 0, 0, 0, 0, 0, 0]^T$
f: Equations (A-71,78,79), (4-33,34,77)	f: Equations (A-71,78,79), (4-51,52,80)

Also, Cartesian space g is Equation (4-13) and curvilinear g is Equation (4-25). u_i which is for both spaces is Equation (4-4).

5-3 Path Following and Trajectory Tracking

In case of path following the time assignment is arbitrary, while for trajectory tracking, the time assignment is predetermined. Desired positions, velocities, accelerations and jerks are obtained by calculation, sensing or mixed. Based on these data, Cartesian space feedback linearization technique can be applied to the system to follow a path or track a trajectory. The external dynamics of the system, by choosing proper values for k_1, k_2 and k_3 (Equation 4-26), will be exponentially stabilized around the path, but internal dynamics issue has also to be addressed. By examining the system, it becomes apparent that steering is the only internal dynamics state variable (section 4-3).

To investigate the stability of this internal dynamics for trajectory tracking where some assumptions of the zero dynamics algorithm, particularly in this case $\omega_1 = 0$, do not hold, a situation in which steering torque would remain zero can be considered. The homogenous differential equation form of (A-75) does not have a closed-form solution. The approach is to check the system close to (one of)equilibrium position(s), $\delta = 0$ in this case, and see under what conditions it stays there and under what conditions it tends to move away. When steering torque is zero and steering angle close to zero, the vehicle will follow an almost straight line. In subsection 4-3-2 an analytical discussion shows

that the internal dynamics for a moving vehicle is exponentially stable if the front wheel angular velocity is greater than zero. For $\omega_1 < 0$ some other equilibrium position(s) may exist.

5-4 Stabilization to a Manifold

Although full state smooth feedback, asymptotic stabilization is not possible for nonholonomic vehicles, for the case of planar motion, the asymptotic stabilization to a one dimensional final manifold (usually orientation is considered as this manifold coordinate) is possible. By input-output feedback linearization, external dynamics can be asymptotically stabilized, and the internal dynamics, which under ideal rolling assumptions with point contact is marginally stable, decides what the final value for the third coordinate(usually orientation) will be. Theoretically this value is known by knowing the initial conditions and the motion from initial to the final point, but it may not be an acceptable value.

5-5 Stabilization to a Position with Orientation. Bounded Stabilization.

By reviewing the literature, it seems that further research is required for solving the asymptotic stabilization problem of dynamics based models of nonholonomic vehicles with front wheel steering. During last few years the evolution of this issue has become faster. What has been tried to do in this research is to find a bounded solution to the stabilization problem of the model that can be verified on an experimental setup. By bounded, an internal dynamics is meant which is bounded stable but not asymptotically stable, and therefore a final position and orientation which are in close vicinity of the desired ones. To do this, it is intended to apply the input-output feedback linearization technique to the curvilinear space coordinates of the vehicle and use "s", the arc length, and "n", the normal to the path of the vehicle at each point, as outputs. This path should connect the initial position and orientation to the desired ones. Also,

this path should be an analytical function of X and Y, or s and n and close to the ends, its curvature(κ) be as much as possible close to zero. The path should be analytical because it is desirable to spend less computing memory and time on path calculations. Then, preferably the definition of the path should be a combination of some of library functions already defined for the computer. Also, the path should be as close as possible to straight lines at the ends, to take advantage of the results on internal stability study close to, but before, the end (section 4-3-2, with this note that, when moving on a straight line Cartesian and curvilinear coordinates coincide). By traveling along this path, closed loop control of s-n will make the vehicle follow the path closely and reach the final position. This, theoretically, means that the orientation remains in an open loop and can be driven to a vicinity of the desired final value. The reason, it is said to a vicinity and not on target, is the steering. For a vehicle without steering, usually the position of the middle point of the rear axle is controlled and not center of mass, and as it moves along a path, its orientation coincides with the tangent to the path at each point. For a vehicle with steering, there will be a difference between vehicle orientation and tangent to the path. For our model, Equations (3-33 and 3-34) show that if $\delta = 0$, then, $\tan\theta = \dot{Y}/\dot{X}$ and orientation and tangent coincide, otherwise, that difference will be present.

5-5-1 Path Planning

Among the suggested analytical paths to connect two end positions and orientations, clothoid pairs with zero end curvature by Kanayama and Miyake [46] seems to be very interesting. In describing the disadvantages of clothoids in which the curvature (κ) is a linear function of s ($\kappa = ks + c_0$), Nelson [47] points out that they have no closed form in terms of Cartesian coordinates, x and y, and also because of that any numerical error in calculations may result in a mismatch in end conditions. These are not valid here because s, n are already being used as the coordinates. Clothoids may

connect the end conditions or two straight lines passing through those ends; Kanayama and Hartman [48] say this transition from one line to the other is non-smooth and may cause slippage. Since closed loop control, and not open loop is to be dealt with in this research, this non-smoothness should not be a major problem. To have better smoothness, cubic spirals which are cubic functions of s ($\theta=As^3+Bs^2+Cs+D$) have been proposed [48]. Also polynomial functions in terms of x, y and polar coordinates have been suggested [47]. The only difficulty with Cartesian cubic polynomial is that their curvature at the ends may not be as desired and if higher order polynomials are going to be used to account for that, more than one saddle point may appear in the middle of the path which is undesirable. An intuitive suggestion is presented in [78]. The initial and desired positions and orientations are defined by $P_i(X_i,Y_i,\theta_i)$ and $P_d(X_d,Y_d,\theta_d)$. The distance between the desired and initial positions is L.(Figure 5-2) The path is calculated in (x_t, y_t) frame whose origin is G_i and where x_t is parallel to $P_i P_d$ and Θ is the angle between x_t and X. The four boundary conditions suggest a forth order differential equation to obtain a smooth path.

Let us consider the equation: $$\frac{d^4y_t}{dx_t^4}-\beta^4 y_t=0$$

Its general solution is a transcendental function of x_t dependent on a parameter "β":

$$y_t=b_1\cos\beta x_t+b_2\sin\beta x_t+b_3\cosh\beta x_t+b_4\sinh\beta x_t \qquad (5\text{-}1)$$

where four coefficients b_1 to b_4 are calculated from the boundary conditions. These boundary conditions in (x_t, y_t) frame are:

$$y_t(0)=0\ ,\ \frac{dy_t}{dx_t}(0)=\tan(\theta_i-\Theta)$$

$$y_t(L)=0\ ,\ \frac{dy_t}{dx_t}(L)=\tan(\theta_d-\Theta) \qquad (5\text{-}2)$$

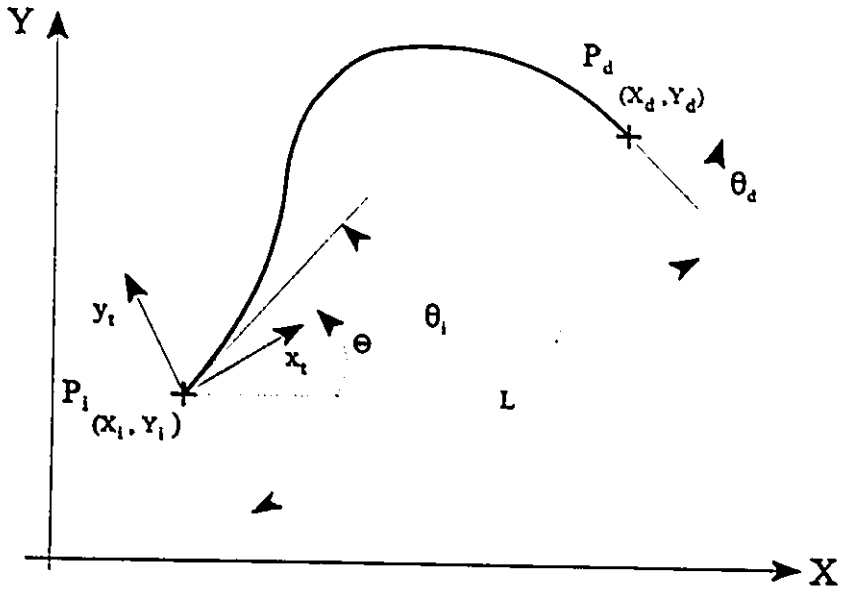

Figure 5-2 Path planning in (x_t, y_t) frame.

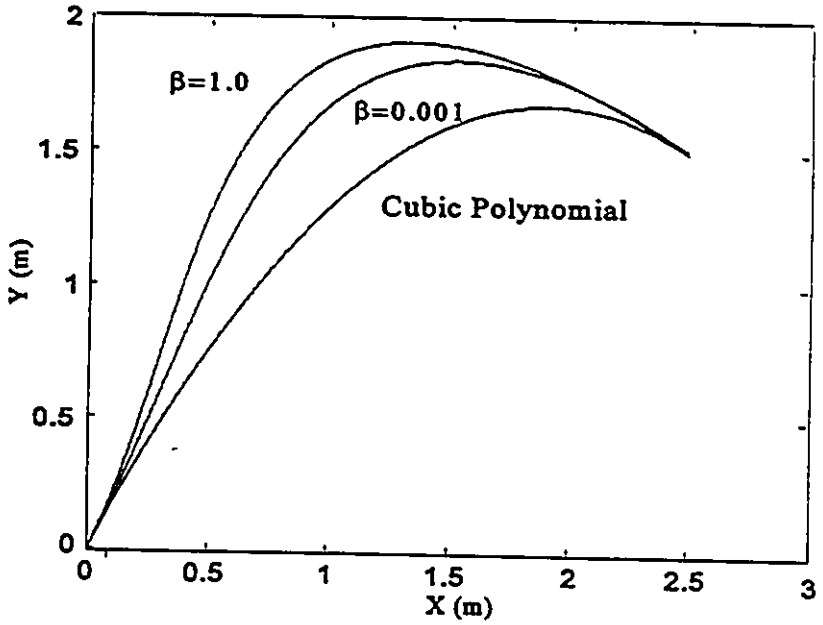

Figure 5-3 Paths for X_i=0, Y_i=0, θ_i=60°, X_d=2.5, Y_d=1.5, θ_d=-30°.

WhereAs it can be seen from Figure (5-3), the suggested path has a more smooth change of curvature than the polynomial path which is more desirable for a good dynamic behavior of the system, particularly in the last quasilinear portion of the path before reaching the final position. This path does not allow the vehicle to reach every point from every initial position. To find a path, defined by a function $y_t=f(x_t)$, which satisfies the boundary conditions of Equation (5-2), the following inequalities in (x_t, y_t) frame have to be verified:

$$-\frac{\pi}{2} \le \theta_i-\Theta < \frac{\pi}{2} \qquad -\frac{\pi}{2} \le \theta_d-\Theta < \frac{\pi}{2} \qquad \text{(5-3)}$$

In this thesis, these paths are not to be compared with each other and to show that the method works, from clothoid, cubic spiral or transcendental functions, which all of them close to the end have acceptable curvatures, the last one is chosen and simulation and experimental results based on this choice will be presented. The reason for this selection is programming availability.

5-5-2 Bounded Stabilization by Feedback Linearization

To justify the method presented in this thesis to achieve bounded stability the following explanation is necessary. As it is known, because of Brockett's theorem, feedback linearization which applies a smooth feedback cannot asymptotically stabilize the wheeled vehicle motion. As long as the vehicle is moving forward on the selected paths, its external as well as internal dynamics are stable; when it gets closer to the end unless a drastic change in steering angle happens, under some realistic conditions the bounded stability is achieved. To have a more realistic representation, a look at the contact area between the wheel and the ground will be very useful (section 4-3-3). Bounded stability of Equation (4-49) will insure that the vehicle(with asymptotically stable external dynamics) will arrive to a small neighborhood of final desired position and orientation.

Chapter 6

Simulation and Experimental Results

The results on motion control problems of autonomous vehicles including trajectory tracking, stabilization to a manifold and bounded stabilization to a position with orientation using suggested methods will be reported in this chapter. The results of the simulation on PC and experiments refer to the vehicle CLAMOR [80]. The simulations have been designed to represent the actual vehicle's platform as accurately as possible. The dimensions and dynamical properties of CLAMOR which have been measured and used in simulations and experiments are given below.

6-1 The Vehicle's Parameters

The dimensions of the CLAMOR are (Figure 3-1):

$r_{w1} = 0.0625$ m	$r_{w2} = 0.075$ m	$r_{w3} = 0.075$ m
$b = 0.381$ m	$c = 0.187$ m	$l = 0.36$ m

and the vehicle's dynamical characteristics are:

$m_0 = 18.0$ kg	$m_1 = 0.1$ kg	$m_2 = 0.15$ kg	$m_3 = 0.15$ kg	$m_{SA} = 6.1$ kg
$J_0 = 2.01$ kg m^2	$J_2 = 0.000844$ kg m^2	$J_3 = 0.000844$ kg m^2	$J_{SA} = 0.354$ kg m^2	
$I_{y1} = 0.000195$ kg m^2	$I_{y2} = 0.000422$ kg m^2	$I_{y3} = 0.000422$ kg m^2		

More of vehicle's dimensions and properties and its mechanical and electrical characteristics can be found in [80].

To avoid actuator saturation, one simple method is time scaling [51]. By knowing the limits, current actuator values and desired commands, if saturation occurs, the calculation backward from the limit(s) to the command jerk(s) will be performed to find the jerk(s) which will not cause the torques to saturate. To make sure this procedure in real time experiment will be done before and not after it is needed, model based prediction in which the commands are assumed constant over a longer period of time can be utilized [81].

To compensate for discontinuous readings (incremental optical encoders have 1000 steps per revolution) and possible perturbations in odometry variables and their derivatives, a low pass filters on odometry data can be utilized. The second order IIR low pass filter has the general form of:

$$y_{filtered} \quad G y_{sensed} \ , \ with \quad G \quad \frac{c_2 z^{\ 2} \quad c_1 z^{\ 1} \quad c_0}{d_2 z^{\ 2} \quad d_1 z^{\ 1} \quad d_0}$$

where $c_0, c_1, c_2, d_0, d_1, d_2$ can be calculated by MATLAB command "butter". This command needs two inputs, first the order of the filter, in this case 2, and a number between 0.0 and 1.0 which is equal to the cutoff frequency of the filter divided by half of the sampling rate of the main program. To take the derivatives of the sensed variables, a simple first order filter is used. It has the form of:

$$y_{new} \quad \frac{2(y_{new} \quad y_{old}) \quad (2T_d \quad T_s) y_{old}}{2T_d \quad T_s}$$

where T_s is the sampling rate and T_d is a function of T_s, here chosen 10 times T_s. These derivatives are then filtered by the IIR filter. The filters on steering angle and front

wheel angular position have the cut-off frequency of 2 Hz. For various motion control problems, the simulation and experimental results are as follow.

6-2 Trajectory Tracking

Most of recent simulation and experimental results on motion control problems of nonholonomic vehicles in the literature are for path following and trajectory tracking. Among them are the results on CLAMOR reported in [80]. Here, the result of input-output feedback linearization approach reported in [13] will be repeated (Figure 6-1). The trajectory starts at (0.5, 0.0) with 45° as the starting orientation, the heading velocity is 0.25 m/s and (rate of change of orientation) of the trajectory is 0.1 rad/s. The vehicle starts at (0.0, 0.5) parallel to X-axis. The same trajectory is tracked with the saturation limits on the inputs (Figure 6-2). For simulation without saturation limits, k_1=5.5, k_2=27.5 and k_3=12.5, and for simulation without saturation limits, k_1 =0.6, k_2 = 2.3175 and k_3= 0.3375 with $\tau_{s\,llim}$=1.6 N.m and $\tau_{d\,lim}$=0.55 N.m have been used.

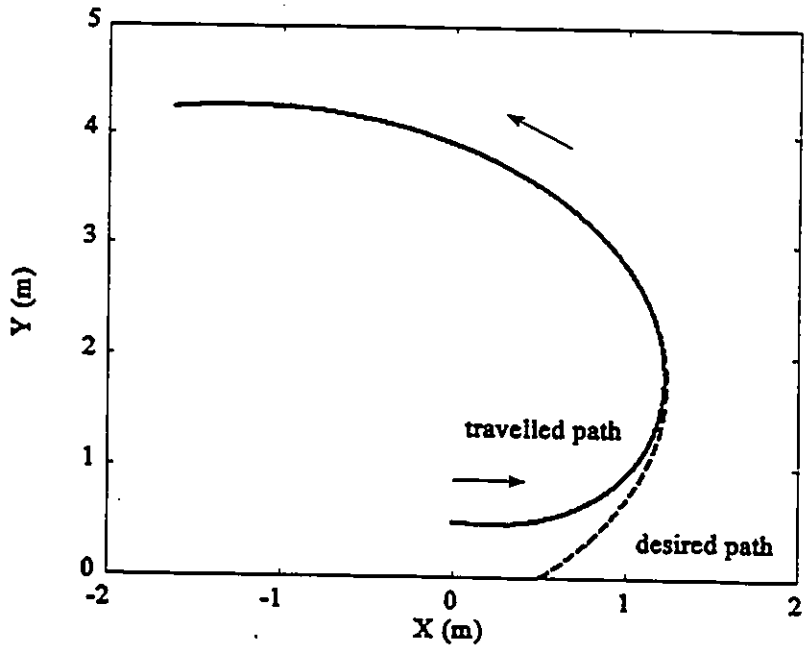

Figure 6-1 Trajectory tracking without saturation.

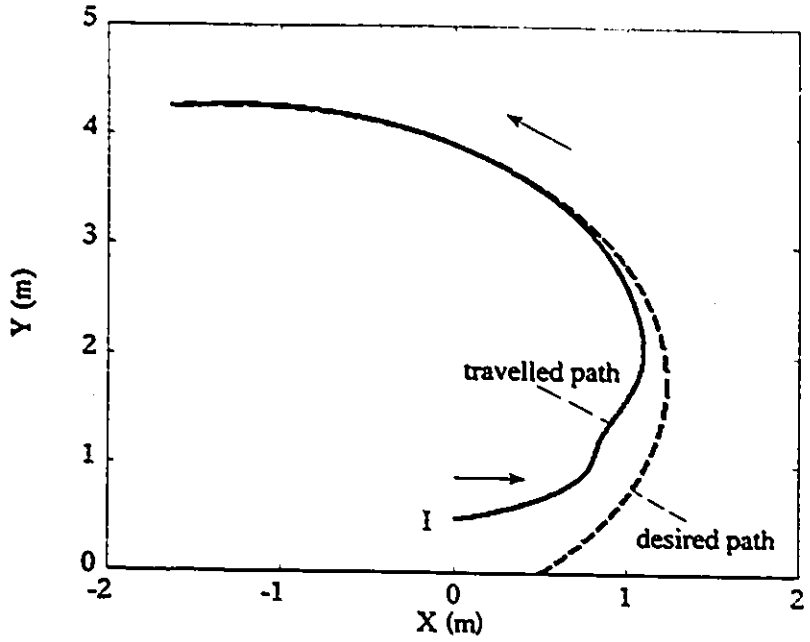

Figure 6-2 Trajectory tracking with saturation limits on input torques.

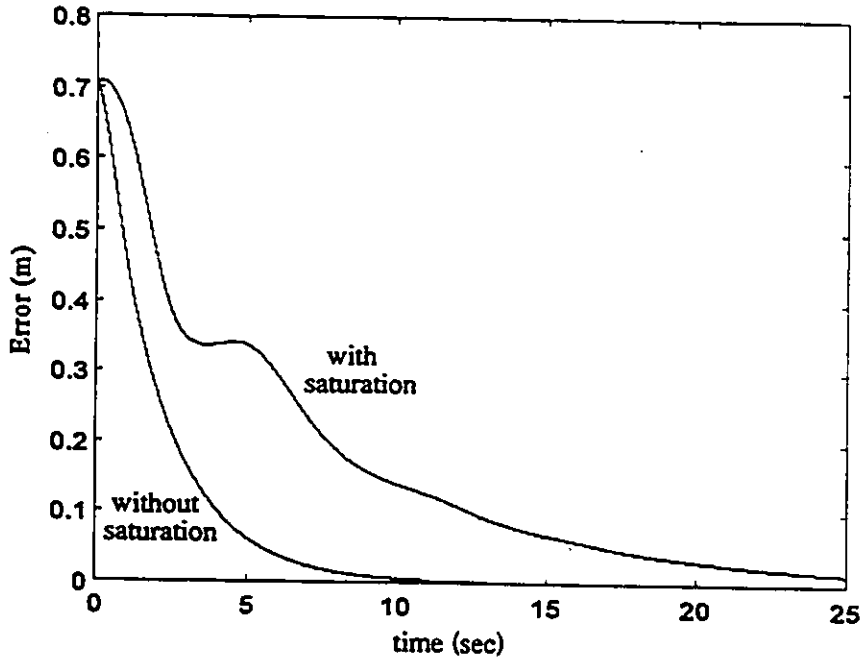

Figure 6-3 Error (distance between desired and real trajectory) versus time for both with and without saturation limits.

Stabilization to a Manifold

Asymptotic stabilization to a manifold of a two DOF vehicle in a planar motion means two out of three variables will be closed loop controlled. Usually orientation is the third variable. To illustrate this the same starting I(1.0, 1.0) and final D(3.0, 2.0) positions as in the previous section with different starting orientations, 0 and 90 degrees (Figures 6-4 and 6-5, respectively), with saturation limits are chosen. These figures clearly show that for different starting orientations (starting and final positions are the same), final orientations will not be alike. This is the main reason why researchers are interested in asymptotic (or bounded) stabilization of the vehicles. The advantage there, is that in a closed-loop (asymptotic stability) or an open-loop (bounded stability) control the vehicle would arrive at the final position with (or close to) the desired orientation.

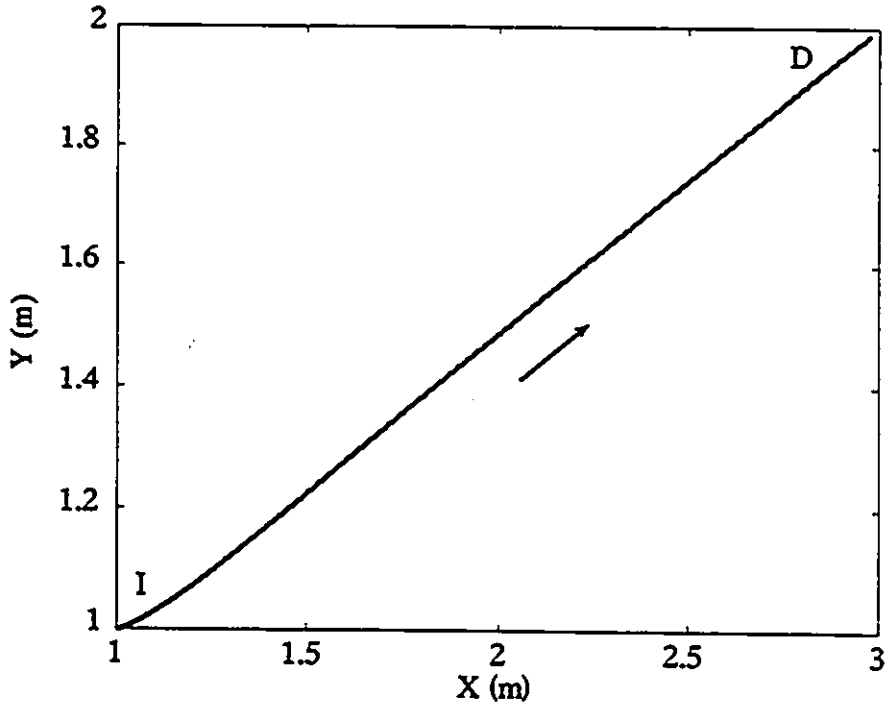

Figure 6-4 Stabilization to a manifold with 0 degree as the starting orientation.

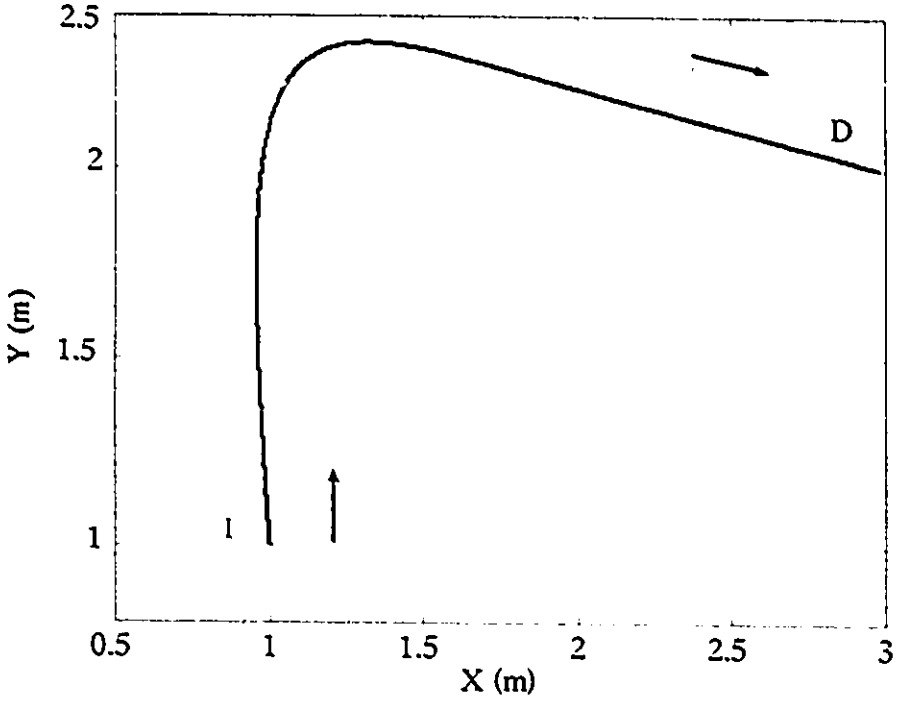

Figure 6-5 Stabilization to a manifold with 90 degree as the starting orientation.

6-4 Simulations on Internal Stability with Non-vanishing Driving Velocity

To show the validity of the discussion of section 4-3-2, two simple simulation have been performed. The initial conditions for both are the same, the vehicle starts from origin with $\delta_i = 0.1$ rad, $|\omega_1| = 0.1$, $\theta_i = 0.0$ and heading velocity ± 0.1 m/s, the only difference is that in the first simulation, it moves forward(Figures 6-6, 6-7), and in the second one, backward (Figures 6-8, 6-9).

These two simulations are not with the same gains. When the gains used for moving forward were applied for moving backward, they resulted in a faster but unstable motion (not shown). Figures (6-8) and (6-9) show a stable but slower mode around $\delta = 180°$ with $\theta = 180°$ and $\omega_1 < 0$ which was not discussed in section 4-3-2. The rotation by 180 degrees of the steering wheel (Figure 6-9) leads in fact to a subsequent forward motion while still $\omega_1 = -0.1$ rad/sec.

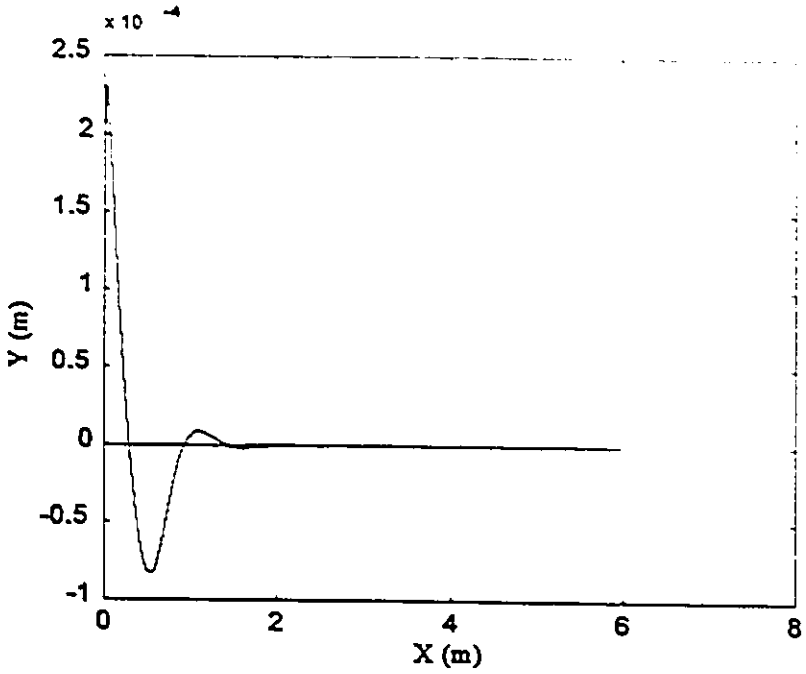

Figure 6-6 Position result of moving forward.

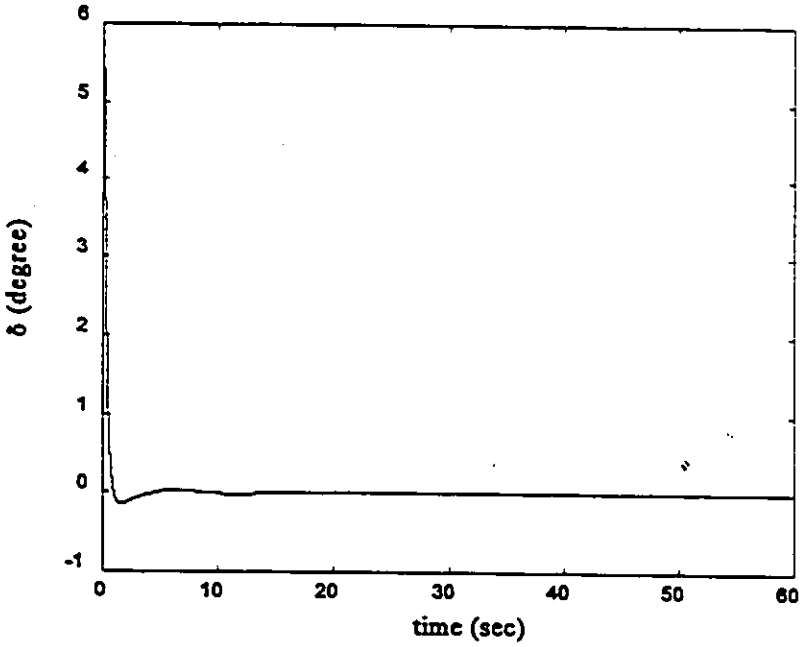

Figure 6-7 Steering angle, moving forward.

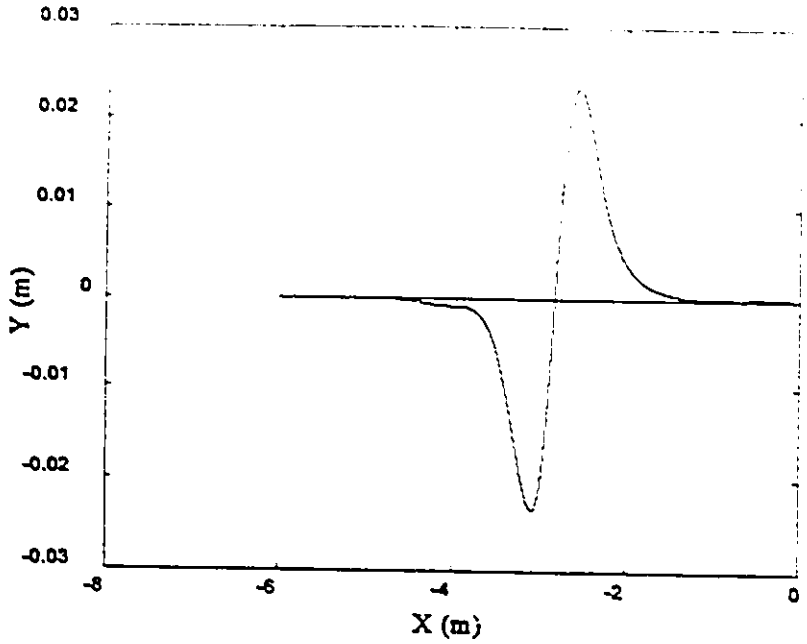

Figure 6-8 Position result of moving backward.

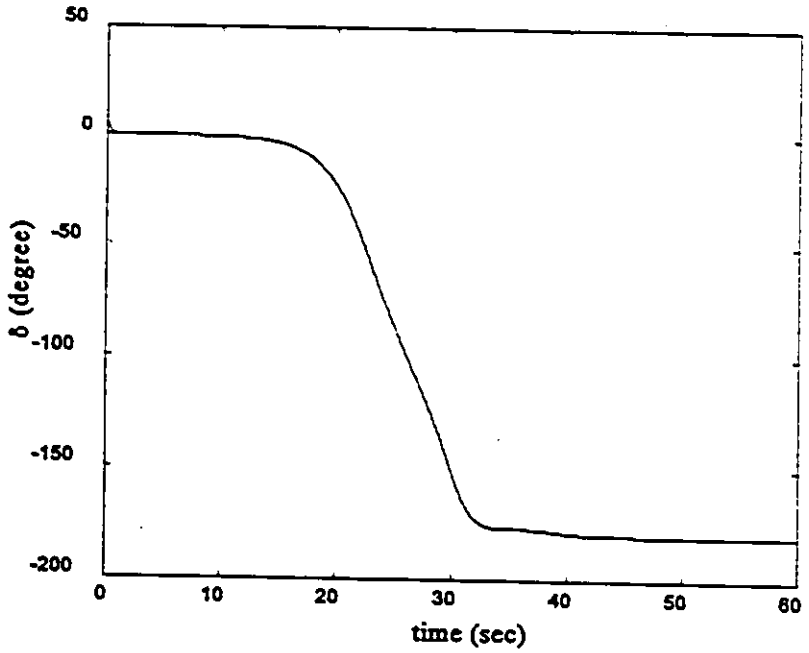

Figure 6-9 Steering angle, moving backward.

6-5 Stabilization to a Position with Orientation. Bounded Stabilization.

Bounded stabilization to a neighborhood of desired position and orientation can be achieved by using feedback linearization in terms of curvilinear space coordinates. To show this by simulation and experiment, four different configurations were chosen. These configurations are listed below:

	Starting Position	Final Position	Starting Orientation	Final Orientation
Test1	(0.0,0.0)	(2.5,1.5)	60°	-30°
Test2	(0.0,0.0)	(2.0,1.0)	30°	60°
Test3	(0.0,0.0)	(2.0,1.0)	0°	60°
Test4	(0.0,0.0)	(2.0,1.0)	0°	90°

The numbers were chosen in order that the experimental tests could be carried out in the available laboratory area. The planned path is given by the transcendental function with $\beta = 0.003$, [78] and (section 5-5-1).

6-5-1 Simulation Results

Simulation results show that by choosing proper gains for the cases of dynamic models with saturation limits on torques and with filters on odometry variables, steering angle and driving angular position, the traveled path can be very close to the planned one. Since, theoretically, the vehicle cannot start from $\omega_1 = 0$ and use input-output feedback linearization (the decoupling matrix will be singular in that case, Equation 4-25), a PD control law on steering and driving variables and their derivatives has been applied for the first two seconds of the traveling [80].

Also, after making sure that the torques are less than or equal their limits, with a safety factor of 90%, a friction model of Bo-Pavelescu type is applied to the torques

to help friction compensation [80]. Bo-Pavelescu model for low speeds is:

$$\tau_{output} = sign\,(\tau_{model})\,(\alpha\, e^{-(\frac{\omega_M}{\epsilon})^{1.5}} + \tau_{dry}) + f_{viscous}\,(\omega_M) + (\tau_{Model})$$

with;

$$V_{output} = K\,\tau_{output} \quad , \quad K = 0.4748\,(\frac{Volt}{N.m})\ for\ experiment,$$

$$K = \quad 1.0\,(\frac{Volt}{N.m})\ for\ simulation.$$

where: α is the Stribek effect coefficient

ω_M is the rotational velocity of the given motor (rad/s)

ϵ is a small rotational velocity, 0.05 (rad/s)

τ_{dry} is the dry friction (N.m)

$F_{viscous}$ is the viscous friction (N.m)

τ_{Model} is the given torque command from the controller

The simulation results were obtained by using k_1=2.4, k_2=1.9 and k_3=0.5, τ_{slim} = 4.5 N.m and τ_{dlim} = 1.35 N.m.

6-5-2 Experimental Results

The programs of the simulation with saturation and filter were modified to perform on dSPACE available at the laboratory. The main difference was that in the experiment, δ and α_1 were measured and not calculated. Also, the vehicle and not its mode, which is not perfect, was utilized. The simulation and experimental results are presented together in order to compare them more easily. Different gains were used for different tests. The results of the experiments will be summarized at the end of this section.

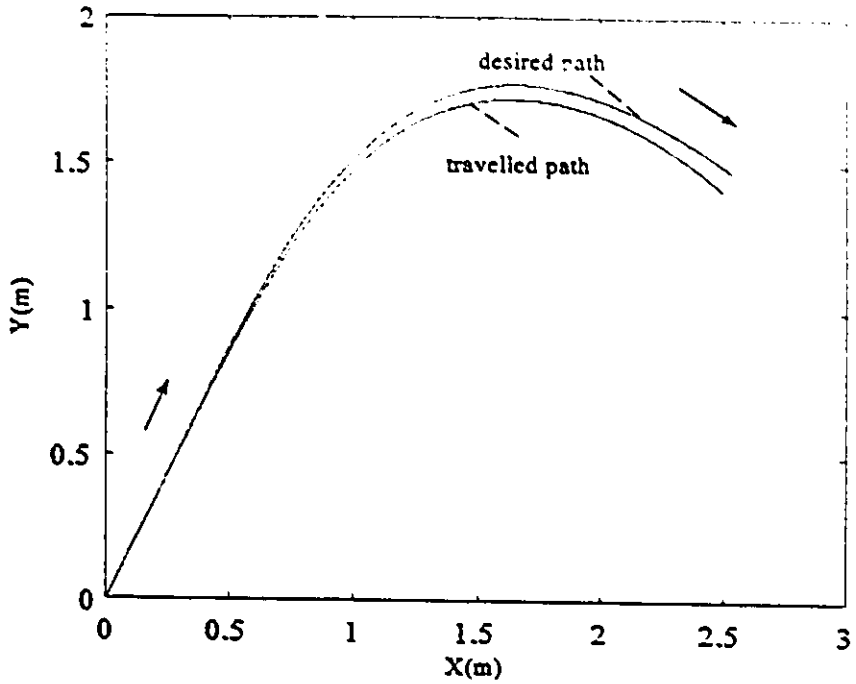

Figure 6-10 Test 1. Experiment. Curvilinear space position control.

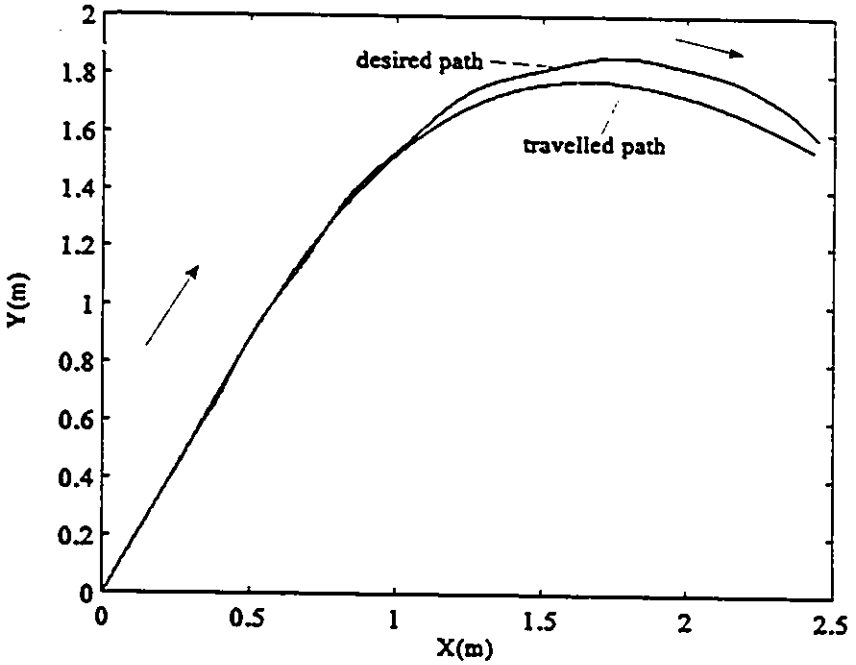

Figure 6-11 Test 1. Simulation. Curvilinear space position control.

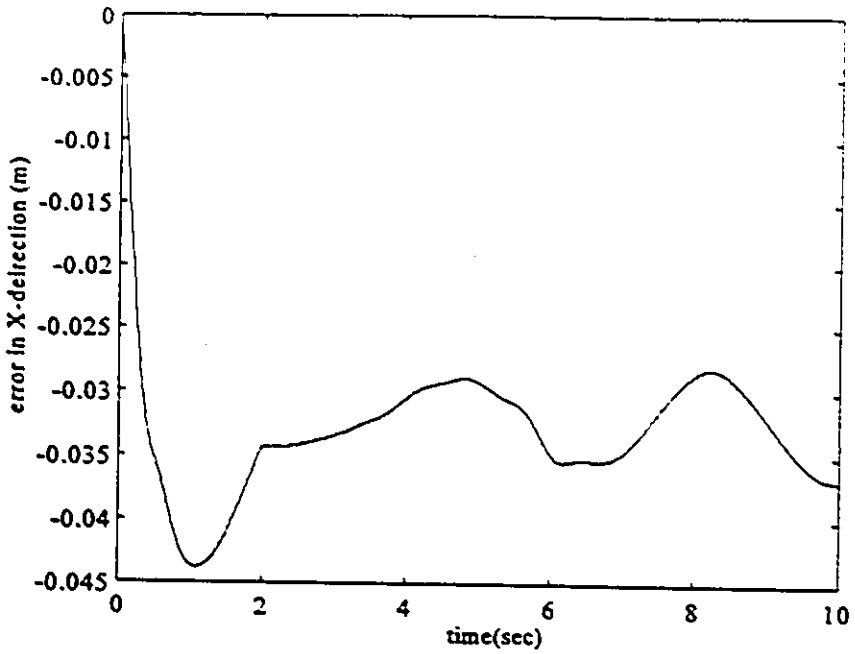

Figure 6-12 Test 1. Experiment. Error in X-direction versus time.

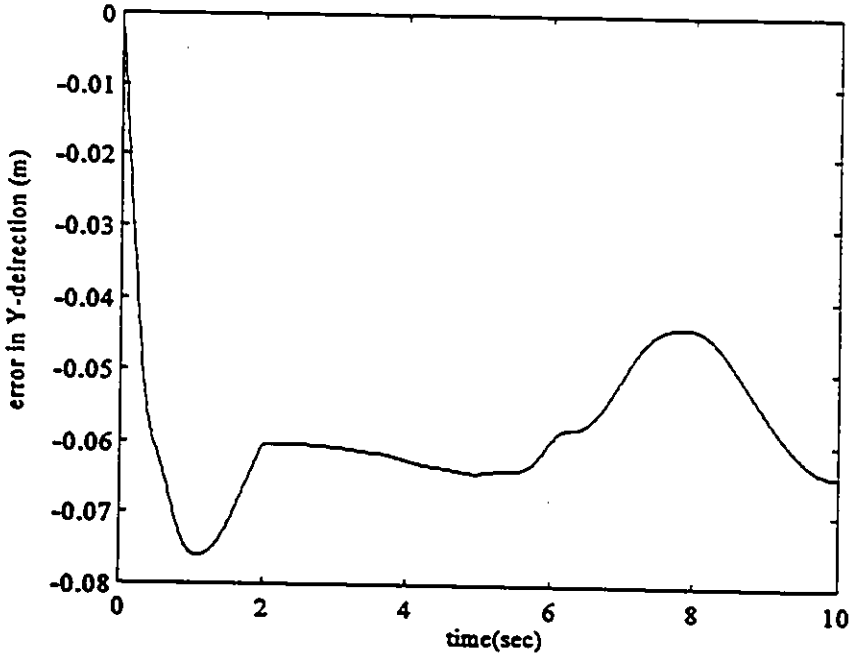

Figure 6-13 Test 1. Experiment. Error in Y-direction versus time.

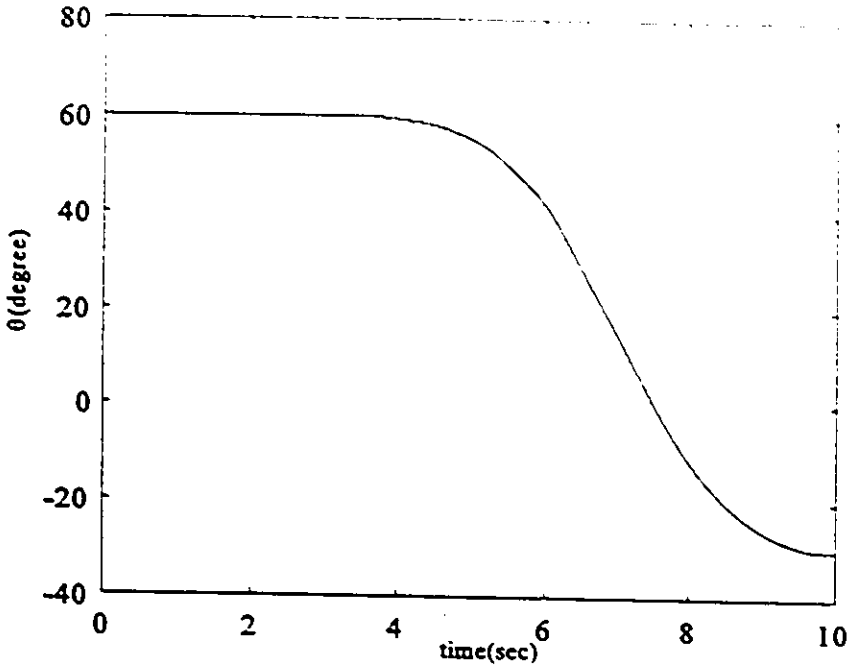

Figure 6-14 Test 1. Experiment. θ (orientation) versus time.

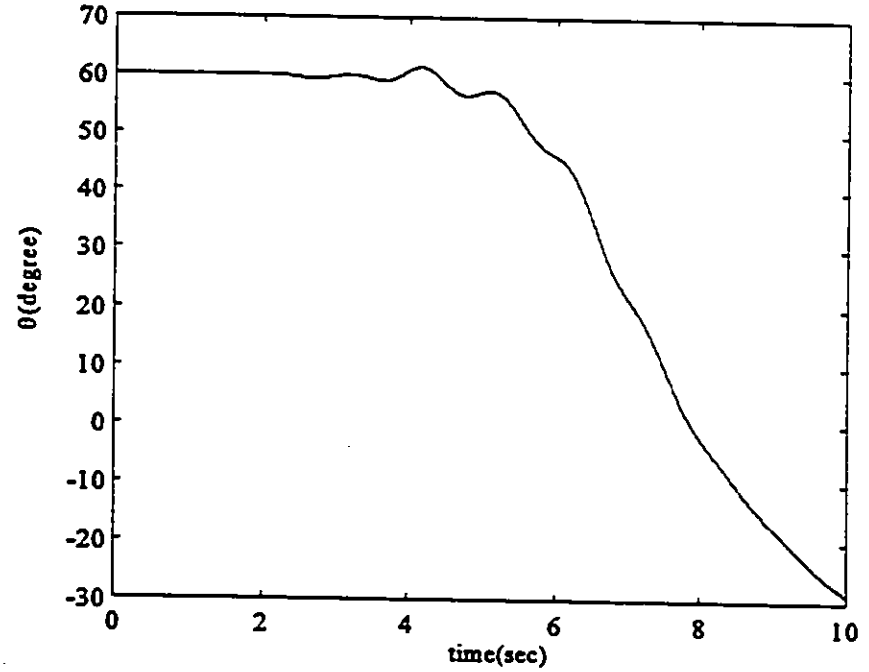

Figure 6-15 Test 1. Simulation. θ (orientation) versus time.

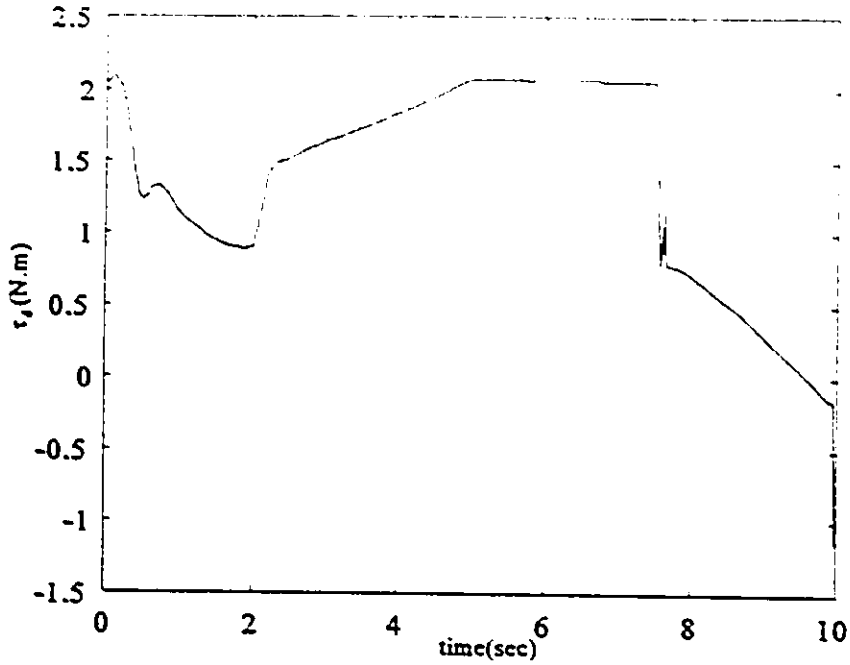

Figure 6-16 Test 1. Experiment. τ_d (driving torque) versus time.

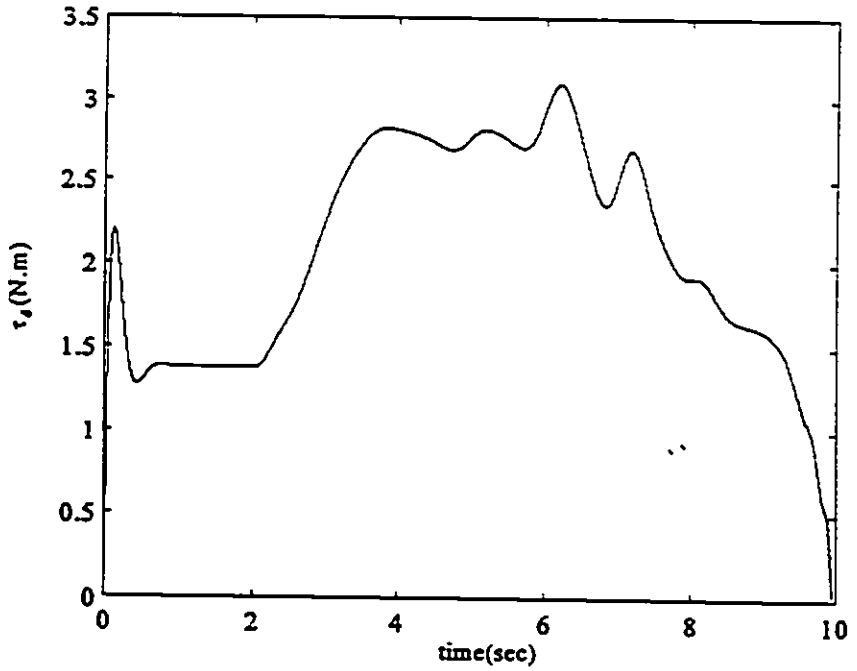

Figure 6-17 Test 1. Simulation. τ_d (driving torque) versus time.

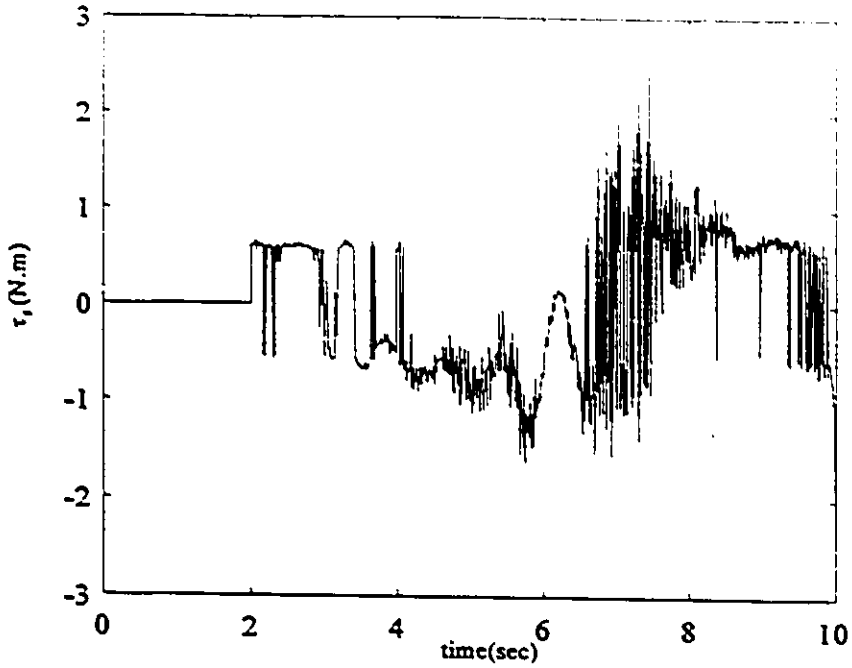

Figure 6-18 Test 1. Experiment. τ_s (steering torque) versus time.

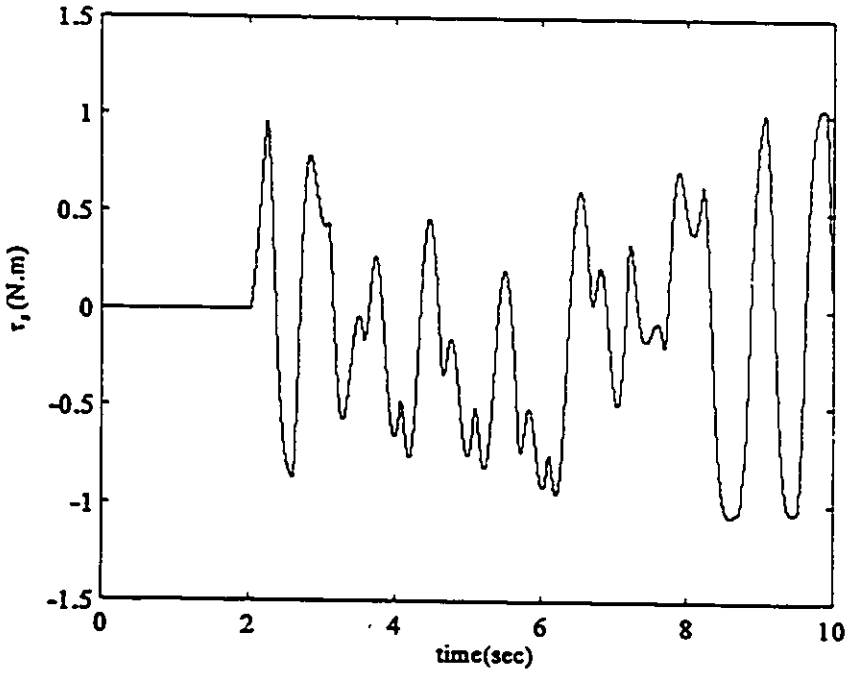

Figure 6-19 Test 1. Simulation. τ_s (steering torque) versus time.

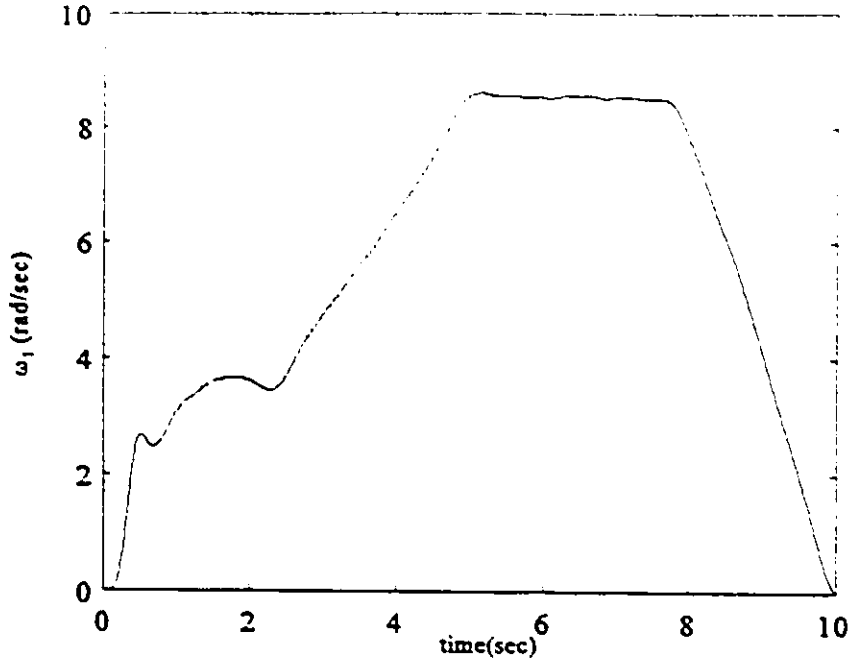

Figure 6-20 Test 1. Experiment. ω_1 versus time.

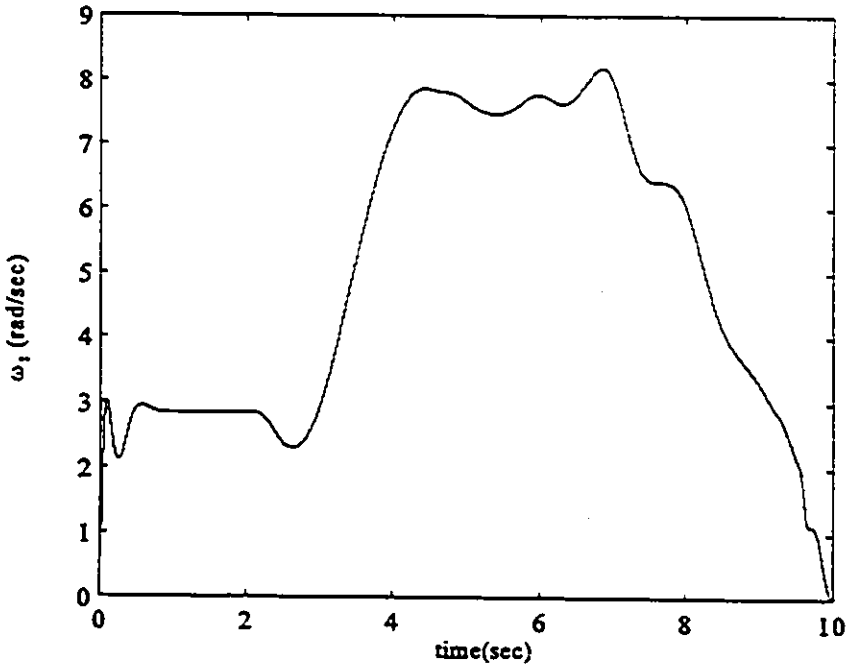

Figure 6-21 Test 1. Simulation. ω_1 versus time.

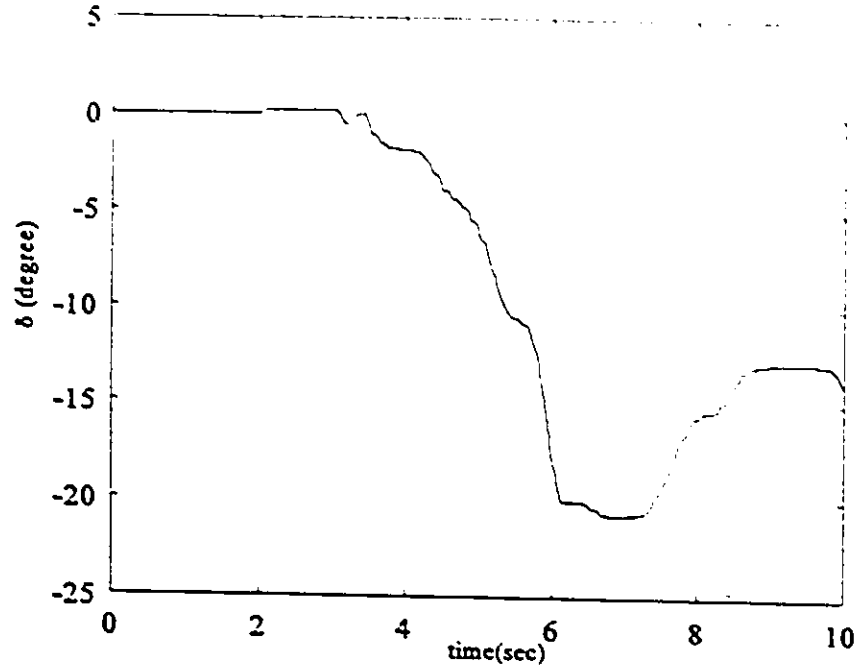

Figure 6-22 Test 1. Experiment. δ (steering angle) versus time.

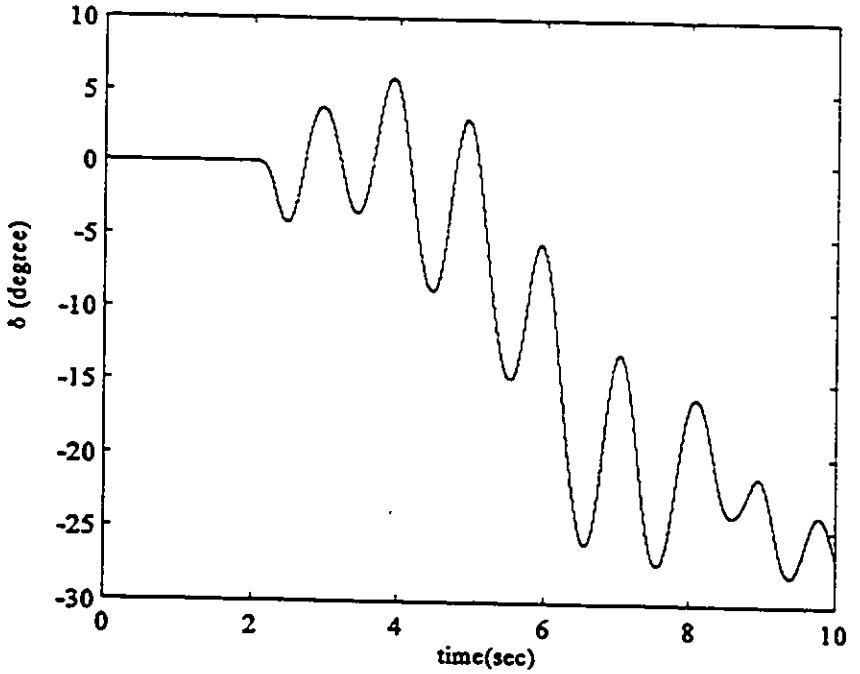

Figure 6-23 Test 1. Simulation. δ (steering angle) versus time.

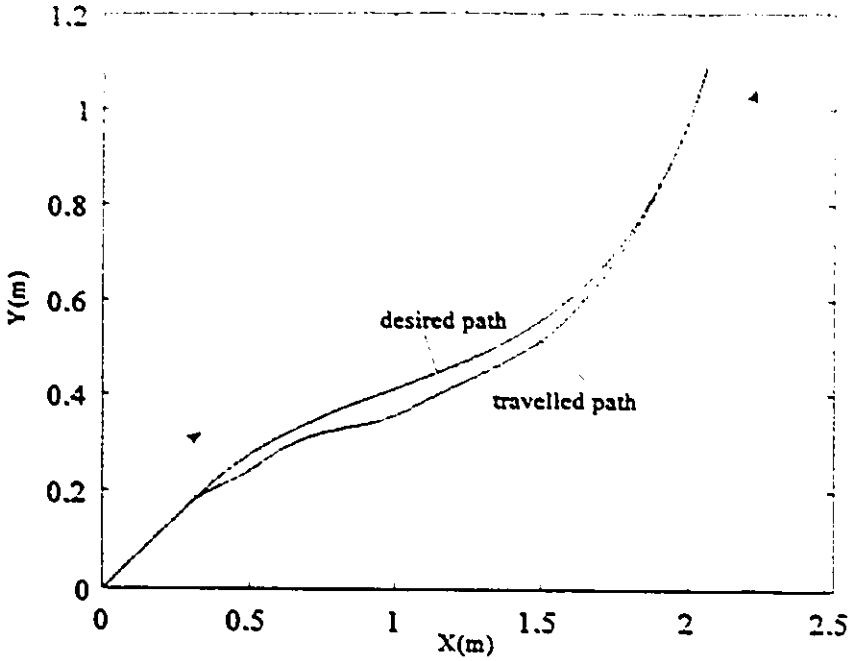

Figure 6-24 Test 2. Experiment. Curvilinear space position control.

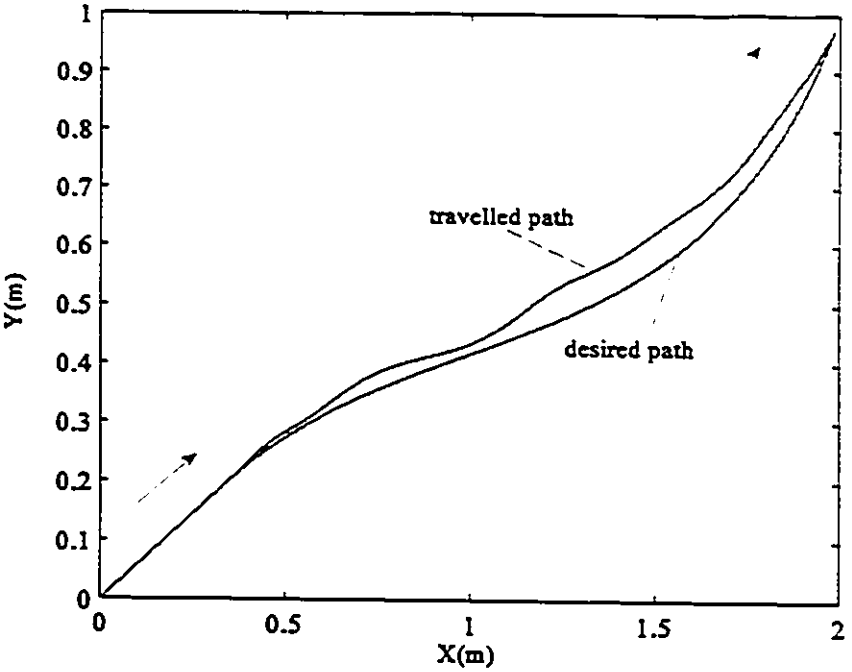

Figure 6-25 Test 2. Simulation. Curvilinear space position control.

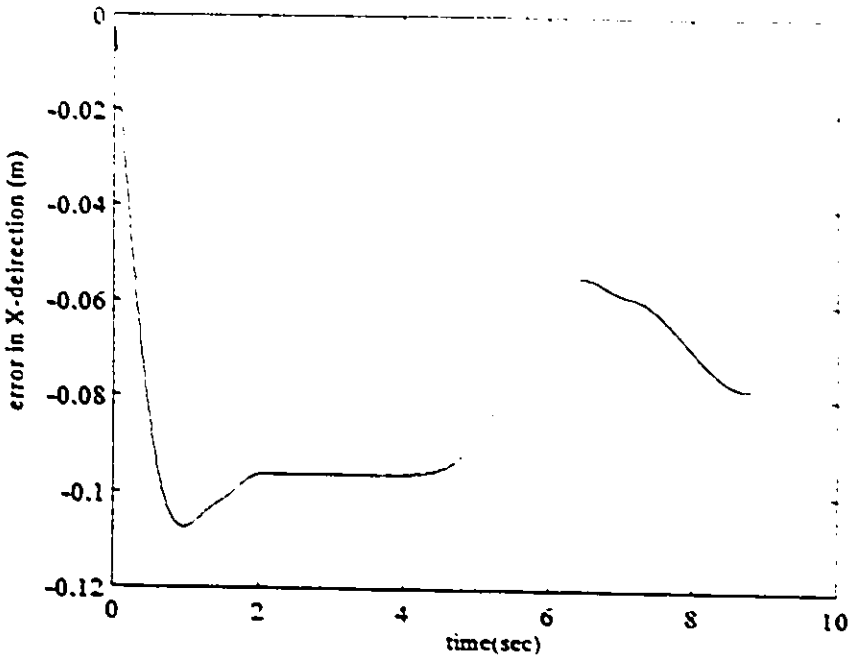

Figure 6-26 Test 2. Experiment. Error in X-direction versus time.

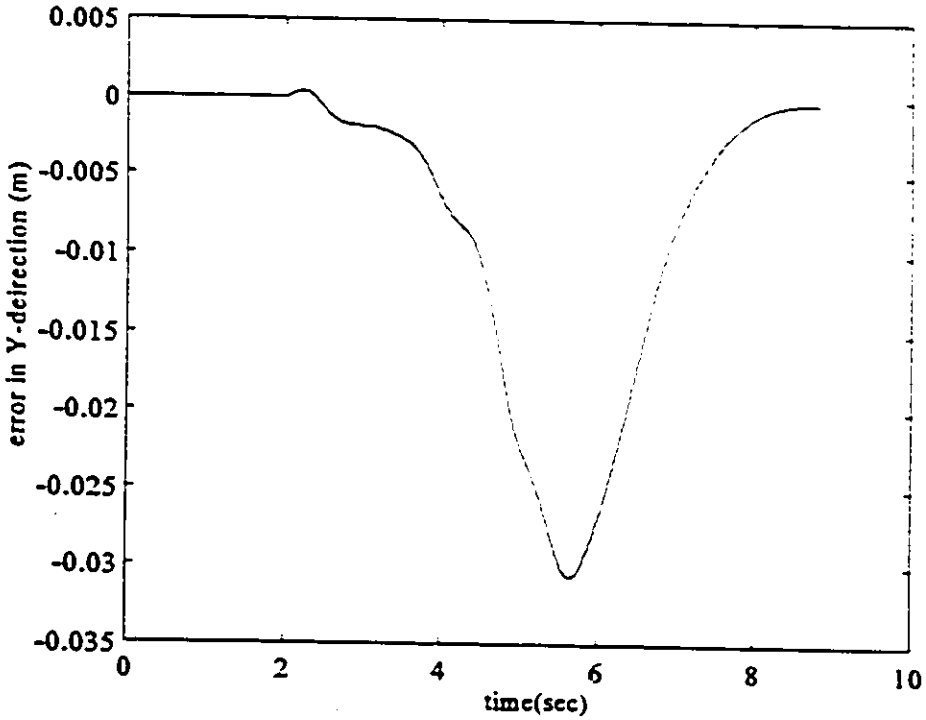

Figure 6-27 Test 2. Experiment. Error in Y-direction versus time.

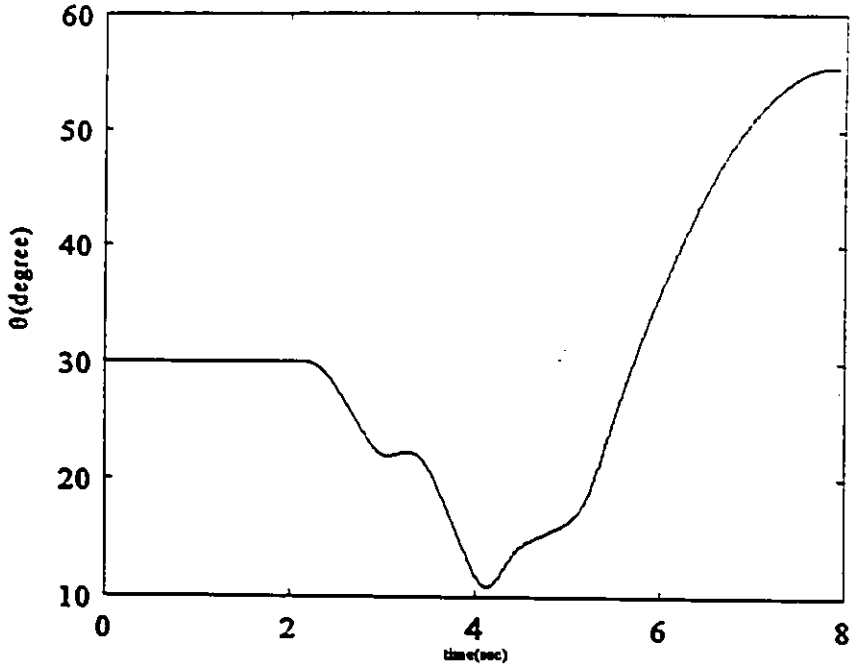

Figure 6-28 Test 2. Experiment. θ (orientation) versus time.

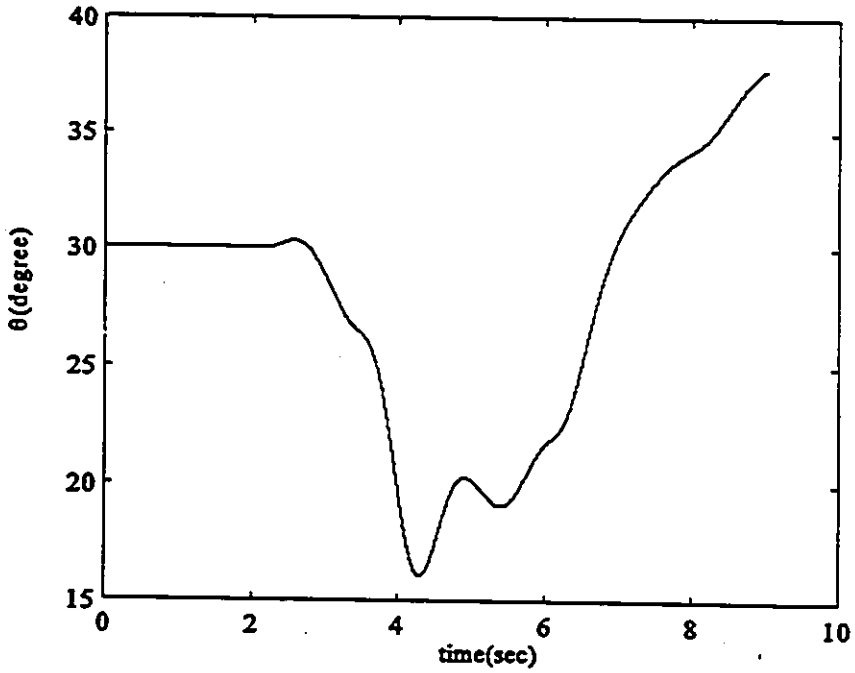

Figure 6-29 Test 2. Simulation. θ (orientation) versus time.

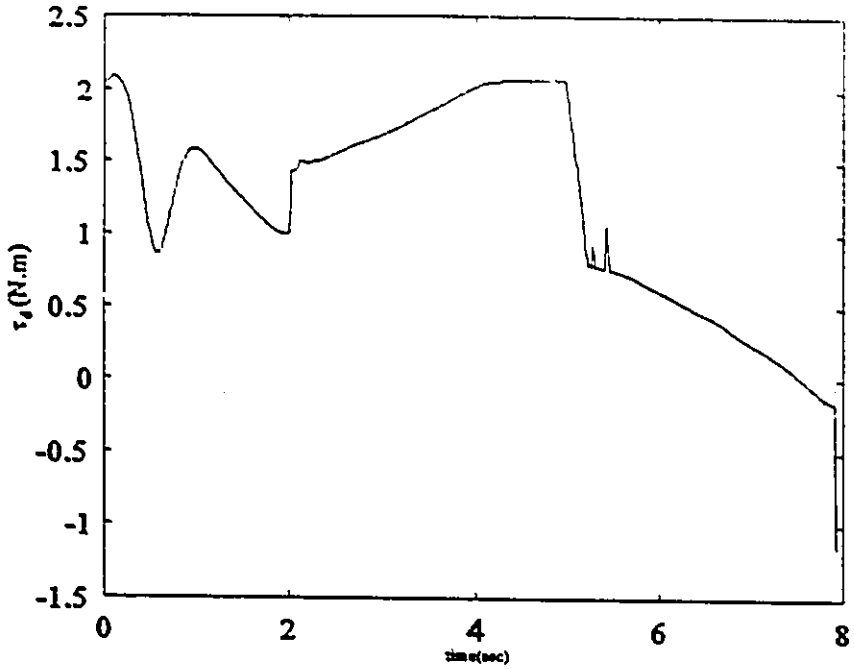

Figure 6-30 Test 2. Experiment. τ_d (driving torque) versus time.

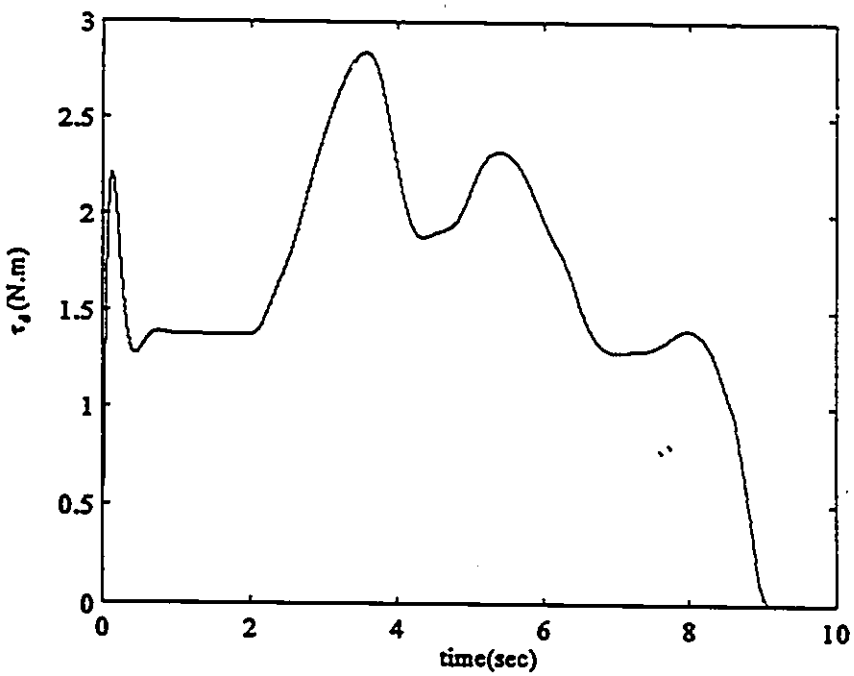

Figure 6-31 Test 2. Simulation. τ_d (driving torque) versus time.

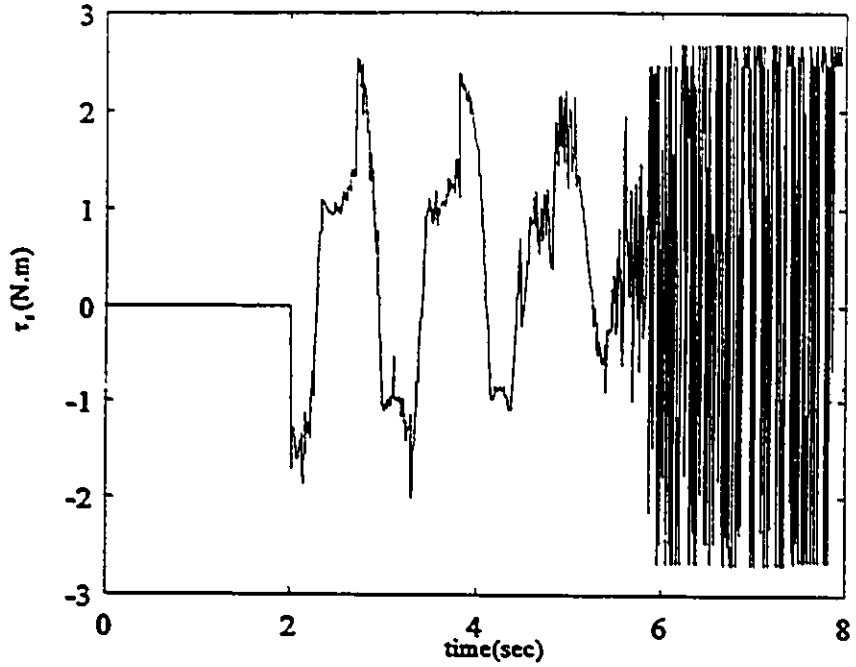

Figure 6-32 Test 2. Experiment. τ_s (steering torque) versus time.

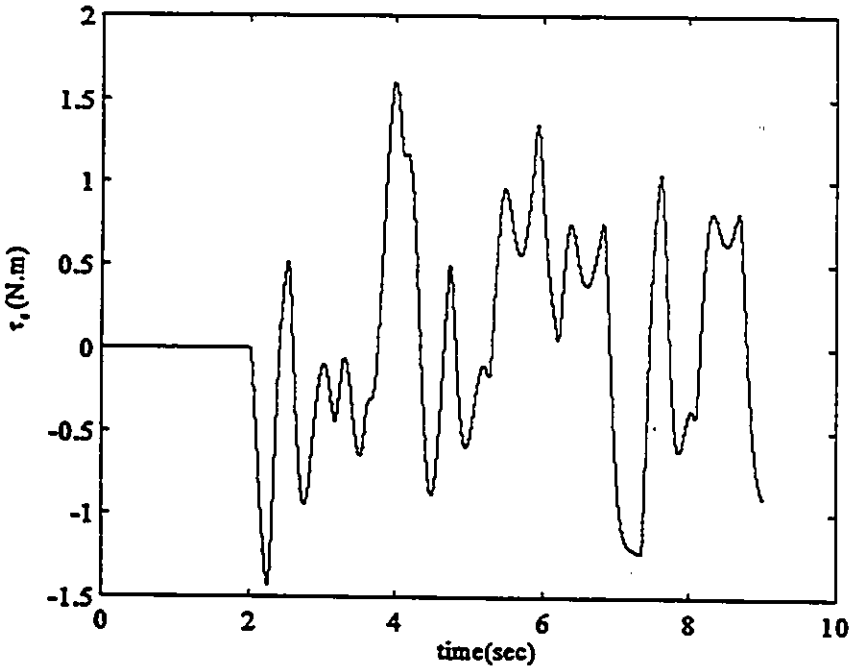

Figure 6-33 Test 2. Simulation. τ_s (steering torque) versus time.

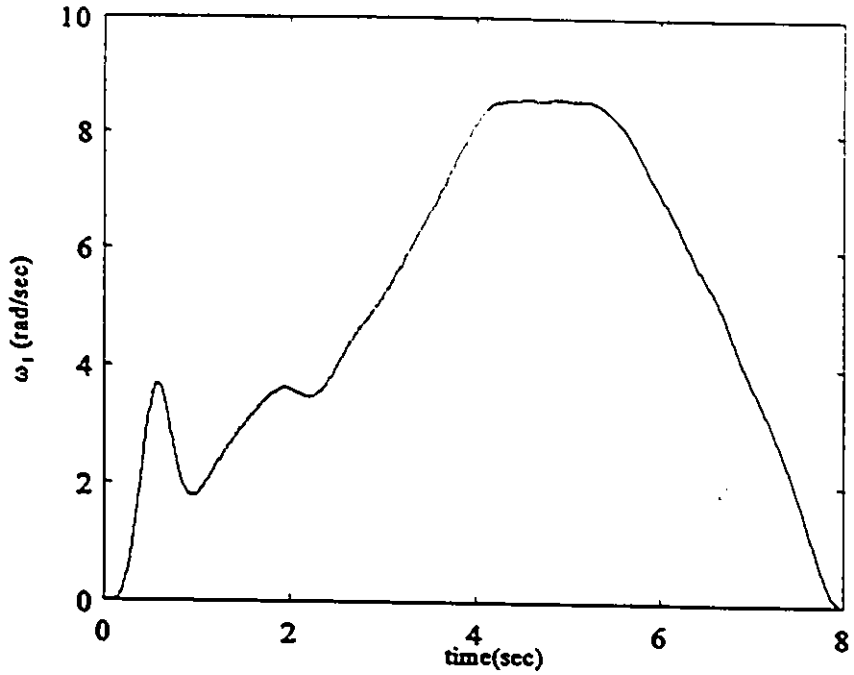

Figure 6-34 Test 2. Experiment. ω_1 versus time.

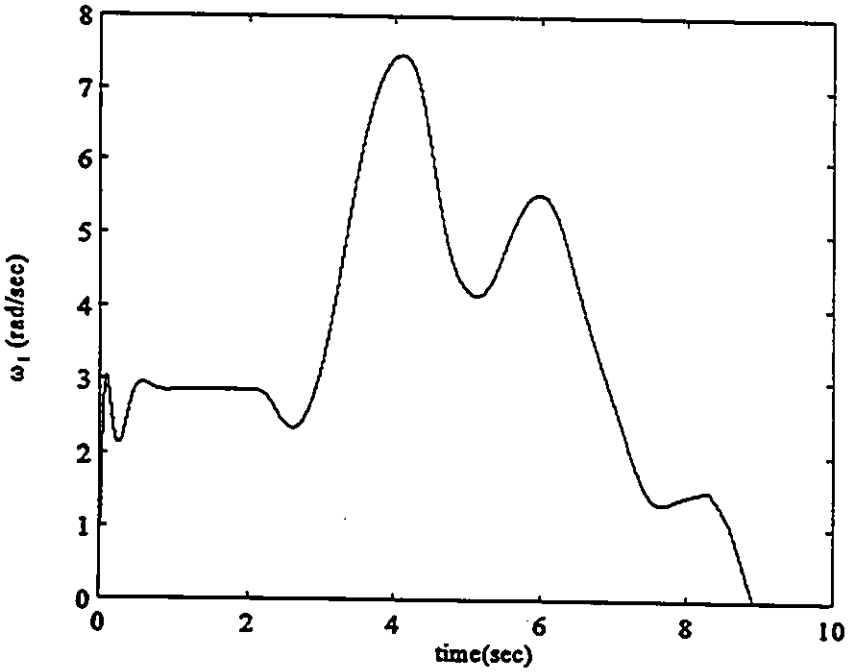

Figure 6-35 Test 2. Simulation. ω_1 versus time.

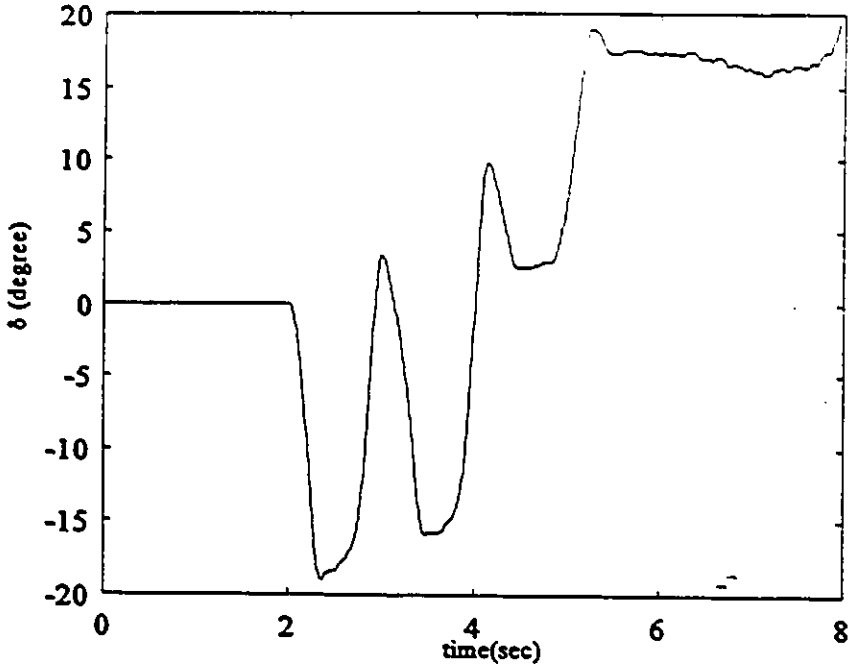

Figure 6-36 Test 2. Experiment. δ (steering angle) versus time.

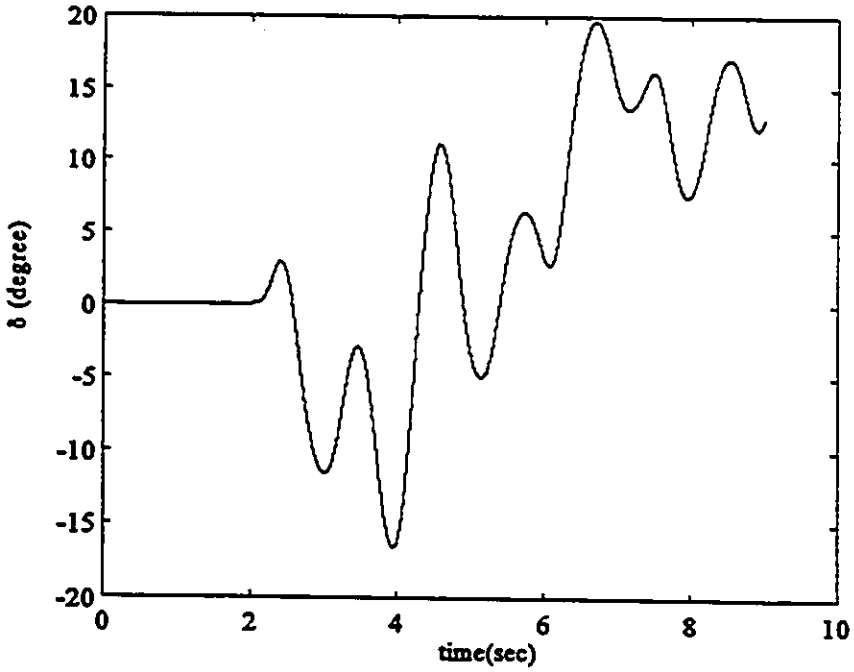

Figure 6-37 Test 2. Simulation. δ (steering angle) versus time.

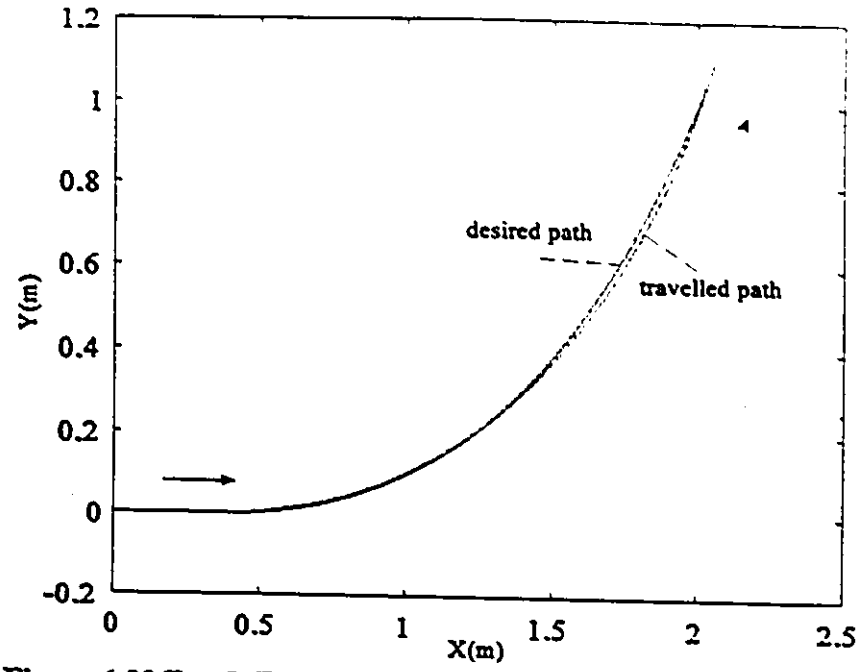

Figure 6-38 Test 3. Experiment. Curvilinear space position control.

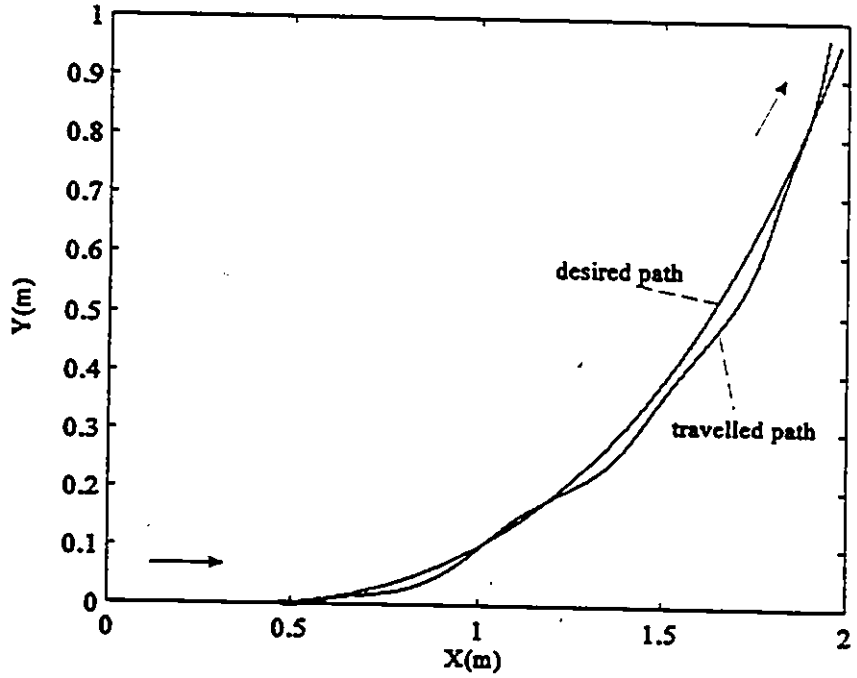

Figure 6-39 Test 3. Simulation. Curvilinear space position control.

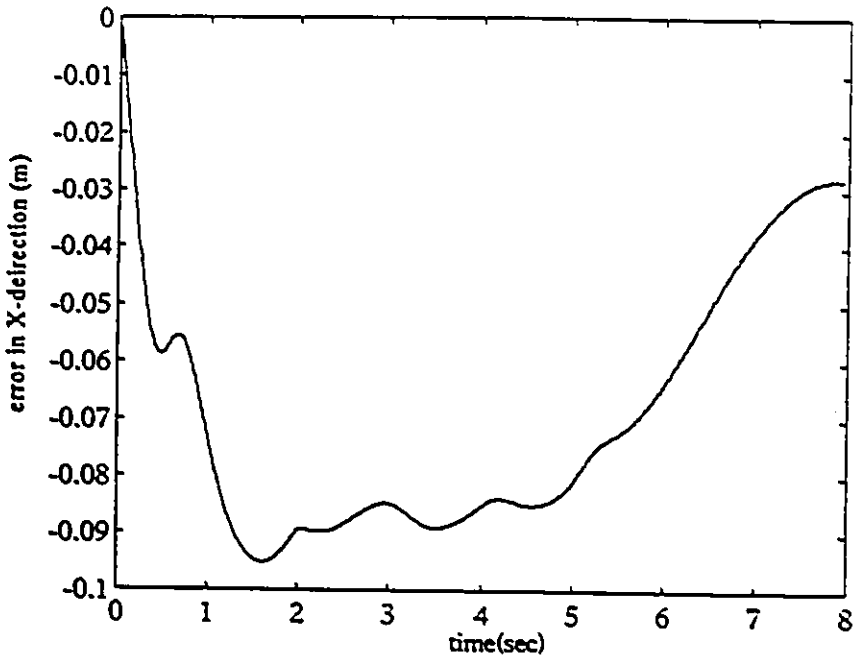

Figure 6-40 Test 3. Experiment. Error in X-direction versus time.

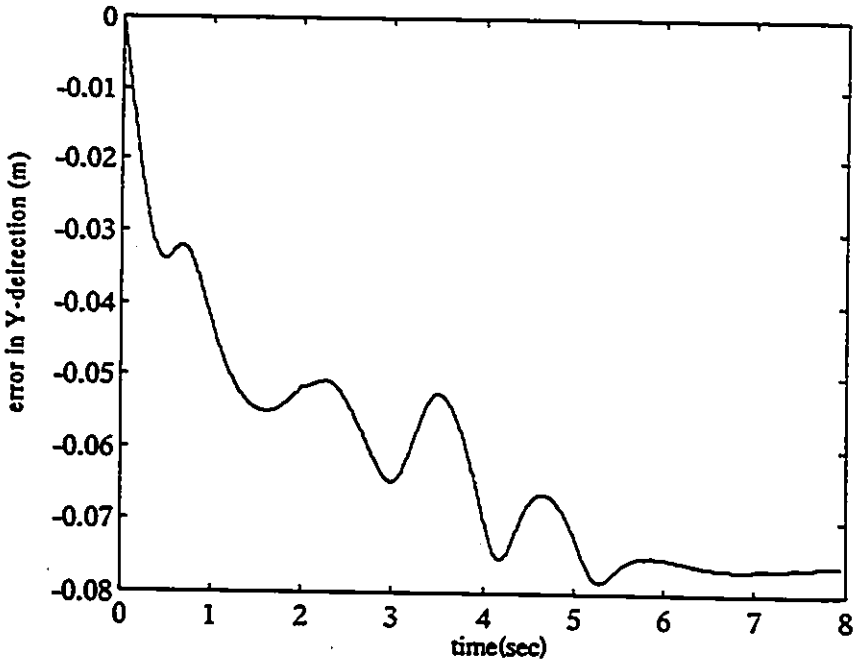

Figure 6-41 Test 3. Experiment. Error in Y-direction versus time.

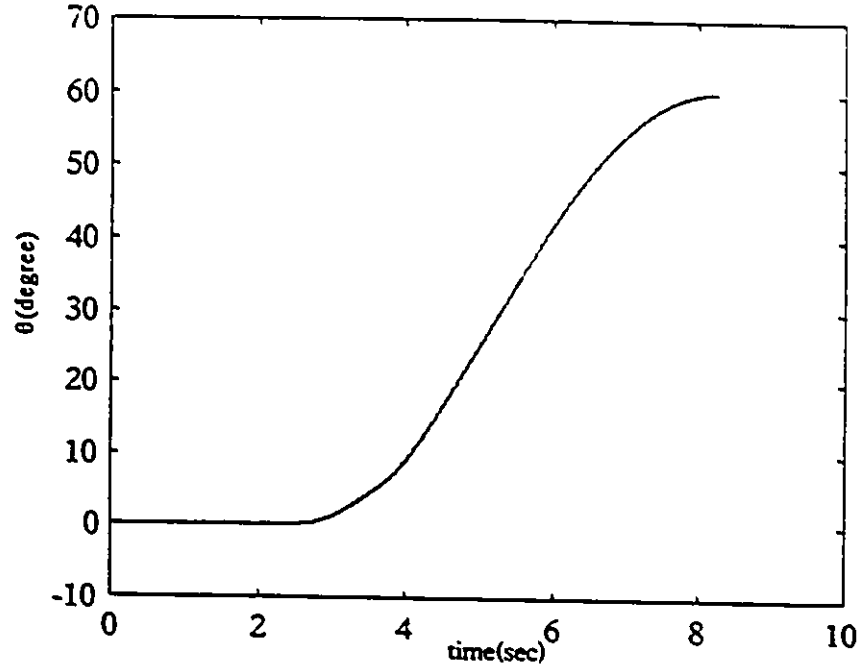

Figure 6-42 Test 3. Experiment. θ (orientation) versus time.

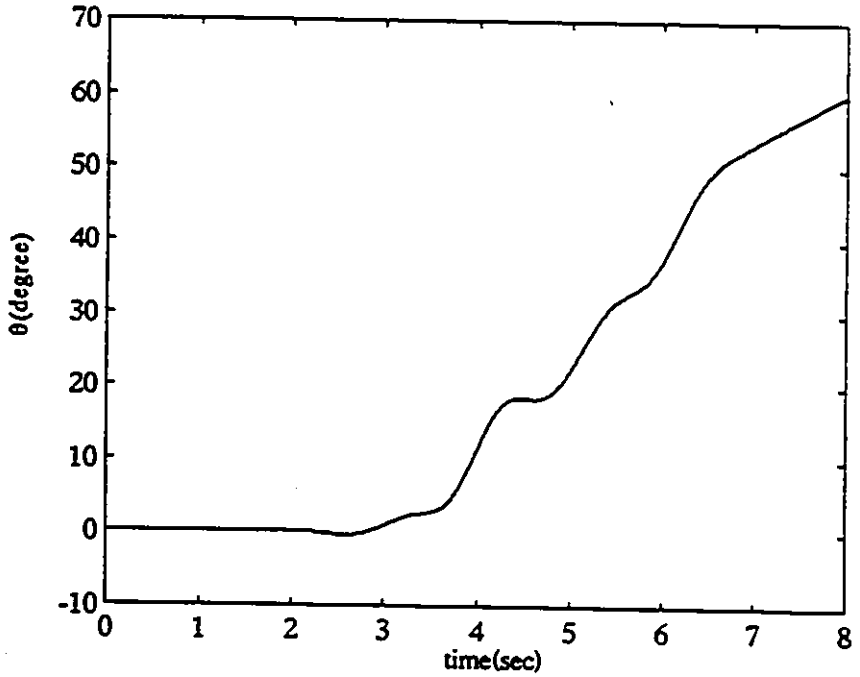

Figure 6-43 Test 3. Simulation. θ (orientation) versus time.

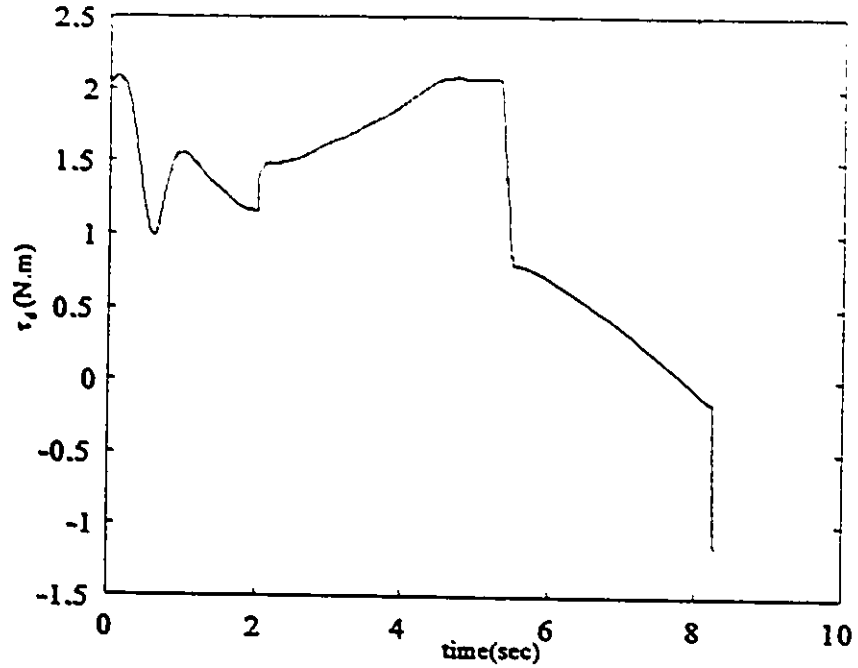

Figure 6-44 Test 3. Experiment. τ_d (driving torque) versus time.

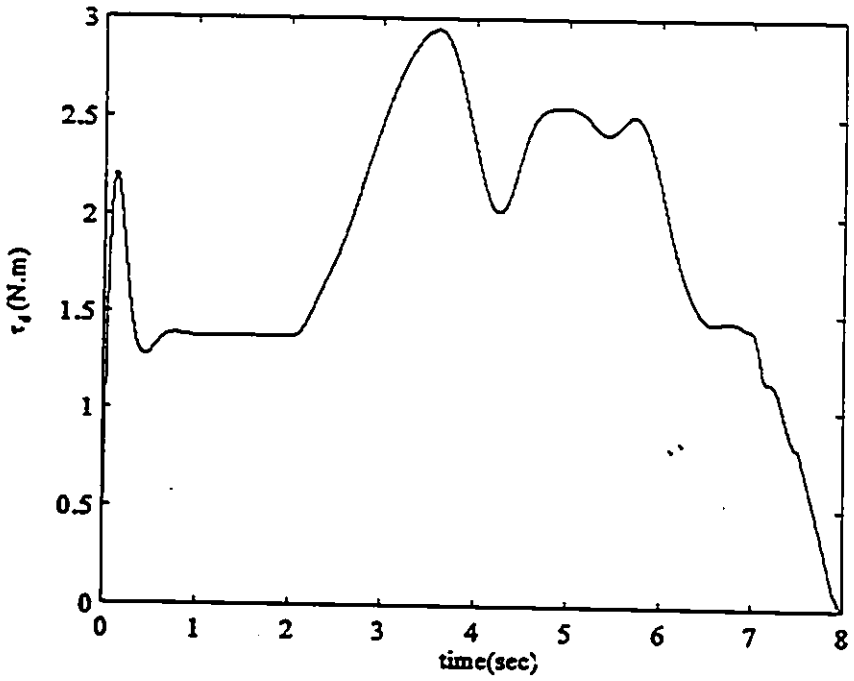

Figure 6-45 Test 3. Simulation. τ_d (driving torque) versus time.

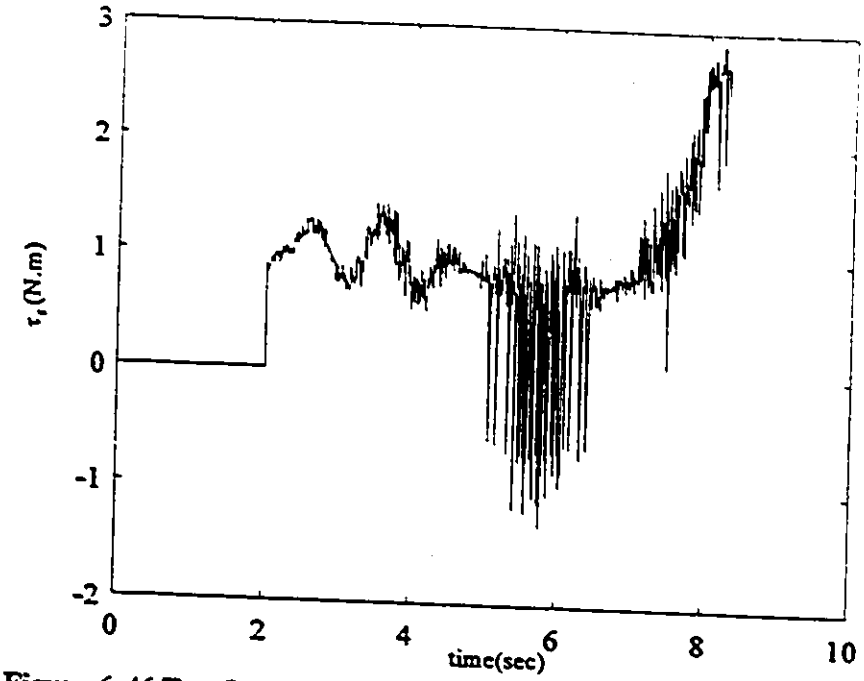

Figure 6-46 Test 3. Experiment. τ_s (steering torque) versus time.

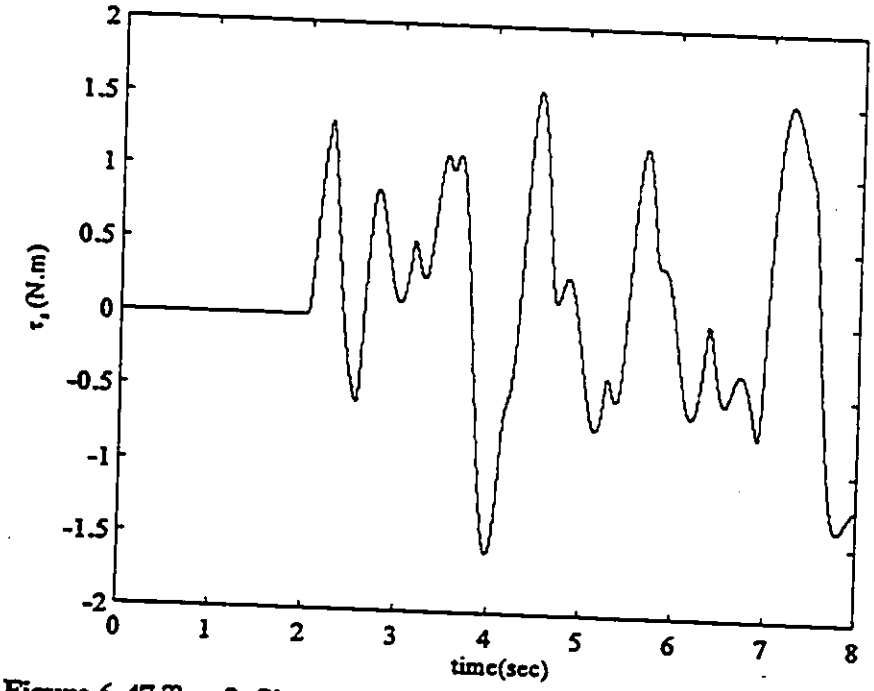

Figure 6-47 Test 3. Simulation. τ_s (steering torque) versus time.

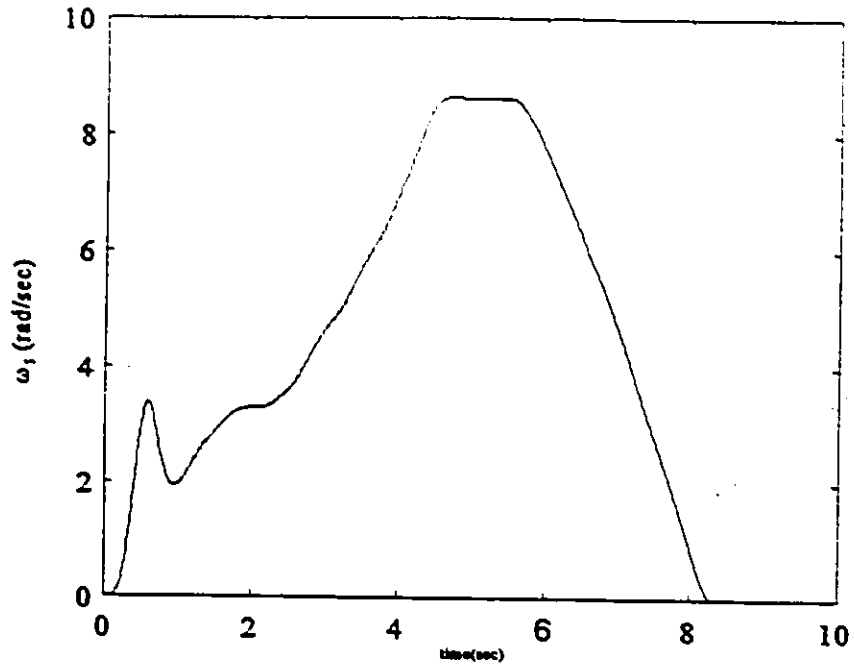

Figure 6-48 Test 3. Experiment. ω_1 versus time.

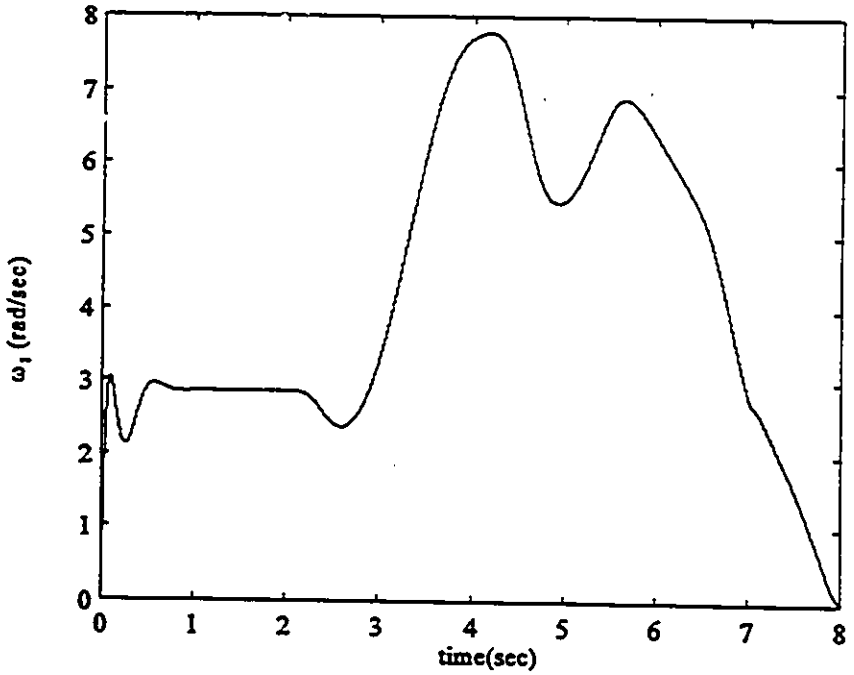

Figure 6-49 Test 3. Simulation. ω_1 versus time.

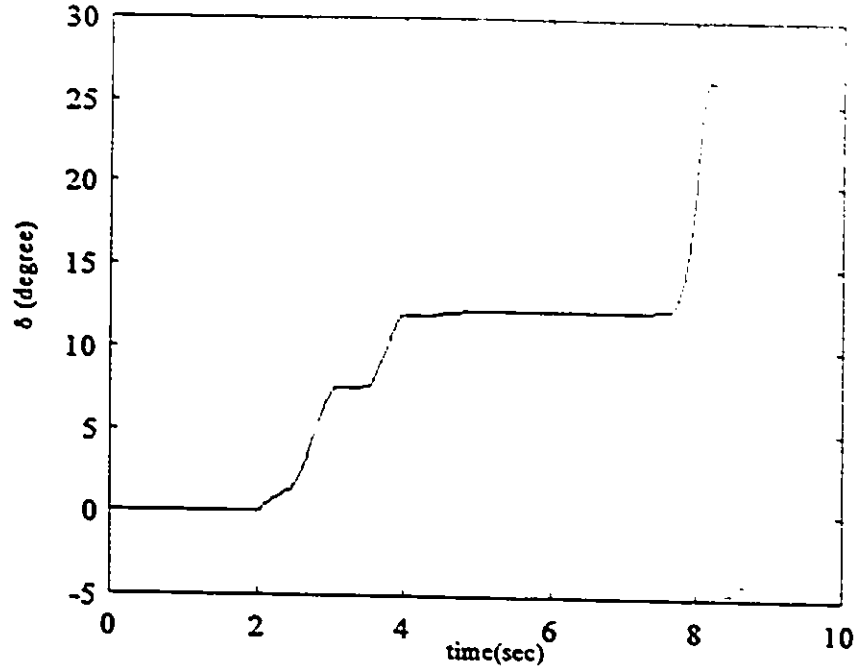

Figure 6-50 Test 3. Experiment. δ (steering angle) versus time.

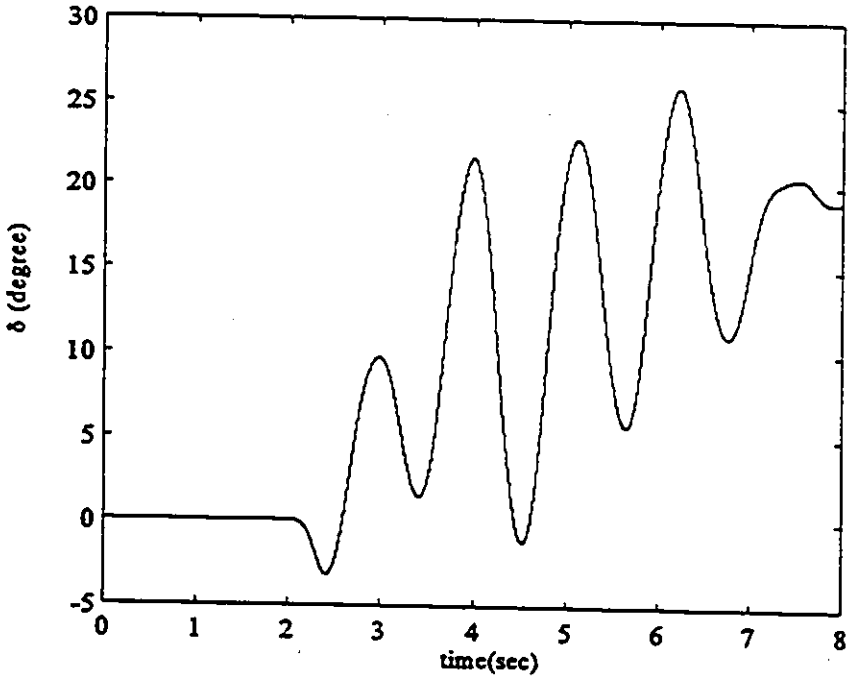

Figure 6-51 Test 3. Simulation. δ (steering angle) versus time.

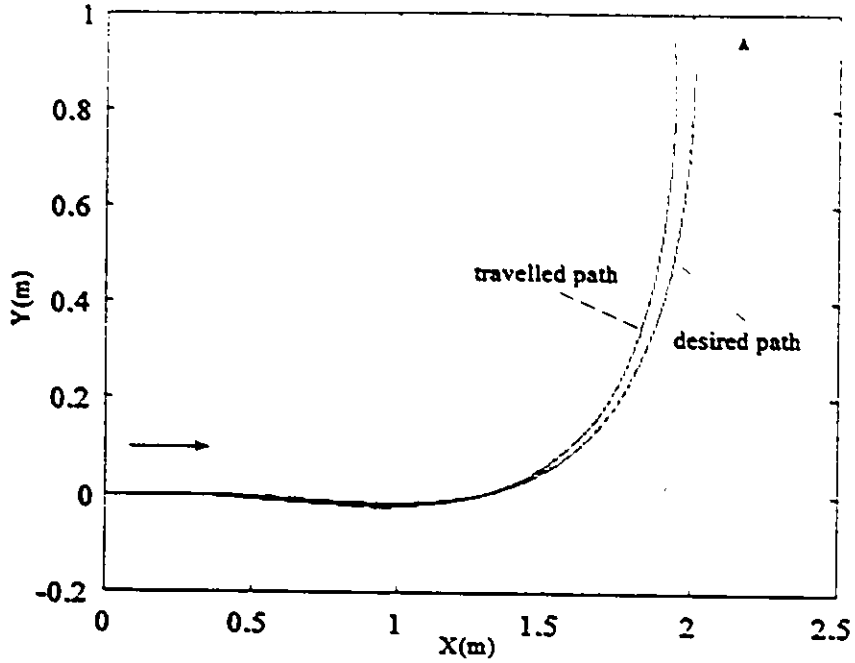

Figure 6-52 Test 4. Experiment. Curvilinear space position control.

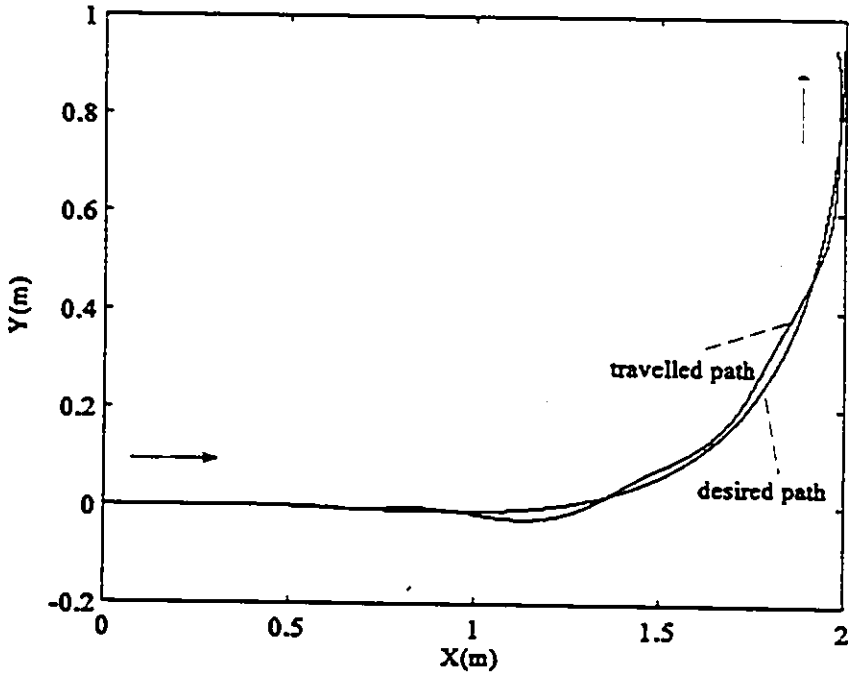

Figure 6-53 Test 4. Simulation. Curvilinear space position control.

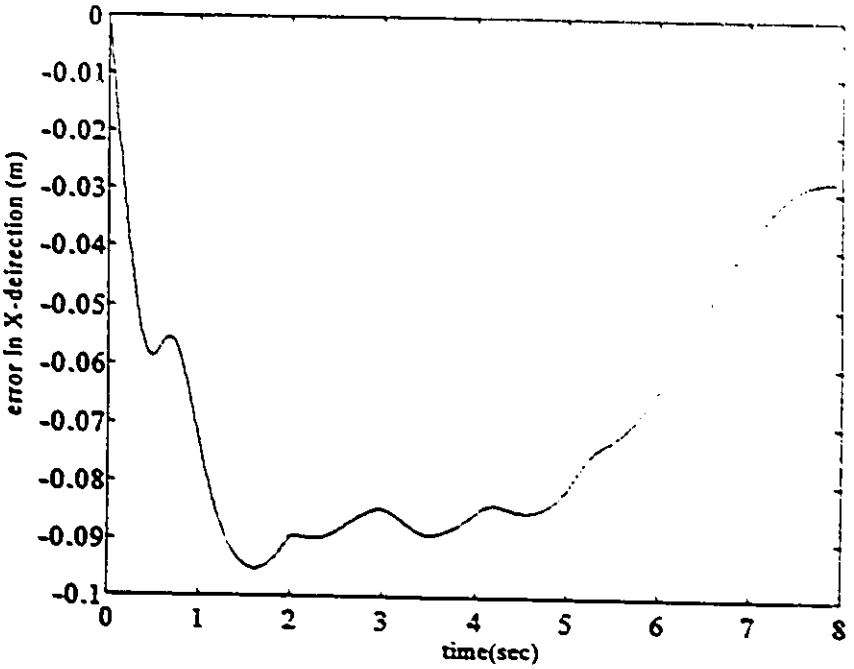

Figure 6-54 Test 4. Experiment. Error in X-direction versus time.

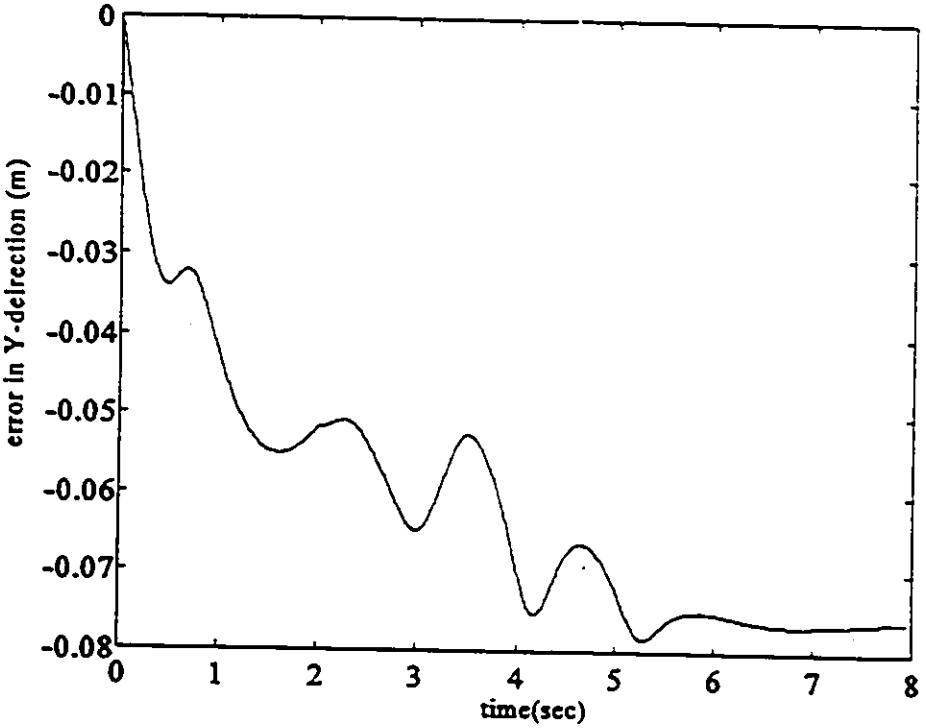

Figure 6-55 Test 4. Experiment. Error in Y-direction versus time.

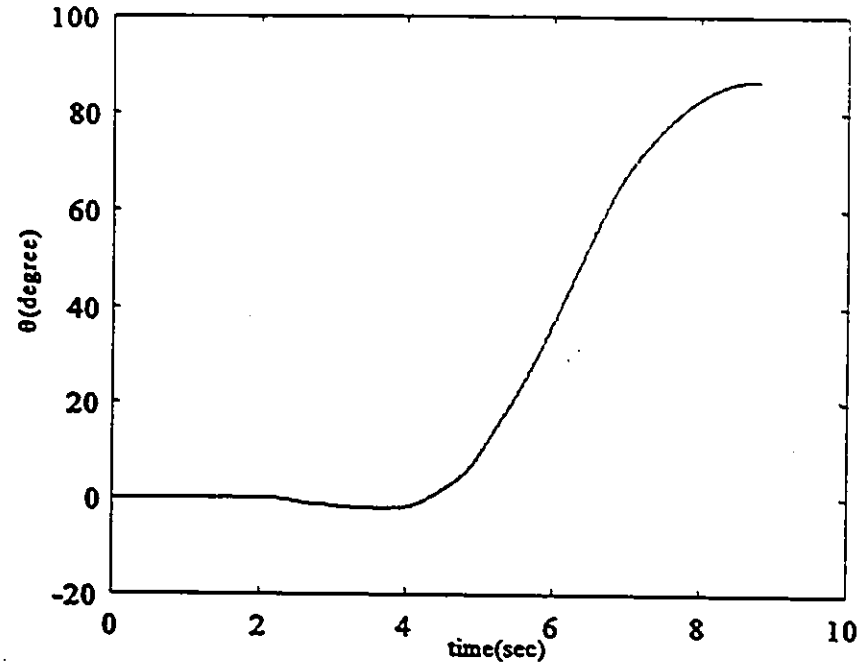

Figure 6-56 Test 4. Experiment. θ (orientation) versus time.

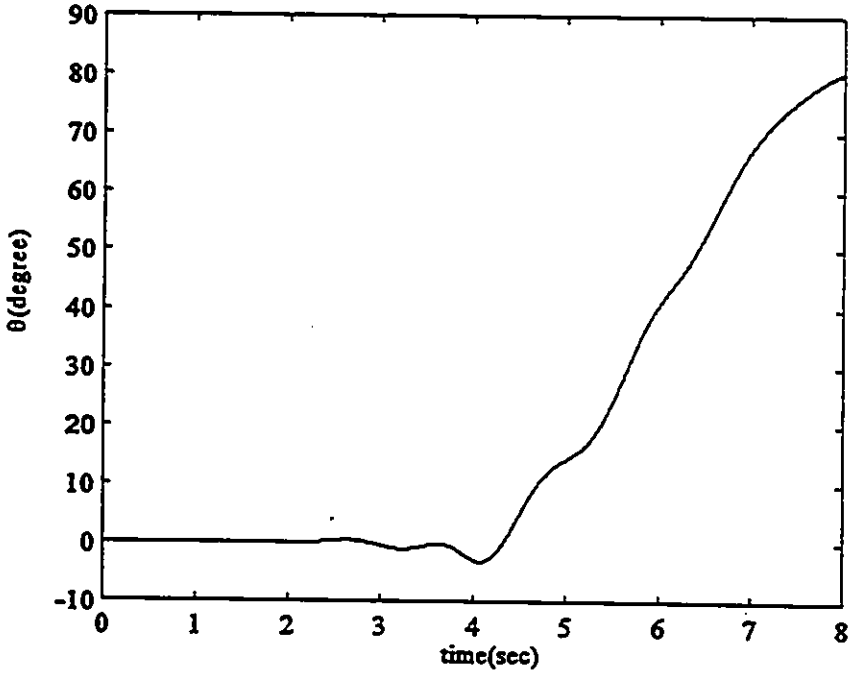

Figure 6-57 Test 4. Simulation. θ (orientation) versus time.

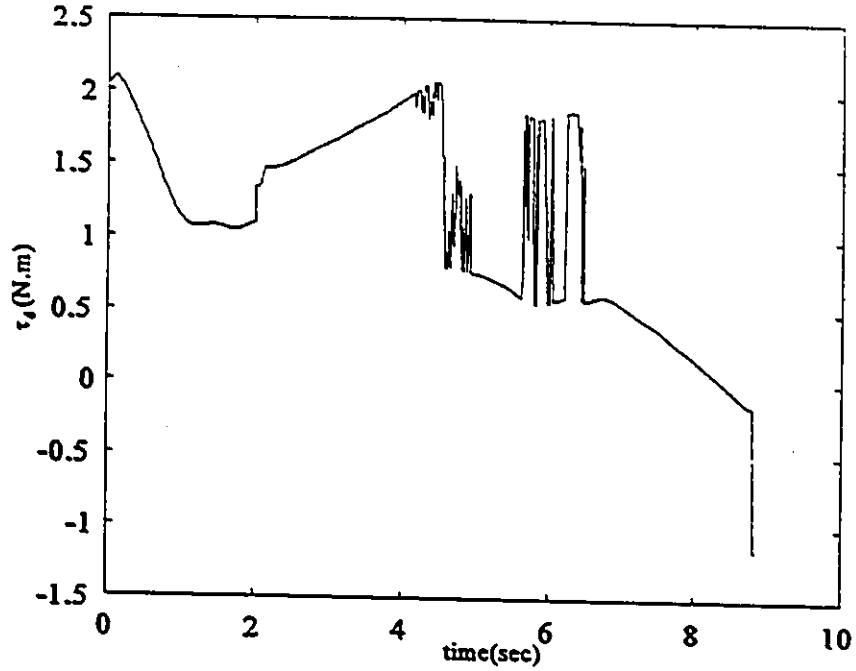

Figure 6-58 Test 4. Experiment. τ_d (driving torque) versus time.

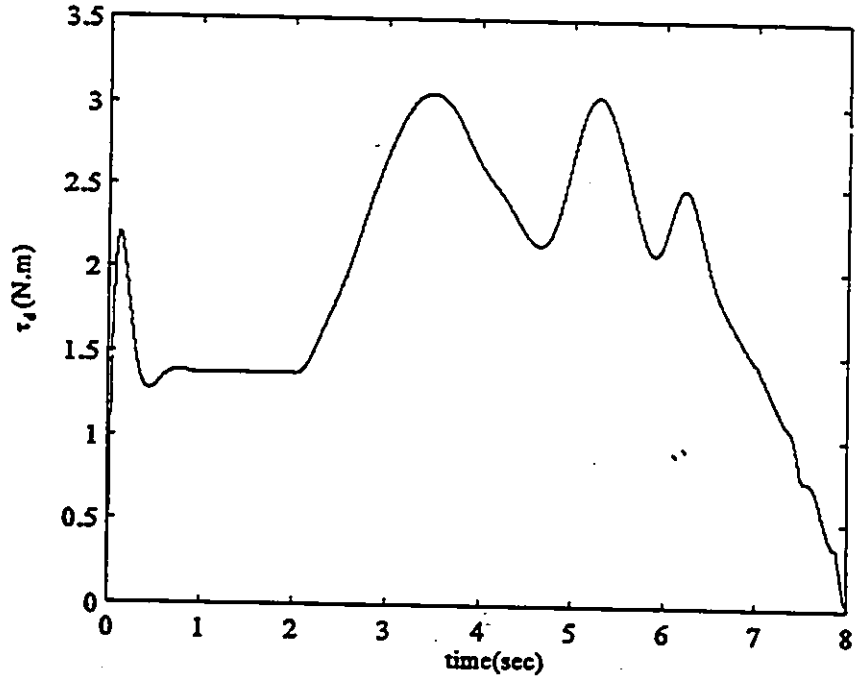

Figure 6-59 Test 4. Simulation. τ_d (driving torque) versus time.

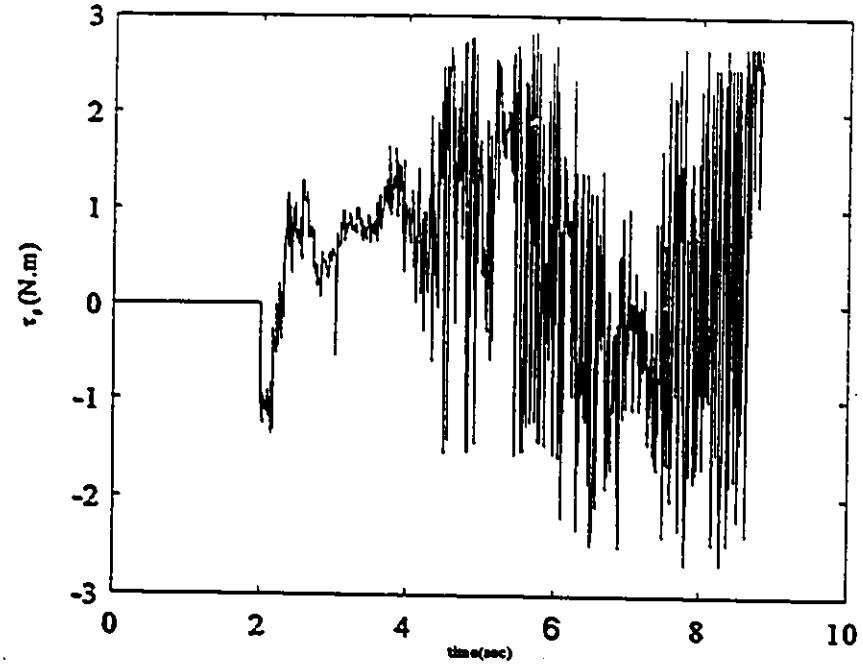

Figure 6-60 Test 4. Experiment. τ_s (steering torque) versus time.

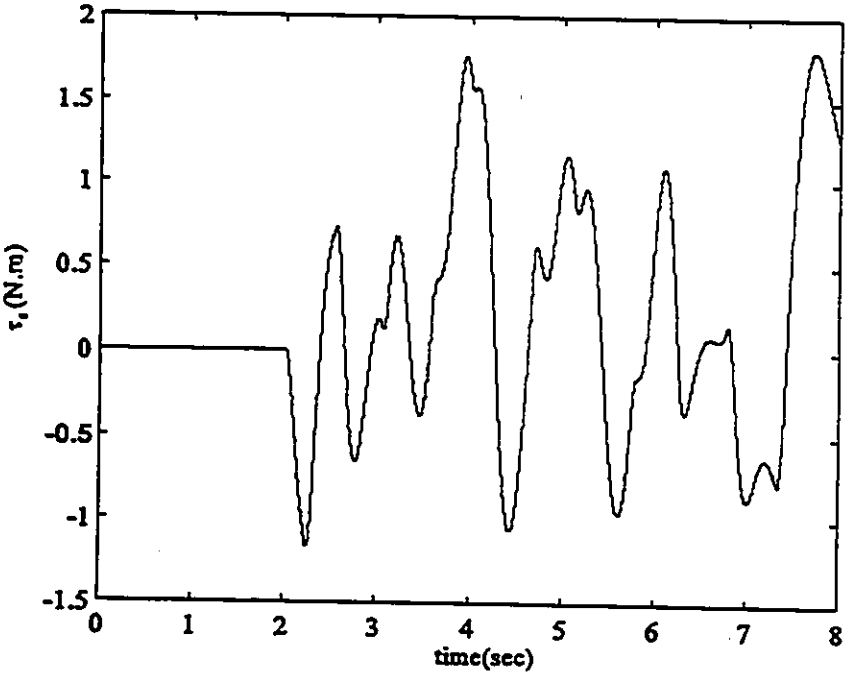

Figure 6-61 Test 4. Simulation. τ_s (steering torque) versus time.

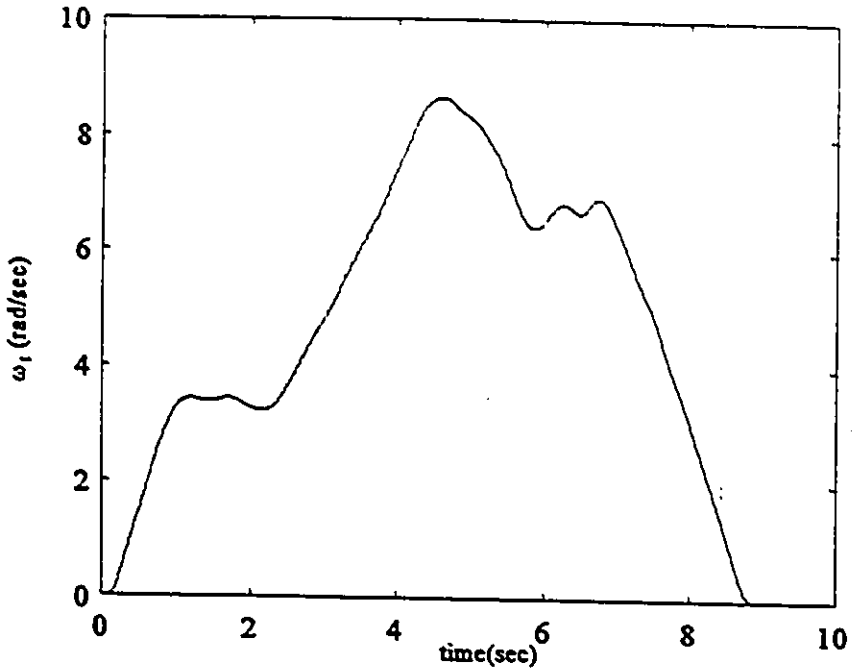

Figure 6-62 Test 4. Experiment. ω_1 versus time.

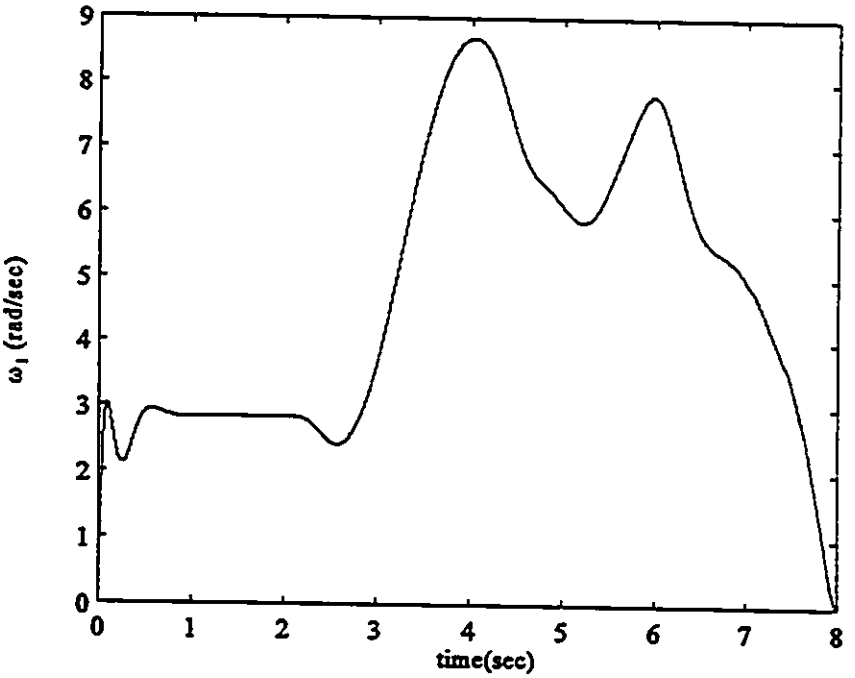

Figure 6-63 Test 4. Simulation. ω_1 versus time.

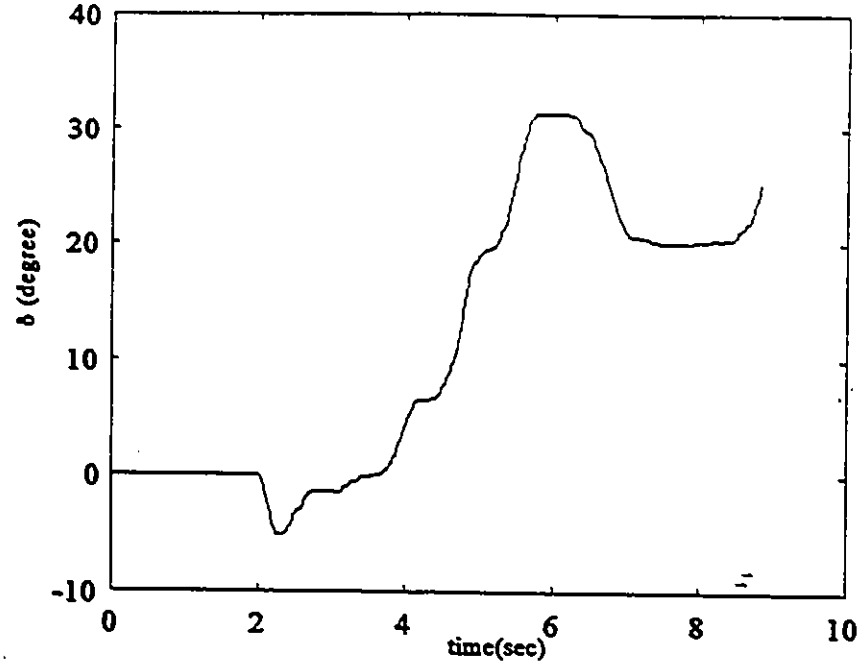

Figure 6-64 Test 4. Experiment. δ (steering angle) versus time.

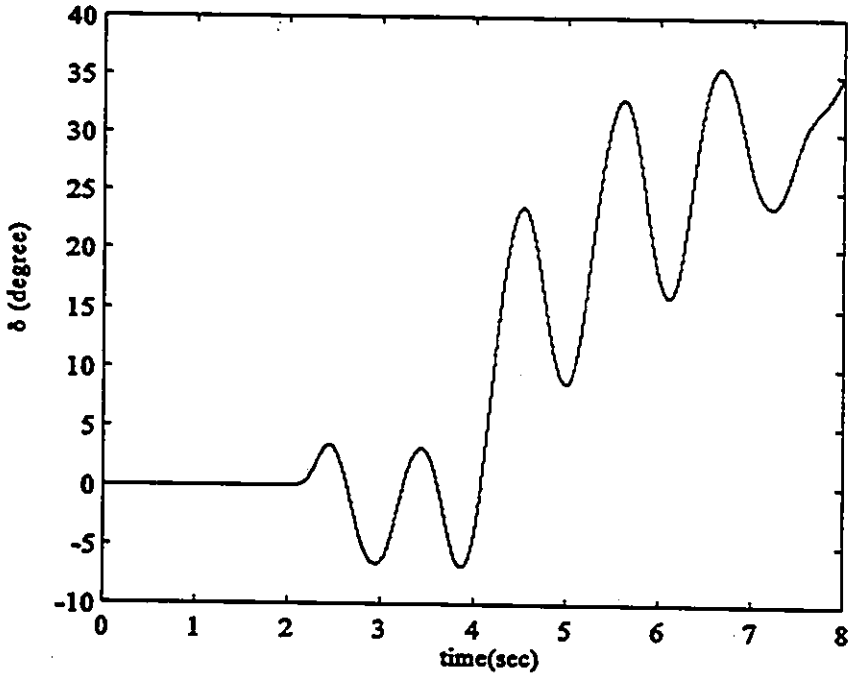

Figure 6-65 Test 4. Simulation. δ (steering angle) versus time.

Some important numbers of the experimental results are reported here:

	time(sec)	final X(m)	final Y(m)	final θ(deg)	k_1	k_2	k_3
Test1	9.990	2.497	1.411	-29.95	11.1	11.1	1.0
Test2	7.950	2.061	1.086	55.50	7.0	14.0	8.0
Test3	8.270	2.027	1.051	60.20	7.55	9.85	3.3
Test4	8.820	1.932	0.961	86.72	8.0	17.0	10.0

6-6 Comments on the Results

- The experimental work reported in [80] demonstrated that Cartesian space feedback linearization can be implemented to work on a real vehicle with steering. The comparison between feedback linearization of the dynamic model and PD control of the kinematic model for trajectory tracking of CLAMOR revealed that both methods can be utilized; input-output feeback linearization performed better when dynamics effects become more important, i.e., at high speeds and sharp turning angles.

- The experimental results on bounded stabilization of curvilinear feedback linearized vehicle show that this method works well enough to be considered as a suitable method to be used for the available and also more complicated dynamic models of the vehicles. Since PD control of kinematic model of the vehicle could not be used for bounded stabilization of orientation, its implementation on the vehicle was not further considered in this work. Other methods presented in the literature have not considered steering dynamics, and they could not be applied to CLAMOR for comparison of the experimental results.

- To carry out the experiments, the intention was to make as few changes as possible in the available setup and programs(hardware and software) and use only three gains, Equation (4-27), to modify the vehicle's performance. Of course, the change from

Cartesian to curvilinear space was inevitable.

- The assumptions made for the theoretical part of the work are quite different from what happens in reality. The laboratory floor is not completely horizontal and flat and there are some embedded materials inside the floor that sometimes cause "slip" during the vehicle's motion. On the other hand, the fact that the measurements are from odometry make system's errors relatively large. As a result of the slips, the chance of the vehicle passing the desired point (and then braking or moving further) or stopping before the desired position will be higher.

- In the experiments, steering torque commands show sometimes oscillatory portions with relatively high amplitudes (Figures 6-18, 32, 46, 60). The same result, with lower frequencies and lower amplitudes can be seen in simulations, Figures (6-19, 33, 47, 61). It was observed that higher cutoff frequencies of filter make steering assembly to shake. On the other hand, reducing the frequency too low tends to cause the vehicle to ignore the changes in the trajectory.[80] The result of using low cutoff frequencies can be high frequency oscillatory portions in torque commands. Equation (A-75) represents a forced nonlinear system an the required torque may change very fast, and even oscillate at high frequency during the motion to compensate for internal and external factors. However, because the overall system is stable (marginally or bounded), no oscillations are noticeable in steering angle. This is confirmed by the results showing no "chattering" in the steering angle (Figures 6-22, 36, 50, 64) as a result of having high frequency of the steering torque commands filtered by the lower natural frequency of the overall closed loop system. It should also be mentioned that higher gains will help reducing the effect of friction, but also may cause this type of oscillations.

- Since for each test (experiment), the vehicle moved on different parts of the laboratory floor with different inclinations which, even small, can produce some forces not accounted for, different gains were had to be chosen for different paths and starting and final positions and orientations.

Chapter 7

Conclusions and Recommendations

7-1 Summary and conclusions

The prime objective of this research is to show that input-output feedback linearization can be used to solve the bounded stabilization problem of the autonomous ground vehicles. Extension of this systematic approach from simpler to more complicated systems is theoretically straightforward. Since smooth state feedback laws cannot be used for asymptotic stabilization of these systems, other methods like time-varying and discontinuous feedback laws have been suggested. Mathematical procedures used in these methods to prove their usefulness are very tedious. This makes the extension of these methods, from currently being applicable to simple systems to be applied on more complex models, very difficult. Input-output feedback linearization applies a smooth state feedback to a nonlinear system, therefore, it cannot be used directly to solve asymptotic stabilization of the nonholonomic vehicles. Two modifications have been suggested in this thesis to fix this difficulty. First, the asymptotic stabilization problem has been reduced to bounded stabilization. From a practical point of view, this reduction will not make much of difference, because in real-time tests those methods will have some bounded errors in position and orientation, too. The other modification is to switch from using Cartesian space coordinates to curvilinear space variables. By having a preplanned path, this allows the vehicle to arrive at a vicinity of the final position and orientation.

One of the major issues involved in applying input-output feedback linearization is that as a consequence of transforming a nonlinear system to a linear one by this method, the system's dynamics will be divided into tow parts, external and internal dynamics. Feedback linearization can only treat the external dynamics. In this research, the internal dynamics of the vehicle "CLAMOR" is examined. The vehicle has a one dimensional internal dynamics which has the steering angle as its governing state. The examination of steering dynamics indicates that when the steering torque is zero, this dynamics is asymptotically stable as long as the vehicle keeps moving forward. This result refers to the asymptotic stabilization of trajectory tracking procedure.

For point stabilization, if close to the end point the path is almost a straight line, internal stability discussion leads to the result that as long as the front wheel angular velocity is positive, the overall system is stable and when this velocity approaches zero, close to the vehicle's stop, unless a drastic change, caused by external contact forces, makes the front wheel to deviate, its orientation remains almost unchanged and near the desired value. Also, it should be mentioned that this deviation of the front wheel orientation may not have enough time to cause the vehicle's orientation change.

Theoretical approaches to control nonholonomic wheeled vehicles have rarely been experimentally verified. The implementation of Cartesian and curvilinear spaces input-output feedback linearization on a tricycle with front wheel steering and driving, CLAMOR, demonstrates the usefulness and capabilities of the approach for trajectory tracking and bounded stabilization.

7-2 Contributions

The major contributions of this research can be summarized as follows:

- A complete dynamic model for a 3-wheel vehicle with front wheel steering and driving is developed.

- Input-output feedback linearization in Cartesian and curvilinear spaces have

been applied on this vehicle. Cartesian space coordinates have been used for trajectory tracking and curvilinear space variables for point stabilization.

- Internal dynamics of the vehicle has been analytically examined. The conditions under which this dynamics is asymptotically stable when the vehicle is in motion are found. Also, bounded stability of the internal dynamics when the vehicle is stopped has been proved.

- By both simulation and experiment, the suggested solutions to the motion control problems of autonomous ground vehicles have been verified.

7-3 Recommendations for Future Work

- Full autonomy for the experimental vehicle by the implementation of an on board computer is needed for performing an extensive experimental study. More accurate models of motors, more advanced techniques to identify its dynamical characteristics, equipping it with inertial sensors along with odometry for position sensing, providing a larger test area that allows more tests at higher speeds, testing its performance on somehow rougher surfaces and also on an inclined plane are recommended. Also more complicated routines and sensors to detect slippage, skid and other practical problems and to compensate for them are required.

- One of the main reasons for using feedback linearization is that it permits to take advantage of the methods applied to linear systems. Among them are robust control and adaptive control that can improve the performance of the system by accounting for unmodeled dynamics and parameter uncertainties.

- As a systematic approach, input-output feedback linearization can be implemented to more complicated vehicles. The difference will be the more lengthy procedure to find the relationships between the inputs to the system, motor torques in this case, and the outputs, the positions and their derivatives.

- From theoretical point of view, smooth and nonsmooth time-varying and discontinuous feedback laws can lead to asymptotic stabilization of nonholonomic systems. On the other hand, input-output feedback linearization applies a smooth state feedback. Exploring the possibilities of making these methods work together to control complicated dynamic models of wheeled vehicles with steering is very interesting.

- As tried in this research, dealing with physical realities as well as theoretical aspects of nonholonomic vehicles at the same time is desirable. To enrich controller designs only improving one side is not effective and complete. Autonomous vehicles for current and possible future applications require improvements of design and mathematical aspects of nonlinear control theory and vehicle's modelling.

References

1. " International Encyclopedia of robotics: Application and Automation", Dorf, R. C., Editor-in-chief, Nof, S. Y., Consulting Editor, Wiley, 1988

2. Campion, G., et al, "Controllability and State feedback Stabilizability of Non Holonomic Mechanical Systems", Proc. of the International Workshop on Nonlinear and Adaptive Control: Issues in Robotics, Grenoble, France, Nov. 21-23, 1990, pp 106-124.

3. Bloch, A. M., and McClamroch, N. H., " Control of Mechanical Systems with Classical Nonholonomic Constraints", The 28th IEEE Conference on Decision and Control, Tampa, Florida, Dec. 1989, pp 201-205.

4. Brockett, R.W., " Asymptotic Stability and Feedback Stabilization", in Differential Geometric Control Theory, Editors: Brockett, R.W., Millman, R.S. and Sussmaan, H.J., Birkhauser, 1983.

5. Shiller, Z. and Gwo, Y.R., "Dynamic Motion Planning of Autonomous Vehicles", IEEE Trans. on Robotics and Automation, Vol. 7, No. 2, April 1991, pp 241-249.

6. Crowley, J.L., "Asynchronous Control of Orientation and Displacement in Robot Vehicles",Proc. 1989 IEEE International Conference on Robotics and Automation, Vol. 3, Scottsdale, Arizona, May 14-19, 1989, pp 1277-1282.

7. Steer, B., "Trajectory Planning for a Mobile Robot", The International Journal of Robotics Research, Vol. 8 No. 5, Oct. 1989, pp 3-14.

8. Hemami, A. et al, "A New Control Strategy for Tracking in Mobile Robot and AGV's" , Proc. 1990 IEEE International Conference on Robotics and Automation, Vol. 2, Cincinnati, Ohio, May 13-18, 1990, pp 1122-1127.

9. Canudas de Wit, C., and Sørdalen, O.J., "Exponential Stabilization of a Mobile Robot with Nonholonomic Constraints", The 30th IEEE Conference on Decision and Control, Dec. 1991, pp 692-697.

10. Samson, C., "Velocity and Torque Feedback Control of a Nonholonomic Cart", Proc. of the International Workshop on Nonlinear and Adaptive Control: Issues in Robotics, Grenoble, France, Nov. 21-23, 1990, pp 125-151.

11. Nelson, W.L., and Cox, I.J., "Local Path Control for an Autonomous Vehicle", Proc. 1988 IEEE International Conference on Robotics and Automation, Vol. 2, Philadelphia, Pennsylvenia, 1988, pp 1504-1510.

12. Necsulescu, D.S., et al "Dynamic Control of an Autonomous Wheeled Ground Vehicle", Trans. of CSME, Vol. 17, No. 4, 1993, pp 735-758.

13. Necsulescu, D. S., Eghtesad, M. And Kalaycioglu, S., " Dynamic Based Linearization and Control of an Autonomous Mobile Robot" , Second Biennial ASME European Conf. on "Engineering, Systems, Design and Analysis", London, England, July 4-7, 1994.

14. Campion, G., et al , "Structural Properties and Classification of Kinematic and

DynamicModels of Wheeled Mobile Robots", Proc. 1993 IEEE International Conference on Robotics and Automation, Vol. 1, pp 462-469.

15. d 'Andrêa- Novel, B., et al, "Modelling and Control of Nonholonomic Wheeled Mobile Robots ", Proc. 1991 IEEE International Conference on Robotics and Automation, Vol. 2, Sacramento, California, April 1991, pp 1130-1135.

16. Campion, G. , "Modelling and State Feedback Control of Nonholonomic Mechanical Systems", The 30th IEEE Conference on Decision and Control, Dec. 1991, pp 1184-1189.

17. Saha, S.K., and Angeles, J., "Kinematics and Dynamics of a Three Wheeled AGV", Proc. 1989 IEEE International Conference on Robotics and Automation, Vol. 3, Scottsdale, Arizona, May 14-19, 1989, pp 1572-1577.

18. Saha, S.K., and Angeles, J., "Dynamics of Nonholonomic MechanicalSystems Using a Natural Orthogonal Complement", ASME Journal of Applied Mechanics, Vol. 58, March 1991, pp 238-243.

19. Ellis, J.R., "Vehicle Dynamics", Business Books, London, 1969.

20. Wong, J.Y., "Theory of Ground Vehicles", John Wiley & Sons, 1978.

21. Muir, P.F., and Neuman, C.P., "Kinematic Modelling of Wheeled Mobile Robots", Journal of Robotic Systems, Vol. 4, No. 2, 1987.

22. D'Souza, A., and Greg, V .K., "Advanced Dynamics: Modelling and Analysis ", Prentice Hall, 1984.

23. Houston, R.L., " Multibody Dynamics", Butterworths- Heinemann, 1990, Boston

24. Haug, E.J., "Intermediate Dynamics", Prentice Hall, 1992.

25. Isidori, A. , "Nonlinear Control Systems, An Introduction", 2nd Edition, Springer-Verlag, 1989.

26. Nijmeijer, H., and Van der Schaft, A.J., "Nonlinear Dynamical Control Systems", Springer-Verlag, 1990.

27. Sussmann, H.J., "A General Theorem on Local Controllability", SIAM Journal on Control and Optimization, Vol. 25, No. 1, January 1987, pp 158-194.

28. Sussmann, H.J., and Jurdjevic, V., "Controllability of Nonlinear Systems", Journal of Differential Equations, Vol. 12, pp 95-116, Academic Press Inc., 1972,

29. Barraquand, J., and Latombe, J.-C., "Controllability of Mobile Robots with Kinematic Constraints", Internal Report, Stanford University, June 1990.

30. Latombe, J.-C., "Robot Motion Planning", Kluwer Academic Publishers, 1991.

31. McKerrow, P.J., "Introduction to Robotics", Addison Wesley, 1991.

32. Li, Z., and Canny, J. F., "Nonholonomic Motion Planning", Kluwer Academic Publishers, 1993.

33. Barraquand, J. , and Latombe, J.-C. , "On Nonholonomic Mobile Robots and Optimal

Maneuvering", In 4th IEEE International Symposium on Intelligent Control, Albany, NY, 1989.

34. Schwartz, J.T. , and Sharir, M., "A Survey of Motion Planning and Related Geometric Algorithms", Artificial Intelligent Journal, Vol. 37, 1988, pp 157-169.

35. Tournassoud, P., and Jehl, O. "Motion Planning for a Mobile Robot with Kinematic Constraint", Proc. 1988 IEEE International Conference on Robotics and Automation, Vol. 2, 1988, pp 1785-1790.

36. Laumond, J.-P., "Feasible Trajectories for Mobile Robots with Kinematic and Environment Constraints" , Proc. of International Conference on Intelligent Autonomous Systems", Amsterdam, The Netherlands, Dec. 1986, pp 346-354.

37. Kolmanovsky, I. and McClamroch, N. H., "Developments in Nonholonomic Control Problems", IEEE Control Systems Mgazine, Vol. 15, No. 6, Dec 1995, pp 20-36.

38. Lafferriere, G., and Sussmann, H., "Motion Planning for Controllable Systems Without Drift", Proc. 1991 IEEE International Conference on Robotics and Automation, Vol. 2, Sacramento, California, April 9-11, 1991, pp 1148-1153.

39. Gurvits, L., "Averaging Approach to Nonholonomic Motion Planning", Proc. 1992 IEEE International Conference on Robotics and Automation, Vol. 3, Nice, France, May 1992, pp 2541-2546.

40. Mukherjee , R., and Anderson, D. P. , "Nonholonomic Motion Planning Using Stokes's Theorem", Proc. 1993 IEEE International Conference on Robotics and Automation, Vol. 3,

pp 802-809.

41. Murray, R.M., and Sastry, S.S., "Steering Nonholonomic Systems Using Sinusoids", The 29th IEEE Conference on Decision and Control, Dec. 1990, pp 2097-2100.

42. Divelbiss, A. W., and Wen, J., "A Global Approach to Nonholonomic Motion Planning", The 31th IEEE Conference on Decision and Control, Dec. 1992, pp 1597-1602.

43. Murray, R.M., and Sastry, S.S., "Steering Nonholonomic Systems in Chained Form", The 30th IEEE Conference on Decision and Control, Dec. 1991, pp 1121-1126.

44. Sussmann, H., "Local Controllability and Motion Planning for some Classes of Systems with Drift", The 30th IEEE Conference on Decision and Control, Dec. 1991, pp 1110-1114.

45. Kanayama, Y., et al "A Locomotion Control Method for Autonomous Vehicles", Proc. 1988 IEEE International Conference on Robotics and Automation, Vol. 2, 1988, pp 1315-1317.

46. Kanayama, Y., and Miyake, N., "Trajectory Generation for Mobile Robots", Journal of Robotics Research, Vol. 3, 1986, pp 333-340.

47. Nelson, W., "Continuous-Curvature Paths for Autonomous Vehicles", Proc. 1989 IEEE International Conference on Robotics and Automation, Vol. 2, 1989, pp 1260-1264.

48. Kanayama, Y., and Hartman, B.I., "Smooth Local Path Planning for Autonomous Vehicles", Proc. 1989 IEEE International Conference on Robotics and Automation, Vol. 2, 1989, pp 1265-1270.

49. Hemami, A., et al "Synthesis of an Optimal Control Law for Path Tracking in Mobile Robots", Automatica, Vol. 28, No. 2, 1992, pp 383-387.

50. Kanayama, Y., et al, "A Stable Tracking Control Method for an Autonomous Mobile Robot", Proc. 1990 IEEE International Conference on Robotics and Automation, Vol. 1, Cincinnati, Ohio, May 13-18, 1990, pp 384-389.

51. Graettinger, T.J., and Krogh, B.H., "Evaluation and Time Scaling of Trajectories for Wheeled Mobile Robots", ASME Journal of Dynamic Systems Measurement and Control, Vol. 111, June 1989, pp 222-231.

52. Dahl, O., and Nielson, L., "Stability Analysis of an On-Line Algorithm for Torque Limited Path Following", Proc. 1990 IEEE International Conference on Robotics and Automation, Vol. 2, Cincinnati, Ohio, May 13-18, 1990, pp 1216-1222.

53. Canudas de Wit, C., and Roskam, R., "Path Following of a 2-DoF Mobile Robot under Path and Input Torque Constraints", Proc 1991 IEEE International Conference on Robotics and Automation, Vol. 2, Sacramento, California, April 9-11, 1991, pp 1142-1147.

54. Sørdalen, O.J., and Canudas de Wit, C., "Path Following and Stabilization of a Mobile Robot", Proc. of the International Workshop on Nonlinear and Adaptive Control: Issues in Robotics, Grenoble, France, Nov. 21-23, 1990, pp 125-151.

55. Shin, D.H., et al "A Partitioned Control Scheme for Mobile Robots Path Tracking", Proc. 1991 IEEE International Conference on Robotics and Automation, Vol. 1, Sacramento, California, April 9-11, 1991, pp 338-342.

56. Samson, C ., "Path Following and Time-Varying Feedback Stabilization of a Wheeled Mobile Robot", Proc. International conference ICARC\ ' 92, Singapore, 1992.

57. Samson, C., and Ait-Abderrahim, K.,"Mobile Robot Control, Part 1: Feedback Control of a Nonholonomic Wheeled Cart in Cartesian Space", Internal Report, INRIA, France, June 8, 1990.

58. Bloch, A.M., et al "Control and Stabilization of Nonholonomic Dynamic Systems", IEEE Trans. on Automatic Control, Vol. 37, No. 11, Nov. 1992, pp 1746-1757.

59. Sussmann, H. J., "Subanalytical Sets and Feedback Control", Journal of Differential Equations, Vol. 31, 1979, pp 31-52.

60. Astolfi, A., "On the Stabilization of Nonholonomic Systems", The 33rd IEEE Conf. on Decision and Control, 1994, pp 3481-3486.

61. Aicardi, M. et al, "Closed Loop Smooth Steering of Unicycle-Like Vehicles", The 33rd IEEE Conf. on Decision and Control, 1994, pp 2455-2458.

62. Bloch, A. and Drakunov, S., "Stabilization of a Nonholonomic System via Sliding Modes", The 33rd IEEE Conf. on Decision and Control, 1994, pp 2961-2963.

63. Samson, C., "Time-Varying Feedback Stabilization of Car-Like Wheeled Mobile Robots", The International Journal of Robotics Research, Vol. 12, No. 1, Feb. 1993, pp 55-64.

64. Coron, J.-M. , "Global Asymptotic Stabilization for Controllable Systems without Drift

", Mathematics of Control, Signals, and Systems, No. 5, 1992, pp 259-312.

65. Pomet, J.-B., "Explicit Design of Time-Varying Stabilizing Control Laws for a Class of Controllable Systems without Drift", Systems and Control Letters, Vol. 18, 1992, pp 147-158.

66. Coron , J.-M., and Pomet , J.-B., "Stabilizing Feedback Laws for Controllable Systems without Drift", IFAC Symposium on Nonlinear Control Systems Design, Bordeaux, France, June 24-26, 1992, pp 397-401.

67. M'Closky, R. T., and Murray, R. M., "Experiments in Exponential Stabilization of a Mobile Robot Towing a Trailer", Proc. Of American Control Conference, 1994, pp 988-993.

68. Sørdalen, O.J., and Egeland, O., "Exponential Stabilization of Nonholonomic Chained Systems", IEEE Trans. on Automatic Control, Vol 40, No. 1, Jan. 1995, pp 35-49.

69. Kolmanovsky, I. et al, "Discontinuous Feedback Stabilization of Nonholonomic Systems in Extended Power Form", The 33rd IEEE Conf. on Decision and Control, 1994, pp 3469-3474.

70. Hauser, J.E., PhD Dissertation, Dept. of Elec. Eng. and Computer Science, Univ. of California at Berkeley, 1989.

71. Slotine, J.-J. E., and Li., W., "Applied Nonlinear Control", Prentice Hall, 1991.

72. d'Andrêa-Novel, B., et al , "Dynamic Feedback Linearization of Nonholonomic Wheeled Mobile Robots", Proc. 1992 IEEE International Conference on Robotics and Automation,

Vol. 3, Nice, France, May 1992, pp 2527-2532.

73. Yun, X., and Yamamoto, Y., "Internal Dynamics of a Wheeled Mobile Robot", Proc. of the IEEE\RJS International Conf. on Intelligent Robots and Systems, Yokohama, Japan, July 26-30, 1993, pp 1288-1294.

74. Deng, Z., and Brady, M., "Dynamic Tracking of a Wheeled Mobile Robot", Proc. of the IEEE\RJS International Conf. on Intelligent Robots and Systems, Yokohama, Japan, July 26-30, 1993, pp 1295-1298.

75. Sarkar, N., et al, "Control of Mechanical Systems With Rolling Constraints: Application to Dynamic Control of Mobile Robots", The Inter. Journal of Robotics Research, Vol. 13, No. 1, Feb. 1994, pp 55-69.

76. Necsulescu, D. S. and Eghtesad, M. "Task Space Motion Control of Autonomous Planetary Vehicles", submitted to CASI, 1995.

77. Isidori, A., and Moog, C.H., "On the Nonlinear Equivalent of the Notion of Transmission Zeros", In Lecture Notes in Control and Information Science, Byrnes, C.I., and Kurszanski, A., eds., No. 105, Springer-Verlag, Berlin, New York, 1988.

78. Necsulescu, D. S., Villien, A. and Eghtesad, M., "Task Space Motion Control of Autonomous Planetary Vehicles", 8th CASI Conf. on Astronotics, Ottawa, Canada, Nov. 7-10 1994, pp. 303-312.

79. Neimark, J. I., and Fufaev, N. A., "Dynamics of Nonholonomic Systems", American Matematical Society, Providence, Rhode Island, 1972.

80. Lonmo, V., "Dynamics Based Control of a Mobile Robot with Non-Holonomic Constraints", M.Sc. Thesis, Dept. of Mechanical Eng., University of Ottawa, 1996.

81. Droguet, E., "Autonomous Robot Control with onstraint Verification", Internal Rerport, Dept. of Mechanical Eng., University of Ottawa, August 1994.

82. Sørdalen, O.J., and Egeland, O., "Exponential Stabilization of Nonholonomic Chained Systems", IEEE Trans. on Automatic Control, Vol. 40, No. 1, January 1995.

Appendix A

The derivations of ω_1 and ω_8 and their derivatives, in terms of the other state variables or their derivatives and the inputs, τ_s and τ_d , based on the kinematic and dynamic equations of the system [12], are presented in this appendix. These derivations are needed in the elimination process of the internal and contact forces and moments. The first step is to define the internal forces and moments based on the other forces and moments and kinematic variables [Equations (3-54 and 55), (3-57 and 58), (3-62 to 64), (3-66 to 69) and (3-71 to 73)]:

$$F_{x2} = G_{x2} - m_2 a_{x2} \tag{A-1}$$

$$F_{y2} = G_{y2} - m_2 a_{y2} \tag{A-2}$$

$$F_{x3} = G_{x3} - m_3 a_{x3} \tag{A-3}$$

$$F_{y3} = G_{y3} - m_3 a_{y3} \tag{A-4}$$

$$M_{z2} = -G_{y2} r_{w2} - I_{z2} \omega_2 \dot{\theta} \tag{A-5}$$

$$M_{z2} = J_2\ddot{\theta} \tag{A-6}$$

$$M_{x3} = -G_{y3}r_{w3} - I_{x3}\omega_3\dot{\theta} \tag{A-7}$$

$$M_{z3} = J_3\ddot{\theta} \tag{A-8}$$

$$\begin{aligned} F_{FSAx}\cos\delta - F_{FSAy}\sin\delta &= -m_0 a_x - F_{x2} - F_{x3} \\ &= -(m_{SA}+m_1)a_{x1} + G_{x1}\cos\delta - G_{y1}\sin\delta \end{aligned} \tag{A-9}$$

$$\begin{aligned} F_{FSAx}\sin\delta + F_{FSAy}\cos\delta &= -m_0 a_y - F_{y2} - F_{y3} \\ &= -(m_{SA}+m_1)a_{y1} + G_{x1}\sin\delta + G_{y1}\cos\delta \end{aligned} \tag{A-10}$$

Equations (A-9 and 10) come after adding $\sum F_x$ and $\sum F_y$ equations of the steering assembly and the front wheel (Equations 3-57,58,72 and 73). From Equations (3-57 to 59), (3-61) and (3-74):

$$F_{SAx}\cos\delta - F_{SAy}\sin\delta = -m_1 a_{x1} + G_{x1}\cos\delta - G_{y1}\sin\delta \tag{A-11}$$

$$F_{SAx}\sin\delta + F_{SAy}\cos\delta = -m_1 a_{y1} + G_{x1}\sin\delta + G_{y1}\cos\delta \tag{A-12}$$

$$M_{SAx} = -I_{xl}(\ddot{\theta}+\ddot{\delta})\omega_1 - G_{yl}r_{wl} \qquad \text{(A-13)}$$

$$M_{SAz} = J_1(\ddot{\theta}+\ddot{\delta}) \qquad \text{(A-14)}$$

$$M_{FSAx} = -I_{SAx}(\ddot{\theta}+\ddot{\delta})\omega_1 - s_b F_{FSAy} - s_a F_{SAy} + M_{SAx} \qquad \text{(A-15)}$$

The next step is to eliminate the wheel- ground contact forces from the equations for the input torques. Equations (3-75 and 76) and (3-61) give:

$$\tau_d = I_{yl}\dot{\omega}_1 + G_{xl}r_{wl} \qquad \text{(A-16)}$$

$$\tau_s = (J_{SA}+J_1)\ (\ddot{\theta}+\ddot{\delta}) \qquad \text{(A-17)}$$

Equation (A-17) is obtained from adding $\sum M_z$ equations of the steering assembly and the front wheel (Equations 3-61 and 3-76). Rewriting Equation (3-56);

$$J_0\ddot{\theta} = (b-c)(F_{FSAx}\sin\delta + F_{FSAy}\cos\delta) + \frac{l}{2}(-F_{x2}+F_{x3}) - c(F_{y2}+F_{y3}) - \tau_s - M_{z2} - M_{z3} \qquad \text{(A-18)}$$

Equations (A-1 to 4),(A-6 and 7), (A-10) and (A-18) give:

$$
\begin{aligned}
J_0\ddot{\theta} = (b-c)[&-(m_{SA}+m_1)a_{y1}+G_{x1}\sin\delta+G_{y1}\cos\delta) \\
&+\frac{l}{2}(-G_{x2}+G_{x3}+m_2a_{x2}-m_3a_{x3}) \\
&-c(G_{y2}+G_{y3}-m_2a_{y2}-m_3a_{y3}) \\
&-\tau_s-J_2\ddot{\theta}\ -J_3\ddot{\theta}
\end{aligned}
\qquad \text{(A-19)}
$$

Equations (3-17 to 19);

$$a_{x1} = a_x-(b-c)\dot{\theta}^2 \qquad \text{(A-20)}$$

$$a_{y1} = a_y+(b-c)\ddot{\theta} \qquad \text{(A-21)}$$

$$a_{x\,2} = a_x+ c\dot{\theta}^2- \frac{l}{2}\ddot{\theta} \qquad \text{(A-22)}$$

$$a_{y2} = a_y- c\ddot{\theta}- \frac{l}{2}\dot{\theta}^2 \qquad \text{(A-23)}$$

$$a_{x\,3} = a_x+ c\dot{\theta}^2+ \frac{l}{2}\ddot{\theta} \qquad \text{(A-24)}$$

$$a_{y3} = a_y - c\ddot{\theta} + \frac{l}{2}\dot{\theta}^2 \qquad \text{(A-25)}$$

can be used to eliminate the accelerations of the moving frames' origins. Combining Equations (A-19) and (A-20 to 25) give:

$$\begin{aligned}(J_0+J_2+J_3)\ddot{\theta} \;=\; & -(b-c)(m_{SA}+m_1)[a_y-(b-c)\ddot{\theta}]+(b-c)(G_{x1}\sin\delta+G_{y1}\cos\delta) \\ & +\frac{l}{2}[m_2(a_x+c\dot{\theta}^2-(l/2)\ddot{\theta})-m_3(a_x+c\dot{\theta}^2+(l/2)\ddot{\theta})]- \\ & +c[m_2(a_y-c\ddot{\theta}-(l/2)\dot{\theta}^2)+m_3(a_y-c\ddot{\theta}+(l/2)\dot{\theta}^2)]-G_{y2}-G_{y3}-\tau_s\end{aligned} \qquad \text{(A-26)}$$

or;

$$\begin{aligned}&[(J_0+J_2+J_3)+(b-c)^2(m_{sa}+m_1)+(c^2+\frac{l^2}{4})(m_2+m_3)]\ddot{\theta} \\ &+a_x(\frac{l}{2})(-m_2+m_3)+a_y[(b-c)(m_{sa}+m_1)-c(m_2+m_3)]= \\ &-c(G_{y2}+G_{y3})+\frac{l}{2}(-G_{x2}+G_{x3})+(b-c)(G_{x1}\sin\delta+G_{y1}\cos\delta)-\tau_s\end{aligned} \qquad \text{(A-27)}$$

All $\sum F_x$ equations can be added together(3-54, 57, 62, 67 and 72) and give:

$$m_0a_x+m_2a_{x2}+m_3a_{x3}+(m_{SA}+m_1)a_{x1}=G_{x1}\cos\delta-G_{y1}\sin\delta+G_{x2}+G_{x3} \qquad \text{(A-28)}$$

Combining Equations (A-28) and (A-20, 22, 24) give:

$$m_0 a_x + m_2\left(a_x + c\dot{\theta}^2 - \frac{l}{2}\ddot{\theta}\right) + m_3\left(a_x + c\dot{\theta}^2 + \frac{l}{2}\ddot{\theta}\right) + (m_{SA} + m_1)[a_x + (b-c)\dot{\theta}^2] = G_{x1}\cos\delta - G_{y1}\sin\delta + G_{x2} + G_{x3} \quad \text{(A-29)}$$

or:

$$(m_0 + m_2 + m_3 + m_{SA} + m_1)a_x + [c(m_2 + m_3) - (m_{SA} + m_1)(b-c)]\dot{\theta}^2 + \frac{l}{2}(-m_2 + m_3)\ddot{\theta} = G_{x1}\cos\delta - G_{y1}\sin\delta + G_{x2} + G_{x3} \quad \text{(A-30)}$$

Adding all $\sum F_y$ equations, (3-55, 58, 63, 68 and 73) gives :

$$m_0 a_y + m_2 a_{y2} + m_3 a_{y3} + (m_{SA} + m_1)a_{y1} = G_{x1}\sin\delta + G_{y1}\cos\delta + G_{y2} + G_{y3} \quad \text{(A-31)}$$

Combining Equations (A-31) and (A-21, 23, 25) will result in:

$$m_0 a_y + m_2\left(a_y - c\ddot{\theta} - \frac{l}{2}\dot{\theta}^2\right) + m_3\left(a_y - c\ddot{\theta} + \frac{l}{2}\dot{\theta}^2\right) + (m_{SA} + m_1)[a_y + (b-c)\ddot{\theta}] = G_{x1}\sin\delta - G_{y1}\cos\delta + G_{y2} + G_{y3} \quad \text{(A-32)}$$

or:

$$(m_0 + m_2 + m_3 + m_{SA} + m_1)a_y + \frac{l}{2}(-m_2 + m_3)\dot{\theta}^2 + [c(m_2 + m_3) - (m_{SA} + m_1)(b-c)]\ddot{\theta} = G_{x1}\sin\delta - G_{y1}\cos\delta + G_{y2} + G_{y3} \quad \text{(A-33)}$$

Equations (A-27), (A-30) and (A-33) can be rewritten as:

$$G_{x1}\cos\delta - G_{y1}\sin\delta + G_{x2} + G_{x3} + P_1 = 0 \qquad \text{(A-34)}$$

$$G_{x1}\sin\delta + G_{y1}\cos\delta + G_{y2} + G_{y3} + P_2 = 0 \qquad \text{(A-35)}$$

$$-c(G_{y2}+G_{y3}) + \frac{l}{2}(-G_{x2}+G_{x3}) + (b-c)(G_{x1}\sin\delta + G_{y1}\cos\delta) + P_3 = 0 \qquad \text{(A-36)}$$

with;

$$P_1 = -Ma_x - Q_3\dot{\theta}^2 - \frac{l}{2}(-m_2+m_3)\ddot{\theta} \qquad \text{(A-37)}$$

$$P_2 = -Ma_y - \frac{l}{2}(-m_2+m_3)\dot{\theta}^2 + Q_3\ddot{\theta} \qquad \text{(A-38)}$$

$$P_3 = -Q_4\ddot{\theta} - \frac{l}{2}(-m_2+m_3)a_x + Q_3a_y - \tau_s \qquad \text{(A-39)}$$

where;

$$M = m_0 + m_1 + m_2 + m_3 + m_{SA} \qquad \text{(A-40)}$$

$$Q_3=[c(m_2+m_3)-(b-c)(m_1+m_{SA})] \tag{A-41}$$

$$Q_4=(U_0+J_2+J_3)+(b-c)^2(m_{SA}+m_1)+(c^2+\frac{l^2}{4})(m_2+m_3) \tag{A-42}$$

From Equations (A-34 to 36), G_{x1} can be written in terms of the other forces:

$$G_{x1}=\frac{G_{x2}(\frac{l}{2}\sin\delta-b\cos\delta)-G_{x3}(\frac{l}{2}\sin\delta+b\cos\delta)-bP_1\cos\delta-(cP_2+P_3)\sin\delta}{b} \tag{A-43}$$

or;

$$G_{x1}=\frac{\frac{l}{2}(G_{x2}-G_{x3})\sin\delta-b(G_{x2}+G_{x3})\cos\delta-bP_1\cos\delta-(cP_2+P_3)\sin\delta}{b} \tag{A-44}$$

Rewriting (3-45);

$$\ddot{\theta}=\frac{1}{c}(-r_{w2}\omega_2\dot{\theta}+a_y-\frac{l}{2}\dot{\theta}^2) \tag{A-45}$$

Equation (A-45) with (3-65 and 70) and (3-44 and 46) give:

$$G_{x2}+G_{x3}=-Q_1a_x-(cQ_1+\frac{l^2}{4}Q_2)\dot{\theta}^2+\frac{lQ_2}{2c}(-r_{w2}\omega_2\dot{\theta}+a_y) \tag{A-46}$$

$$G_{x2}-G_{x3}=-Q_2 a_x-(cQ_2+\frac{l^2}{4}Q_1)\dot{\theta}^2+\frac{lQ_1}{2c}(-r_{w2}\omega_2\dot{\theta}+a_y) \qquad \text{(A-47)}$$

where;

$$Q_1=\frac{I_{y2}}{r_{w2}^2}+\frac{I_{y3}}{r_{w3}^2} \qquad \text{(A-48)}$$

$$Q_2=\frac{I_{y2}}{r_{w2}^2}-\frac{I_{y3}}{r_{w3}^2} \qquad \text{(A-49)}$$

On the other hand, Equations (A-35 and 36) give:

$$\begin{aligned} cP_2+P_3=&-(\frac{l}{2})(-m_2+m_3)a_x+(-cM+Q_3)a_y \\ &+(cQ_3-Q_4)\ddot{\theta}-c(\frac{l}{2})(-m_2+m_3)\dot{\theta}^2-\tau_s \end{aligned} \qquad \text{(A-50)}$$

Equations (A-45 and 50) will result in:

$$\begin{aligned} cP_2+P_3=&-(\frac{l}{2})(-m_2+m_3)a_x+(-cM+Q_3+Q_3-\frac{Q_4}{c})a_y \\ &+(\frac{l}{2})[-c(-m_2+m_3)-Q_3+\frac{Q_4}{c})]\dot{\theta}^2-(r_{w2}\omega_2\dot{\theta})(Q_3-\frac{Q_4}{c}) \end{aligned} \qquad \text{(A-51)}$$

or;

$$cP_2+P_3=(\frac{l}{2})(m_2-m_3)a_x+(-cM+Q_3-Q_5)a_y \\ +(\frac{l}{2})[c(m_2-m_3)+Q_5]\dot{\theta}^2+Q_5(r_{w2}\omega_2\dot{\theta})-\tau_s \quad \text{(A-52)}$$

where;

$$Q_5= -Q_3+\frac{Q_4}{c} \quad \text{(A-53)}$$

$$P_1=Ma_x+(\frac{l}{2c})(-m_2+m_3)r_{w2}\omega_2\dot{\theta}-(\frac{l}{2c})(-m_2+m_3)a_y+[(\frac{l^2}{4c}(-m_2+m_3)-Q_3]\dot{\theta}^2 \quad \text{(A-54)}$$

Also, Equations (A-37, 44 to 47 and 53) have this result:

$$G_{xl}=[-\frac{l}{2b}Q_7\sin\delta+Q_6\cos\delta]a_x+[\frac{Q_8}{b}\sin\delta-\frac{l}{2c}Q_7\cos\delta]a_y \\ +[\frac{l}{2b}(-cQ_7-\frac{l^2}{4c}Q_1-Q_5)\sin\delta+(cQ_1+\frac{l^2}{4c}Q_7+Q_3)\cos\delta]\dot{\theta}^2 \quad \text{(A-55)} \\ +[-\frac{1}{b}(Q_5+\frac{l^2}{4c}Q_1)\sin\delta+\frac{l}{2c}Q_7\cos\delta](r_{w2}\omega_2\dot{\theta})+\frac{\sin\delta}{b}\tau_s$$

where;

$$Q_6= Q_1+M \quad \text{(A-56)}$$

$$Q_7 = Q_2 + m_2 + m_3 \tag{A-57}$$

Equations (3-10, 11, 23, 42, 43, 77) and (A-55) give:

$$\begin{aligned} G_{xl} = &[Q_6\cos^2\delta + \frac{c}{b^2}Q_8\sin^2\delta - \frac{l}{b}Q_7\sin\delta\cos\delta]r_{wl}\dot{\omega}_1 \\ &+[\frac{l}{2b}Q_7(\sin^2\delta - \cos^2\delta) + Q_{12}\sin\delta\cos\delta]r_{wl}\dot{\theta}\dot{\delta} \\ &+\frac{r_{wl}^2}{b^2}[(\frac{l}{2}Q_7 + \frac{l}{2b}Q_3)\sin^3\delta + (Q_{14} - bQ_6 + q_8 - Q_{11})\cos\delta\sin^2\delta]\dot{\theta}^2 + \frac{\sin\delta}{b}\tau_s \end{aligned} \tag{A-58}$$

where;

$$Q_8 = \frac{l^2}{4c}Q_1 + cM - Q_3 + Q_5 \tag{A-59}$$

$$Q_9 = -(c + \frac{l^2}{4c})Q_7 - Q_5 \tag{A-60}$$

$$Q_{10} = cQ_1 + \frac{l^2}{4c}Q_7 + Q_3 \tag{A-61}$$

$$Q_{11} = \frac{l^2}{4c}Q_1 + Q_5 \tag{A-62}$$

$$Q_{12} = -Q_6 + \frac{c}{b^2} Q_8 \tag{A-63}$$

$$\begin{aligned} Q_{13} &= Q_9 + (b-c)Q_7 + Q_{11} \\ &= -bQ_7 \end{aligned} \tag{A-64}$$

$$Q_{14} = Q_{10} + (b-c)Q_6 - \frac{l^2}{4c} Q_7 \tag{A-65}$$

The following relationships can be obtained from the Q_i's definitions:

$$Q_{14} - bQ_6 + Q_8 - Q_{11} = 0 \tag{A-66}$$

$$\frac{l}{2} Q_7 + \frac{l}{2b} Q_{13} = 0 \tag{A-67}$$

Then, Equation (A-58) can be rewritten in this reduced form:

$$\begin{aligned} G_{xl} = &[Q_6 \cos^2\delta + \frac{c}{b^2} Q_8 \sin^2\delta - \frac{l}{b} Q_7 \sin\delta\cos\delta] r_{wl} \dot{\omega}_1 \\ &+ [\frac{l}{2b} Q_7 (\sin^2\delta - \cos^2\delta) + Q_{12} \sin\delta\cos\delta] r_{wl} \omega_1 \dot{\delta} \\ &+ \frac{\sin\delta}{b} \tau_s \end{aligned} \tag{A-68}$$

Combining Equations (A-16) and (A-68) will result in:

$$\tau_d=[I_{yl}+(Q_6\cos^2\delta+\frac{c}{b^2}Q_8\sin^2\delta-\frac{l}{b}Q_7\sin\delta\cos\delta)r_{wl}^2]\dot{\omega}_1 +[\frac{l}{2b}Q_7(\sin^2\delta-\cos^2\delta)+Q_{12}\sin\delta\cos\delta]r_{wl}^2\omega_1\dot{\delta} +\frac{r_{wl}\sin\delta}{b}\tau_s \quad \text{(A-69)}$$

or:

$$\tau_d -[\frac{l}{2b}Q_7(\sin^2\delta-\cos^2\delta)+Q_{12}\sin\delta\cos\delta]r_{wl}^2\omega_1\dot{\delta} -\frac{r_{wl}\sin\delta}{b}\tau_s =[I_{yl}+(Q_6\cos^2\delta+\frac{c}{b^2}Q_8\sin^2\delta-\frac{l}{b}Q_7\sin\delta\cos\delta)r_{wl}^2]\dot{\omega}_1 \quad \text{(A-70)}$$

Then:

$$\dot{\omega}_1 =\frac{\tau_d -Num(\delta)r_{wl}^2\omega_1\dot{\delta} -\frac{r_{wl}\sin\delta}{b}\tau_s}{Den(\delta)} \quad \text{(A-71)}$$

where;

$$Num(\delta) = \frac{l}{2b}Q_7(\sin^2\delta-\cos^2\delta) +Q_{12}\sin\delta\cos\delta \quad \text{(A-72)}$$

$$Den(\delta) = I_{yl}+[Q_6\cos^2\delta+\frac{c}{b^2}Q_8\sin^2\delta-\frac{l}{b}Q_7\sin\delta\cos\delta]r_{wl}^2 \quad \text{(A-73)}$$

Equations (3-10, 11, 23) and (A-17 and 45) give:

$$\begin{aligned}\ddot{\delta} &= \frac{\tau_s}{J_{SA}+J_1} - \ddot{\theta} \\ &= \frac{\tau_s}{J_{SA}+J_1} - \frac{1}{c}(-r_{w1}\dot{\theta}\omega_1\cos\delta + \frac{l}{2}\dot{\theta}^2 + a_y - \frac{l}{2}\dot{\theta}^2) \\ &= \frac{\tau_s}{J_{SA}+J_1} - \frac{1}{c}(-r_{w1}\dot{\theta}\omega_1\cos\delta + a_y) \\ &= \frac{\tau_s}{J_{SA}+J_1} - \frac{1}{c}(-r_{w1}^2\omega_1^2\sin\delta\cos\delta + a_y)\end{aligned} \tag{A-74}$$

Then;

$$\ddot{\delta} = \frac{\tau_s}{J_{SA}+J_1} - \frac{1}{b}(r_{w1}\dot{\omega}_1\sin\delta + r_{w1}\omega_1\dot{\delta}\cos\delta) \tag{A-75}$$

Equation (A-75) can be deducted from (A-74), (3-43) and (A-45), since:

$$\begin{aligned}a_y &= \frac{c}{b}[r_{w1}\dot{\omega}_1\sin\delta + r_{w1}(\dot{\theta}+\dot{\delta})\omega_1\cos\delta + (\frac{b-c}{c})r_{w2}\omega_2\dot{\theta} + \frac{l}{2}(\frac{b-c}{c})\dot{\theta}^2] \\ &= \frac{c}{b}[r_{w1}\dot{\omega}_1\sin\delta + r_{w1}(\frac{r_{w1}}{b}\omega_1\sin\delta+\dot{\delta})\omega_1\cos\delta \\ &\qquad + (\frac{b-c}{c})(r_{w1}\omega_1\cos\delta - \frac{l}{2}\dot{\theta})\dot{\theta} + \frac{l}{2}(\frac{b-c}{c})\dot{\theta}^2] \\ &= \frac{c}{b}[r_{w1}\dot{\omega}_1\sin\delta + r_{w1}(\frac{r_{w1}}{b}\omega_1\sin\delta+\dot{\delta})\omega_1\cos\delta + (\frac{b-c}{c})r_{w1}\omega_1\dot{\theta}\cos\delta] \\ &= \frac{c}{b}[r_{w1}\dot{\omega}_1\sin\delta + r_{w1}(\frac{r_{w1}}{b}\omega_1\sin\delta+\dot{\delta})\omega_1\cos\delta + (\frac{b-c}{c})\frac{r_{w1}^2}{b}\omega_1^2\sin\delta\cos\delta] \\ &= \frac{c}{b}[r_{w1}\dot{\omega}_1\sin\delta + r_{w1}\dot{\delta}\omega_1\cos\delta + (1+\frac{b-c}{c})\frac{r_{w1}^2}{b}\omega_1^2\sin\delta\cos\delta] \\ &= \frac{c}{b}(r_{w1}\dot{\omega}_1\sin\delta + r_{w1}\dot{\delta}\omega_1\cos\delta) + \frac{r_{w1}^2}{b}\omega_1^2\sin\delta\cos\delta]\end{aligned} \tag{A-76}$$

Combining Equations (A-71) and (A-75);

$$\ddot{\delta} = -\left(\frac{r_{wl}}{b}\sin\delta\right)\left[\frac{\tau_d - \frac{r_{wl}}{b}\tau_s\sin\delta - r^2_{wl}\omega_1\dot{\delta}Num(\delta)}{Den(\delta)}\right] - \frac{r_{wl}}{b}\omega_1\dot{\delta}\cos\delta + \frac{\tau_s}{J_{SA}+J_1} \qquad \text{(A-77)}$$

By having this definition:

$$\omega_\delta = \dot{\delta} \qquad \text{(A-78)}$$

Equation (A-77) can be rewritten in this form:

$$\dot{\omega}_\delta = \tau_s\left[\frac{1}{J_{SA}+J_1} + \frac{r^2_{wl}\sin^2\delta}{b^2 Den(\delta)}\right] - \left(\frac{r_{wl}}{b}\sin\delta\right)\left[\frac{\tau_d}{Den(\delta)}\right] + \frac{r_{wl}}{b}\omega_1\omega_\delta\left[\frac{Num(\delta)}{Den(\delta)}r^2_{wl}\sin\delta - \cos\delta\right] \qquad \text{(A-79)}$$

Appendix B

Study of Some Other Methods

In this appendix, some of other suggested methods in the literature will be studied. There will not be a direct comparison between their results and input-output feedback linearization approach results presented in this thesis, rather the differences will be qualitatively discussed. These methods are: PD control, time-varying control and discontinuous control.

B-1 PD Control

PD control is one of the simplest methods available. Usually more advanced methods are to be compared with these simple methods in order to show their differnces and the advantages of applying advanced control methods. Also, they may be utilized as a part of a robust control method. PD control in its direct form can not be categorized as a method that may be used for asymptotic or bounded stabilization problems of nonholonomic vehicles. The reason is that it cannot direct the vehicle to the desired orientation in a planar motion if the position coordinates are closed-loop controlled. To show this fact, a simple PD control law has been applied on the dynamic model of CLAMOR with the same saturation limits on input torques given in chapter 6. The same PD control law was used for trajectory tracking of the same vehicle [80]. First, a P controller gives resolved speeds (c stands for command):

$$\dot{X}^{(c)} = (X_D - X)K_P \quad , \quad \dot{Y}^{(c)} = (Y_D - Y)K_P \qquad \text{(B-1)}$$

The relationships between the outputs (in this case δ, steering angle, and ω_1, front wheel angular velosity) and the inputs (τ_s and τ_d) are:

$$\tau_s = (\dot{\delta}_D - \dot{\delta})K_{DS} + (\delta_D - \delta)K_{PS} \quad , \quad \tau_d = (\omega_{1D} - \omega_1)K_t \qquad \text{(B-2)}$$

Here, "D" represents the desired values.

By using K_P =0.429, K_{DS} =4.5, K_{PS} =25.0 and K_t =1.0, the following results for position and orientation of the vehicle when it starts from (0.0, 0.0) with angle as the starting orientation and moves towards (2.5, 1.5) are obtained:

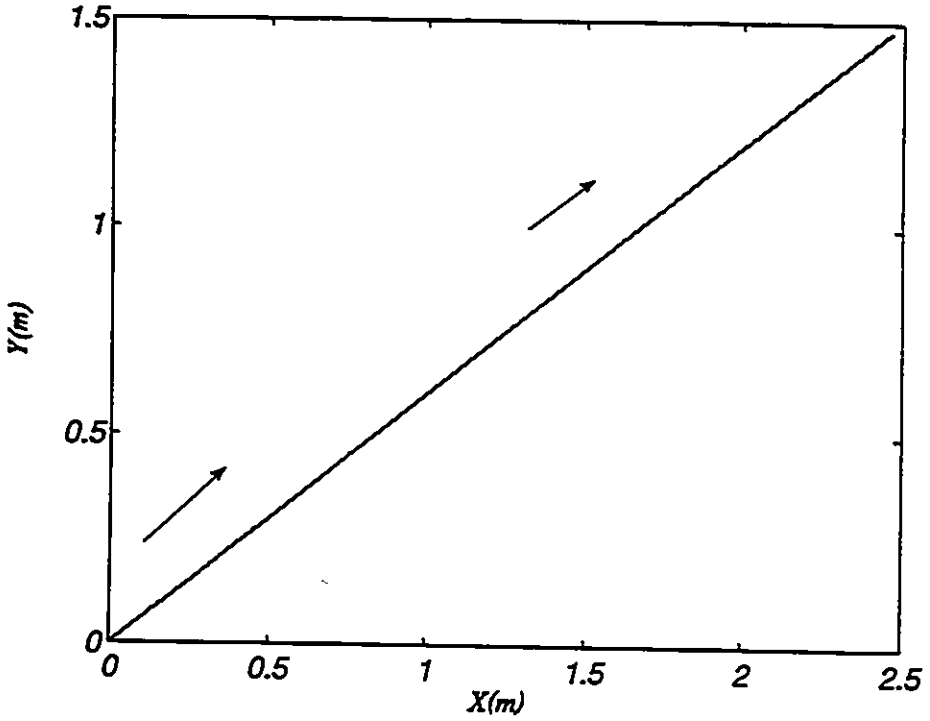

Figure B-1 PD position control.

This result could be repeated for other starting and desired positions and orientation, but the result would be the same and there would be no control over final orientation value.

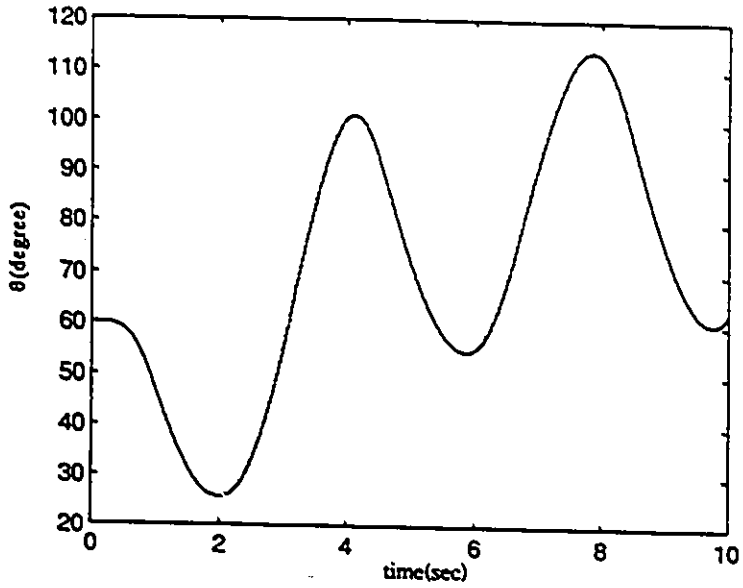

Figure B-2 PD Control. Orientation versus time.

B-2 Time-Varying Control

Samson's results presented in [63] for a kinematic model of a vehicle with steering in the form of:

$$\dot{x} = v(1+1/e)y\tan(\delta) \quad , \quad \dot{y} = -v(1/e)x\tan(\delta)$$

$$\dot{\theta} = v(1/e)\tan(\delta) \quad , \quad \frac{d}{dt}\tan(\delta) = [1+\tan^2(\delta)]\,\dot{\delta} \qquad \text{(B-3)}$$

where x and y are vehicle's moving frame Cartesian coordinates, θ is the orientation, v is the heading velosity and δ is the steering angle are regenerated by using the same gains. Although the orientation angle as shown in the following results is moving towards its desired value (here 0°), system's dynamic behavior is not very desirable. Two simulations are performed; starting "S" and final "F" positions and orientations are S_1(0., 1., 0°), S_2(0.,0., 90.°), F_1(0.,0., 0°) and F_2(2.5,1.5, 0°), respectively.

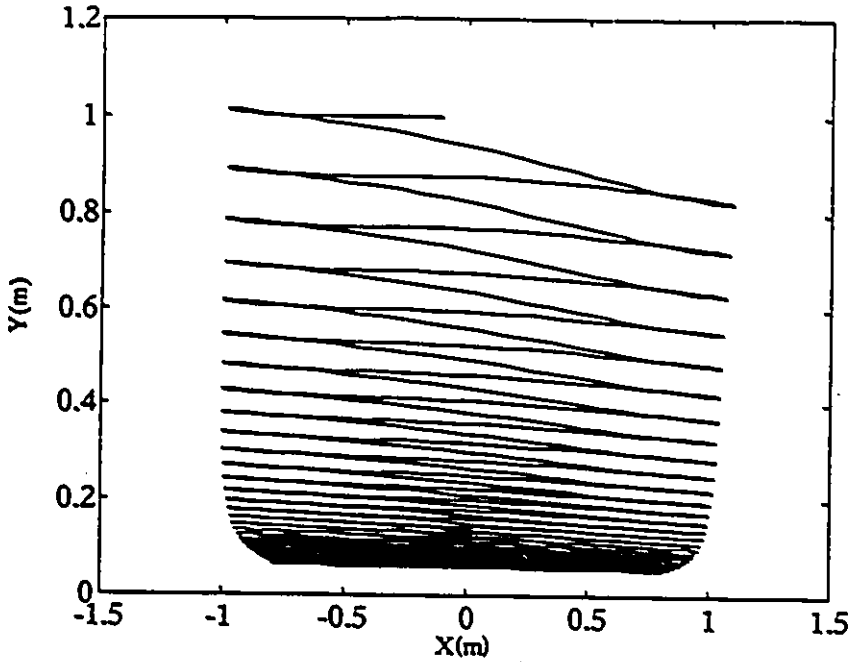

Figure B-3 Time-Varying Control. Simulation 1. Position.

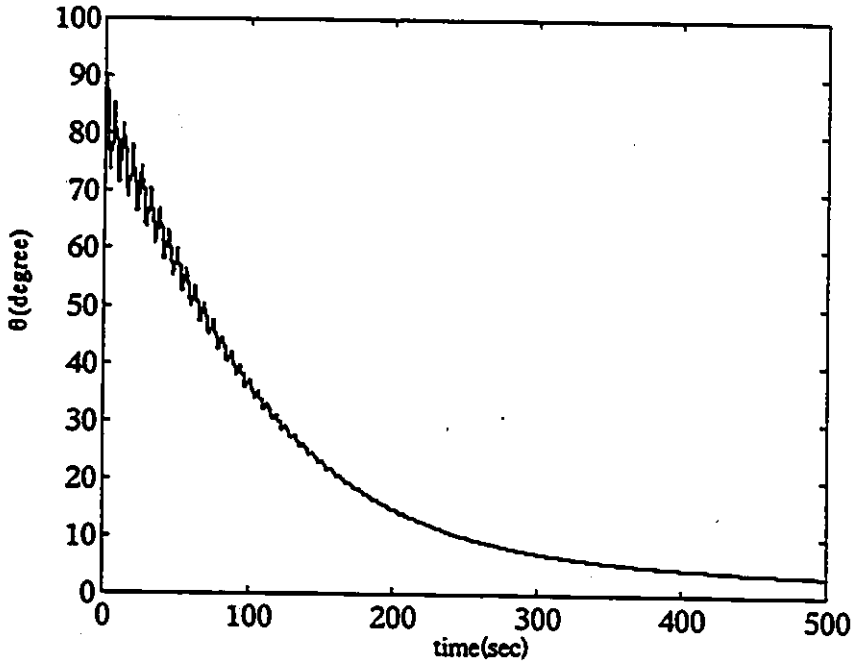

Figure B-4 Time-Varying Control. Simulation 1. Orientation versus time.

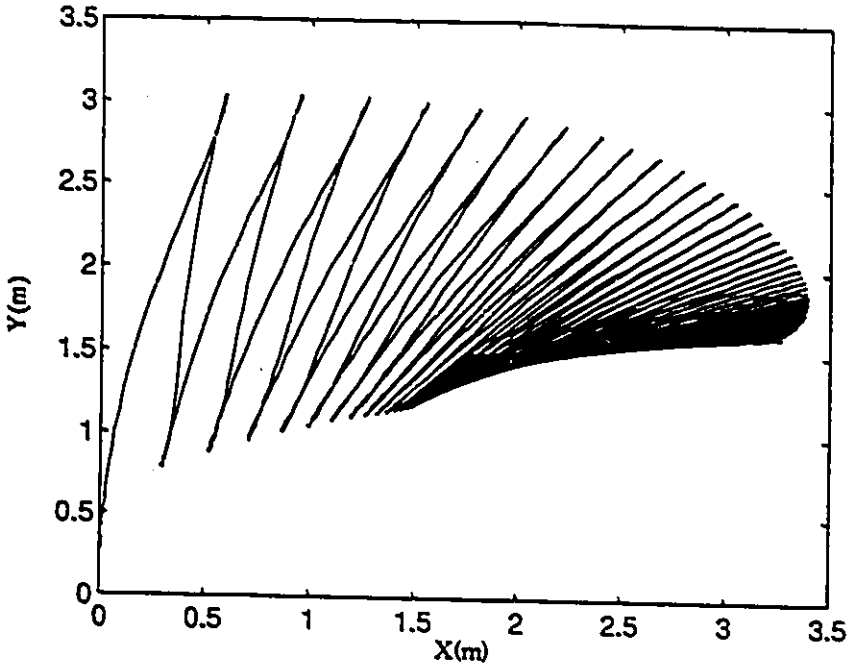

Figure B-5 Time-Varying Control. Simulation 2. Position.

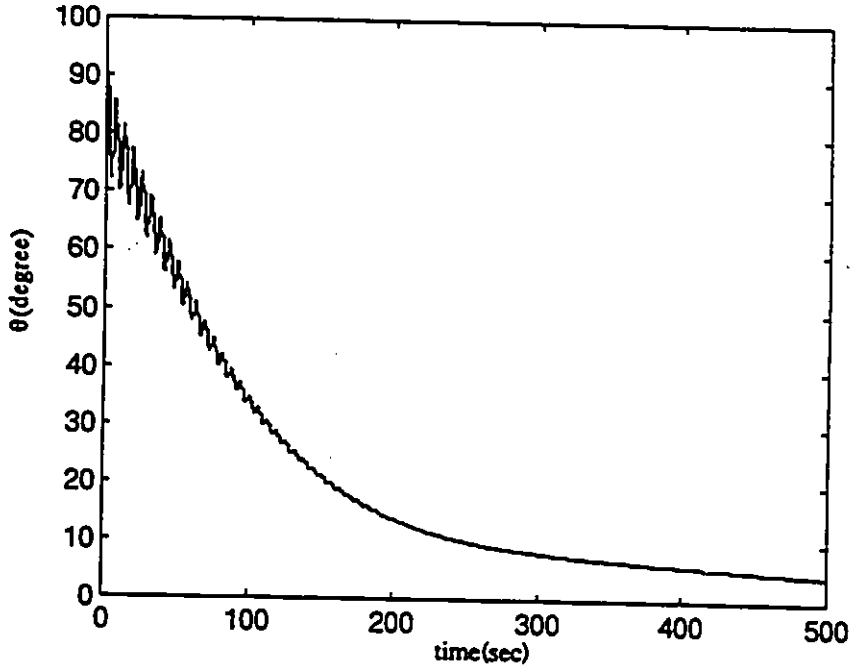

Figure B-6 Time-Varying Control. Simulation 2. Orientation versus time.

B-3 Discontinuous Control

Canudas and Sørdalen's results were given in [9] for a very simple kinematic model of a two rear wheel driven vehicle. The system's model is:

$$\begin{aligned} \dot{x} &= v\cos(\theta) \\ \dot{y} &= v\sin(\theta) \\ \dot{\theta} &= \omega \end{aligned} \qquad \text{(B-4)}$$

where x and y are the Cartesian inertial coordinates, v is the heading velocity and θ is the orientation angle and ω is the planar angular velocity of the vehicle. The vehicle starts from (-0.707,-0.707) with 90° as the orientation angle and moves towards the origin horizontally.

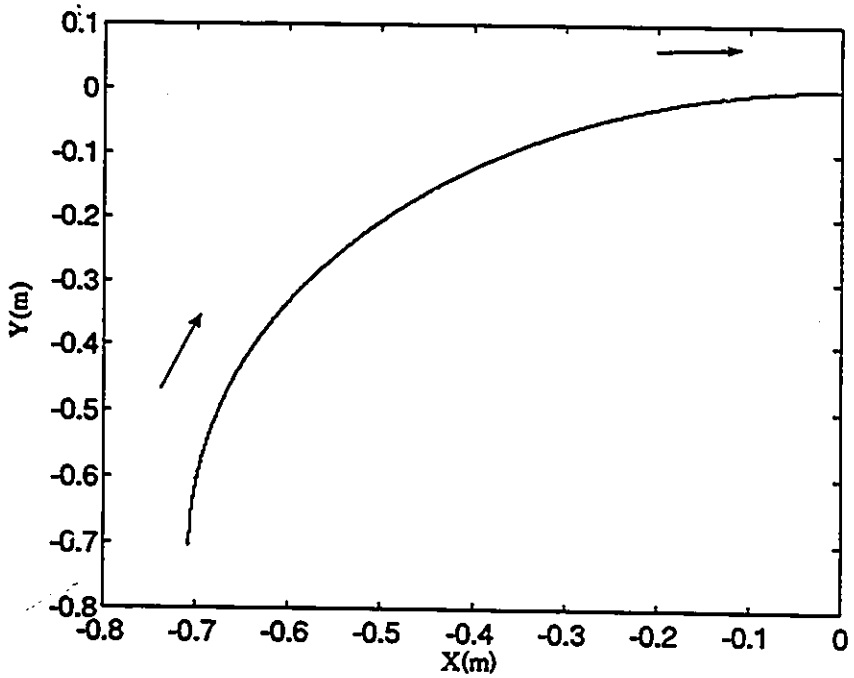

Figure B-7 Discontinuous Control. Position.

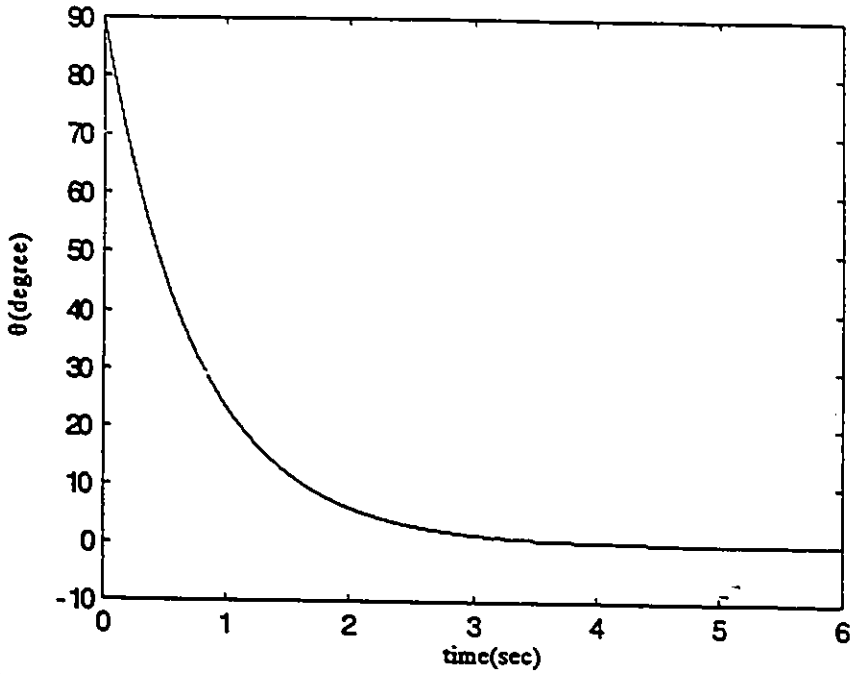

Figure B-8 Discontinuous Control. Orientation versus time.

The simulations show that this method has very interesting results, but this method has not been applied on a dynamic model of a vehicle that has the steering angle as one of its main state variables. The nature of the mathematical proof of the asymptotic stability for this method makes it very difficult, if not impossible, to validate the same type of stability for more complcated models. Recently, discontinuous control laws for models in chained form have been introduced and discussed in the literature [82].